

Clemson University

TigerPrints

All Dissertations

Dissertations

5-2020

Modeling Energy Expenditure and Recovery in Cycling

Vijay Sarthy Mysore Sreedhara

Clemson University, vsreedh@g.clemson.edu

Follow this and additional works at: https://tigerprints.clemson.edu/all_dissertations

Recommended Citation

Sreedhara, Vijay Sarthy Mysore, "Modeling Energy Expenditure and Recovery in Cycling" (2020). *All Dissertations*. 2605.

https://tigerprints.clemson.edu/all_dissertations/2605

This Dissertation is brought to you for free and open access by the Dissertations at TigerPrints. It has been accepted for inclusion in All Dissertations by an authorized administrator of TigerPrints. For more information, please contact kokeefe@clemson.edu.

MODELING ENERGY EXPENDITURE AND RECOVERY IN CYCLING

A Dissertation
Presented to
the Graduate School of
Clemson University

In Partial Fulfillment
of the Requirements for the Degree
Doctor of Philosophy
Mechanical Engineering

by
Vijay Sarthy Mysore Sreedhara
May 2020

Accepted by:
Dr. Gregory Mocko, Committee Chair
Dr. Ardalan Vahidi, Committee Member
Dr. Ethan Kung, Committee Member
Dr. Randolph Hutchison (Furman University), Committee Member

ABSTRACT

The power-duration relationship, comprised of the parameters Critical power (CP) and work capacity (\dot{V}), has been used to model energy expenditure in cycling. For modeling recovery, the W'_{bal} model has been used but lacks validation. Additionally, existing literature has not focused on quantifying or estimating the inherent trial-to-trial variability at the subject level, called the intra-individual variability (IIV), of CP and \dot{V} , posing challenges in modeling and optimization of performance. Thus, the objectives of this research are (i) to establish a method to quantify the IIV of CP and \dot{V} as determined from the 3-minute all-out test (3MT), (ii) to develop a testing protocol to understand expenditure and recovery of power and \dot{V} , (iii) to establish \dot{V} recovery profiles in terms of recovery power (P_{rec}) and recovery duration (t_{rec}), and (iv) to present a case of cycling performance optimization using the energy management system based on athlete-specific models. Competitive amateur cyclists participated in two cycle ergometer studies: (i) repeatability of 3MTs to quantify IIV and (ii) intermittent cycling, in the laboratory to establish \dot{V} recovery profiles. The studies included an incremental ramp test to determine gas exchange threshold (GET), two or four 3MTs to determine CP and \dot{V} , and nine intermittent cycling tests to understand recovery of \dot{V} . From the repeated 3MT study, a new method was proposed to compare any two pairs of the 3MT at the individual level and estimate the IIVs associated with CP and \dot{V} . In the second study, a statistically significant two-way interaction effect between P_{rec} and t_{rec} on \dot{V} recovery was observed followed by simple main effects seen only with respect to P_{rec} at each t_{rec} . This indicates that P_{rec} has a greater

influence on the recovery of Υ in a recovery interval lasting 2-15 minutes that follows a semi-exhaustive exertion interval above CP. The overestimation of the actual Υ -balance at the end of the recovery interval by the W'_{bal} models highlights the need for athlete-specific recovery parameters or models. Finally, the optimization tests conducted with one subject provide encouraging signs for the use of individualized recovery models in real-time in-situ performance optimization.

DEDICATION

*To all the subjects who participated in the experimental studies that are presented
in this dissertation.*

ACKNOWLEDGMENTS

“Alone we can do so little, together we can do so much” - Helen Keller

This work presented in this dissertation is a culmination of the work by many students over the past six years. Firstly, I would like to express my earnest gratitude to my advisor Dr. Gregory Mocko for his knowledge, support, and guidance since my Master’s, making it a great learning and enjoyable experience. I would like to convey my heartfelt thanks to Dr. Randy Hutchison for being an amazing co-advisor and helping me navigate this non-conventional topic. I would like to thank Dr. Ardalan Vahidi for his belief in this work and constant encouragement and Dr. Ethan Kung for being on my committee and guiding me through this journey.

I would like to thank the research group from the early days of my Ph.D. in 2016: Phoebe Bickford, for piquing my interest in this topic and laying the groundwork, Faraz Ashtiani, for helping me through this project over the past four years, and Palmer Primm for being our pilot subject. We have come far from doing the extremely hard cycling tests in Dr. Mocko’s basement.

I would like to thank Furman University students: Lee Shearer, Nicholas Hayden, Sunyeop Lee, Frank Lara, Mason Coppi, Jake Ogden, and Brendan Rhim for their assistance in conducting the experiments and data collection.

I would like to express my extreme gratitude for the sweat and selfless commitment shown by all our subjects who were a part of this work for no reason other than that of scientific endeavor. I thank all the members of Clemson Engineering Design Applications

and Research (CEDAR) laboratory, both past and present, for their good-hearted humor, knowledge, and thoughtfulness during this journey.

I would like to acknowledge the Mechanical Engineering department which gave me financial support during my doctoral program. I would also like to thank the administrative staff of the Mechanical Engineering department for all their help throughout this program.

I would like to thank my parents and my grandmother for their unconditional love, belief, and emotional support. It would be remiss of me not to thank my girlfriend Shraddhaa Narasimha for her unconditional support during this journey. Last but not the least, I thank all my friends for making me feel at home away from home.

TABLE OF CONTENTS

	Page
ABSTRACT	ii
DEDICATION	iv
ACKNOWLEDGMENTS	v
TABLE OF CONTENTS	vii
LIST OF TABLES	xi
LIST OF FIGURES	xiii
NOMENCLATURE	xvii
CHAPTER ONE: INTRODUCTION	1
1.1. Background.....	1
1.2. Understanding fatigue.....	2
1.3. Critical Power (CP) and Work Capacity (Υ) in brief	4
1.4. Research goals	5
1.5. Outline of the dissertation.....	5
CHAPTER TWO: LITERATURE REVIEW	6
2.1. Critical power concept.....	6
2.2. Methods and protocols to estimate CP and Υ	13
2.2.1. Limitations of the protocols used to determine CP and Υ	16
2.3. Adding recovery to the 2-parameter model	21
2.3.1. Applications of a combined expenditure-recovery model of Υ	25
2.4. Research opportunities in modeling human performance	27

2.5. Key conclusions and research objectives.....	30
CHAPTER THREE: REPEATABILITY AND VARIABILITY OF THE 3MT AT THE	
SUBJECT LEVEL	33
3.1. Background.....	33
3.2. Estimating the repeatability and IIV.....	35
3.3. Experimental Procedures and Analyses.....	37
3.3.1. Subjects.....	37
3.3.2. Procedures.....	37
3.3.3. Incremental ramp test.....	38
3.3.4. 3min all out test.....	40
3.3.5. Statistical Analyses.....	41
3.4. Results.....	42
3.5. Discussion.....	49
3.6. Key findings.....	56
CHAPTER FOUR: MODELING THE RECOVERY OF $\dot{V}O_2$	57
4.1. Hypothesized behavior of recovery of $\dot{V}O_2$	57
4.2. Experimental Procedures and Analyses.....	60
4.2.1. Subjects.....	60
4.2.2. Procedures.....	60
4.2.3. Incremental ramp test and the 3MTs.....	61
4.2.4. Intermittent cycling tests.....	61
4.2.5. Optimization tests.....	63

4.2.6. Statistical analysis.....	63
4.3. Results.....	64
4.3.1. Repeatability of 3MTs and the intermittent test	66
4.3.2. Effect of recovery power (P_{rec}) and recovery duration (t_{rec}) on \dot{V} recovery	67
4.3.3. Comparison of actual \dot{V} -balance (A_3) and W'_{bal} predicted by SK2 and BAR models.....	74
4.3.4. Influence of intermittent test on CP	74
4.3.5. Optimization tests	75
4.4. Discussion.....	79
4.5. Key findings.....	83
CHAPTER FIVE: CONCLUSIONS AND FUTURE WORK	85
5.1. Conclusions.....	85
5.2. Future Work.....	87
5.2.1. Reducing the number of testing days.....	87
5.2.2. Surrogate models using muscle-oxygenation (MO_2) and heart rate	89
5.2.3. In-situ testing and validation using a multiple sensor network.....	89
5.2.4. Modeling performance of endurance sports	91
5.2.5. Training and in-game strategies for team sports.....	91
5.2.6. Exercise and health	91
5.3. Research Contributions.....	92
5.3.1. Publications.....	93
REFERENCES	95

LIST OF TABLES

Table	Page
Table 2-1. Models that address the limitations of the 2-parameter model.....	10
Table 2-2. Summary of estimates from all models fit to the data presented by Gaesser and colleagues [48].....	12
Table 2-3. Research opportunities and applications of human performance modeling.	28
Table 3-1. Summary of parameters from the ramp test: VO_{2max} , GET, and VO_{2peak} for all subjects.	42
Table 3-2. Summary of the parameters form the four trials of the 3MT for all subjects.....	43
Table 3-3. ICCs, TEs, CVs, and their 95% CIs for consecutive pairs of trials in parentheses.....	46
Table 3-4. Results from Bland-Altman analysis on all parameters from consecutive pairs of trials.	47
Table 3-5. One-way repeated measures, ICCs, TEs, CVs, their 95%CI, and δg for CP, Y, Pp, and TW for the four trials.	49
Table 3-6. Comparison of average CV at the subject level for CP and Y computed from Triska and colleagues [93].	52
Table 4-1. Summary of parameters from the ramp test: VO_{2max} , GET, and VO_{2peak} for all subjects.	65

Table 4-2. Summary of the parameters form the four trials of the 3MT for all subjects. Data presented as Mean \pm SD.	66
Table 4-3. Summary of the reliability metrics with their 95% CI for the repeated trials of the 3MT and the intermittent test.	67
Table 4-4. Mean Υ_{rec} at different t_{rec} and P_{rec} with summary of simple main effects of P_{rec} at each t_{rec}	73
Table 4-5. Comparison of results between self-strategy and optimal strategy tests.	76
Table 5-1. Proposed testing schedule to reduce the number of testing days.	88
Table A-1. E_{rec} (%) during each intermittent cycling test for all subjects.	121
Table A-2. Results of the repeated measures ANOVA.	121
Table A-3. Results of the simple main-effects analysis at each t_{rec} *	122
Table A-4. Results of the simple main-effects analysis at each P_{rec}	122
Table A-5. Υ_{bal} actual (A_3) vs. Υ_{SK2} and Υ_{BAR} for all subjects*	123
Table A-6. Mann-Whitney U test results for A_3 vs. Υ_{SK2}	125
Table A-7. Mann-Whitney U test results for A_3 vs. Υ_{BAR}	125
Table A-8. CP_{fr} and CP_{ft} for all subjects.	127
Table A-9. Mann-Whitney U test results excluding Subject 7*	129
Table A-10. Independent t-test results for Subject 1	130
Table A-11. Independent t-test results for Subject 2	130
Table A-12. Independent t-test results for Subject 4	131
Table A-13. Independent t-test results for Subject 6	131

LIST OF FIGURES

Figure	Page
Figure 1-1. The hyperbolic relationship between power (P) and time-to-exhaustion t_{Lim}	4
Figure 2-1. The 2-parameter model, (a) the hyperbolic form and (b) the linear transformation with Critical Power (CP) as the y-intercept and curvature constant (Υ) as the slope.....	8
Figure 2-2. The 2-parameter model and its limitations. As t_{Lim} tends to 0, P tends to ∞ , and Critical Power (CP) is the power asymptote at $t_{Lim} = \infty$	9
Figure 2-3. The 2-parameter model (solid line), the 3-parameter model (dashed line), and the exponential model (dotted line) fitted to the same experimental data (solid circles) presented by Gaesser and colleagues [48]. Data extracted from Figure 2 in [34] (p. 1434) and redrawn with permission using the values reported in the original article.....	12
Figure 2-4. Schematic representation of a 3-min all-out test to determine Critical Power (CP) and the curvature constant (Υ). The average power of the last 30s yields CP and the area below the curve and above CP yields Υ	15
Figure 2-5. Repeated constant work-rate (CWR) tests to capture intra-individual variability (IIV) associated with Critical Power (CP) and curvature constant (Υ) estimates. The dotted, dashed, and dot-dashed lines show the fits to the different sets of data and their respective asymptotes. The grand means for	

CP and Υ are obtained by averaging the respective parameters estimates from each curve fitting.....	18
Figure 2-6. model [66] plots showing positive inertial resistance of ergometer flywheel, P_{IN} (solid line) and negative P_{IN} (dashed line). The positive P_{IN} term does not yield the shape shown in Figure 2-4.	20
Figure 2-7. Critical power (CP) concept using Morton’s hydraulic vessel analogy [52]: Energy domains show sub-CP and supra-CP vessels connected by a tube of fixed diameter. Morton’s aerobic and anaerobic vessels are replaced by $<CP$ and $>CP$ respectively as the curvature constant (Υ) and Anaerobic Work Capacity (AWC) cannot be used interchangeably.....	22
Figure 3-1. Schematic representation of the incremental ramp test protocol.	39
Figure 3-2. Schematic representation of the 3-minute all-out test protocol.	41
Figure 3-3. Bland-Altman plots for consecutive trials. Panel A, B, C: Plots for CP, panels D, E, F: Plots for Υ , panels G, H, I: Plots for P_p , and panels J, K, L: Plots for TW.....	45
Figure 3-4. Group and subject level probability density functions (PDF) of CP plotted with $\pm 3SD$. Subjects 3 and 6 were shown as they had the highest and the lowest CP among the group respectively. Solid line shows the group PDF. Dash-dot line shows Subject 3’s PDF, and dotted line shows Subject 6’s PDF. The figure illustrates the overestimation of IIVs by the group level SDs.....	52

Figure 3-5. Comparison of average CP and \dot{V} from CWR tests with multiple trials at each work-rate (total number of CWR tests ≥ 6 with at least two per work-rate) with those from multiple 3MT trials (total number of repeats ≥ 3)..... 55

Figure 4-1. Example of an intermittent cycling session; A1 and A2 are areas of the two exertion intervals..... 58

Figure 4-2. Hypothesized behavior of % \dot{V} recovered, (a) as a function of recovery power (β) and (b) as a function of recovery duration t_{rec} 59

Figure 4-3. Schematic representation of the intermittent cycling test protocol..... 62

Figure 4-4. Recovery profiles of all subjects. Subject A: (i) and (ii), Subject B: (iii) and (iv), Subject 1: (v) and (vi), Subject 2: (vii) and (viii), Subject 4: (ix) and (x), Subject 6: (xi) and (xii), and Subject 7: (xiii) and (xiv). 68

Figure 4-5. Interaction plots. A: \dot{V}_{rec} vs P_{rec} , and B: \dot{V}_{rec} vs t_{rec} . Simple main effects are present at all t_{rec} between mean \dot{V}_{rec} at the three P_{rec} , there are no simple main effects at all P_{rec} between mean \dot{V}_{rec} at the three t_{rec} 72

Figure 4-6. Results from the optimization tests: (a) Power vs distance profile for self-strategy, (b) Power vs distance profile for optimal strategy, and (c) \dot{V} -balance vs distance for the optimal strategy test. The course grade is shown below the power profiles and is plotted on the secondary axis..... 78

Figure 5-1. Multiple sensor network for real-time in-situ performance optimization. 90

Figure A-1. Dissimilar frequency distributions of A_3 and \dot{V}_{SK2} 125

Figure A-2. Dissimilar frequency distributions of A_3 and \dot{V}_{BAR} 126

Figure A-3. Dissimilar frequency distributions of CP_{fr} and CP_{ft} 130

NOMENCLATURE

3MT	3-minute all-out test.
A3	Amount of Υ expended in the 3-minute all-out interval of the intermittent test. Also, the amount of Υ remaining at the end of the recovery interval (Joule).
AWC	Anaerobic Work Capacity (Joule).
CNS	Central Nervous System.
CP	Critical Power, asymptote of the power and time relationship (Watts).
CP4	Power at which a subject will completely expend their Υ in 4 minutes (Watt).
CP_{fr}	CP determined by the 3MT (Watt).
CP_{ft}	CP determined from the 3min all out interval of the intermittent test (Watts).
CV	Coefficient of Variation (%).
CWR	Constant Work Rate test.
D_{CP}	Difference between CP and recovery power (Watt).
GET	Gas Exchange Threshold: a non-invasive surrogate of Maximal Lactate Steady State (MLSS) given by the point at which CO ₂ expiration increases relative to O ₂ consumption (Liter/minute).
I₀	Instantaneous maximum inclination (%).
I_∞	Inclination corresponding to infinite time (%).
ICC	Intraclass correlation coefficient.

IIV	Intra-individual variability.
I_t	Inclination at time t (%).
MLSS	Maximal Lactate Steady State: the highest blood lactate concentration that can be maintained without further accumulation.
P	Power (Watt).
P_{aer, R}	Maximum aerobic power (Watt).
P_{GET}	Power at GET (Watt).
P_{max}	Maximum available anaerobic power/ Instantaneous maximum power (Watt).
P_{mech max}	Maximum power for a 3 second effort (Watt).
P_{mx}	Maximum power observed during the incremental ramp test (Watt).
P_p	Peak power observed during the 3MT (Watt).
P_r	Power output of interval below CP (Watt).
P_{rec}	Power held during the recovery interval of the intermittent test (Watt).
P_w	Power output of interval above CP (Watt).
TE	Typical error of measurement.
t_{LIM}	Time to exhaustion (second).
T_{Pp}	Time taken to reach the peak power P _p in a 3MT (second).
t_r	Duration of interval below CP (Watt).
t_{rec}	Duration of the recovery interval of the intermittent test (second).
TW	Total work done during the 3MT (Joule).
t_w	Duration of interval above CP (Watt).

$\dot{V}O_2$	Volume of oxygen uptake (Liter/minute).
$\dot{V}O_{2max}$	Maximum oxygen uptake (Liter/minute).
$\dot{V}O_{2peak}$	Peak oxygen uptake (Liter/minute).
W'_{exp}	Amount of Υ expended (Joule).
δ	Ratio of the absolute difference between two trials and the average of the two trials (%)
λ, k_{cycle}	Model constants (1/second)
τ, τ_w, k	Time constants (second).
Υ, W', W'_0	Work Capacity, curvature constant of the power and time relationship (Joule).
$\Upsilon_{SK2}, \Upsilon_{BAR}, W'_{bal}$	Model predicted amount of Υ remaining; SK2: Skiba 2 model and BAR: Bartram model (Joule).

CHAPTER ONE: INTRODUCTION

The purpose of this chapter is:

- *To explain the motivation behind the work presented in this dissertation.*
- *To give an overview of fatigue in relation to power and introduce the critical power concept.*

1.1. Background

The study of human fatigue, energy expenditure, and to a lesser degree recovery, has been a focal area of research since the early 1900s. Seminal works in the fields of exercise physiology and performance modeling by Hill [1], Monod and Scherrer [2], and Ward-Smith [3] have laid the groundwork for modeling energy expenditure during prolonged exertion. Recently, researchers have developed formal mathematical models that aid in better management of performance and push limits of human endurance. Most available models have originated from cycle ergometer tests [4] due to the ease of measuring power in cycling and then applied to other forms of exercise like running [5], swimming [6], and rowing [7]. Additionally, most of these models focus on energy exertion with only a few publications that focus on energy recovery, which could give us valuable insight into the physiological underpinnings of fatigue, recovery, and ultimately optimizing performance. Furthermore, developing models of human performance and fatigue lead to applications such as mission planning of soldiers, and investigating the influence of physical activity of cardio-vascular and overall health of a human being.

1.2. Understanding fatigue

From an overall human body perspective, the occurrence of fatigue is governed by both the central nervous system (CNS) and the muscular system (peripheral system) [8], [9]. The CNS mobilizes muscles by stimulating the motor units which results in contraction of the muscles producing force or power. Central fatigue occurs due to the failure of the CNS to drive and maintain muscle activity [10]–[14]. Whereas, changes within the muscular and metabolic system results in peripheral fatigue [11], [15], [16]. It is shown that in healthy individuals, central fatigue contributes about 15%-22% towards fatigue during muscle contraction [15], [17], [18]. Thus, it is practical to consider fatigue as a result of concurrent occurrence of central and peripheral mechanisms [17], [19], [20].

There are several definitions of fatigue across researchers that limit the ability to measure and develop mathematical models [21], [22]. Fatigue is defined as the progressive loss of the ability of the muscular system to sustain this power (energy exertion) over a desired duration of time [15]. Fatigue is also defined as an impairment in performance due to increase in perceived effort coupled with the inability to produce the desired force [23]. For the purpose of this manuscript, fatigue is defined as an exercise induced progressive loss of the ability to sustain maximum power (energy exertion) over a desired duration of time [12], [15], [21], [22], [24]. Thus, fatigue is a dynamic process that leads to a drop in the required exercise intensity, which eventually leads to termination of exercise due to exhaustion [16], [25]–[28].

Exercise intensity is generally categorized as severe, heavy, or moderate [29], [30] based on blood lactate levels [31], maximum oxygen uptake ($\dot{V}O_{2\max}$) [32], [33], or power output

[33]. Maximal Lactate Steady State (MLSS) is often used to categorize exercise intensity. MLSS is the highest blood lactate concentration that can be maintained without further accumulation during sub-maximal work [34], [35]. The exercise intensity associated with MLSS indicates the highest intensity that can be supported by aerobic mechanisms [34], [36] and thus, differentiates the aerobic and anaerobic domains. There are many methods developed to determine MLSS, however, all of them involve taking blood samples to measure the lactate concentration.

Critical power can also be used to determine exercise intensity [33], [37]. Critical power (CP) represents a power output beyond which muscle metabolic homeostasis cannot be attained [38]–[40]. CP is shown to be in close vicinity to the power at which MLSS occurs [41]–[43]. Therefore, CP provides a convenient and non-invasive way of determining exercise intensity. The $\dot{V}O_2$ and blood lactate levels attain a steady state during exercise below CP and hence can be classified as either moderate (below lactate threshold) or heavy (from lactate threshold to CP) intensities [33], [37]. However, exercise above CP is categorized as severe intensity as $\dot{V}O_2$ and blood lactate levels cannot attain a steady state [33]. Thus, CP represents the boundary between heavy and severe intensity exercises [39]. Exertion below CP can last for a long time as the fuel capacity is large. Whereas, exertion above CP is limited in capacity and relatively lasts for a shorter duration. This limited capacity above CP is referred to as work capacity (Υ), which is a finite energy reservoir for exercise intensities above CP.

1.3. Critical Power (CP) and Work Capacity (Y) in brief

Critical Power (CP) and work capacity (Υ) are the power asymptote and the curvature constant respectively of the hyperbolic relationship between power and time-to-exhaustion. CP represents the highest power output above which muscle metabolic steady state cannot be attained [38]–[40] and Υ represents a finite amount of work that can be done at intensities above CP [44], [45]. The hyperbolic relationship was proposed by Monod and Scherrer [2] by conducting a series of constant load dynamic exercises pertaining to specific muscle groups. Moritani and colleagues [4] extended the CP concept to cycling using a series of constant work-rate (CWR) tests to exhaustion (See Figure 1-1).

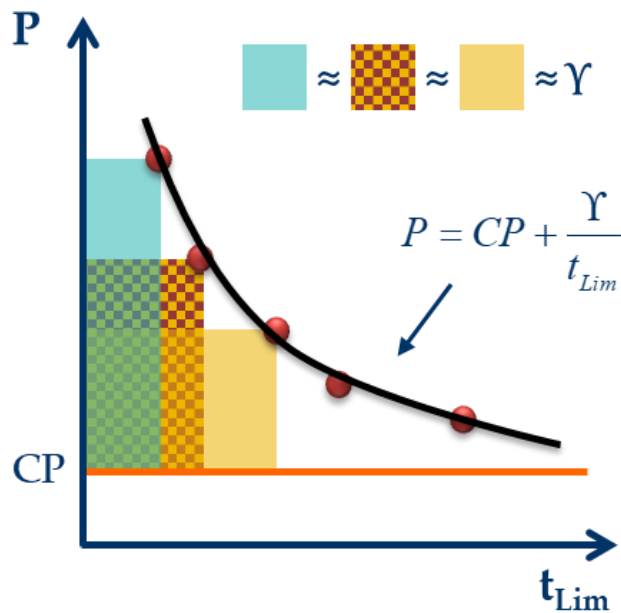


Figure 1-1. The hyperbolic relationship between power (P) and time-to-exhaustion t_{Lim}

The CP concept has a potential application in modeling an energy management system for the human body for a physical task. The physical task is chosen to be cycling in this research due to the relative ease with which power can be measured. The rate of discharge and recharge of Υ can be used to develop a combined expenditure-recovery model for a

cyclist, which would be representative of an energy management system. The amount of Y remaining would represent the state of fatigue of the cyclist leading to better informed strategies to improve and optimize performance. The cyclist will be able to pace themselves better, thereby, meeting their training/race goals and improving their performance.

1.4. Research goals

The goals of this research are to (i) understand the recovery of Y in relation to different recovery powers and recovery durations, (ii) investigate the possibility of a combined expenditure-recovery model of Y to develop an energy management system and optimize cycling performance. These goals are accomplished in the following chapters whose organization is described in the next section.

1.5. Outline of the dissertation

This dissertation is presented in five chapters. The current chapter describes the motivation behind the project, introduces the critical power concept, and defines the scope of the work. Chapter 2 surveys the literature for power-based fatigue models to identify research opportunities and formulate objectives specific to achieving the research goals. Chapter 3 describes the method proposed to estimate the individual variability of CP and Y . Chapter 4 describes the hypothesized behavior of recovery of Y with respect to recovery power and duration and describes the experimental protocol with results. Conclusions, future work, and research contributions are discussed in Chapter 5.

CHAPTER TWO: LITERATURE REVIEW¹

The purpose of this chapter is:

- *To conduct a review of power-based fatigue and recovery models available in literature.*
- *To identify research opportunities and define the scope of this research.*

2.1. Critical power concept

The critical power concept was introduced by Monod and Scherrer [2] using a linear relationship between total work done and time-to-exhaustion. Monod and Scherrer's work was based on Hill's [1] observations pertaining to athletic records in different sports. Monod and Scherrer coined the terms Critical Power (CP) and limit work (W_{Lim}). They defined CP as the power output that an athlete can generate indefinitely and W_{Lim} as the total work done until exhaustion at a constant work-rate above CP related by a linear relationship given by,

$$W_{Lim} = a + b \cdot t_{Lim} \quad (1)$$

where, 'a' is an energy reserve in the units of work (Joules) and the constant 'b' is the critical power in Watts, and t_{Lim} is time-to-exhaustion in seconds. Monod and Scherrer derived a hyperbolic form for t_{Lim} by substituting W_{Lim} as,

¹ The work presented in this chapter stems from the following paper:

Sreedhara, V. S. M., Mocko, G. M., & Hutchison, R. E. "A survey of mathematical models of human performance using power and energy". Accepted (December 2019), Sports Medicine – Open.

$$W_{Lim} = P \cdot t_{Lim} \quad (2)$$

Using Equation 2 and transforming Equation 1 as:

$$t_{Lim} = \frac{a}{P - b} \quad (3)$$

where, P is power in Watts. Moritani and colleagues [4] extended the critical power concept to cycling using a series of cycle ergometry tests and called the term ‘a’ as anaerobic reserve deriving the linear relationship between P and 1/t_{Lim} from Equation 3 given by,

$$P = \frac{a}{t_{Lim}} + b \quad (4)$$

Whipp and colleagues [46] then fit a hyperbolic curve between P and t_{Lim} with a time asymptote at a power level that is equal to CP and denoted the anaerobic reserve term as W'. The anaerobic reserve term, W' has since been referred to as anaerobic work capacity (AWC) and these two terms have been used interchangeably. However, it has been shown that W' is not equal to AWC and the two terms should not be used interchangeably [28], [47]. Additionally, it should be noted that W' (pronounced W prime) may lead to confusion in mathematical modeling as it is common notation to use “prime” to represent the first derivative with respect to time. Hence, W' is referred to as Y hereafter. Rewriting Equation 4 by replacing ‘a’ with Y and ‘b’ with CP yields the following relationship,

$$P = CP + \frac{Y}{t_{Lim}} \quad (5)$$

Equation 5, widely regarded as the 2-parameter model, has been transformed to its linear form, first seen in [4] and later in [2], [48]–[50], by plotting power versus 1/t_{Lim} with CP and Y representing the y-intercept and slope respectively as shown in Figure 2-1. The CP

concept has been applied to running [5], swimming [6], and rowing [7] with analogous parameters such as Critical Velocity (CV) and distance capacity (D') instead of CP and Υ respectively.

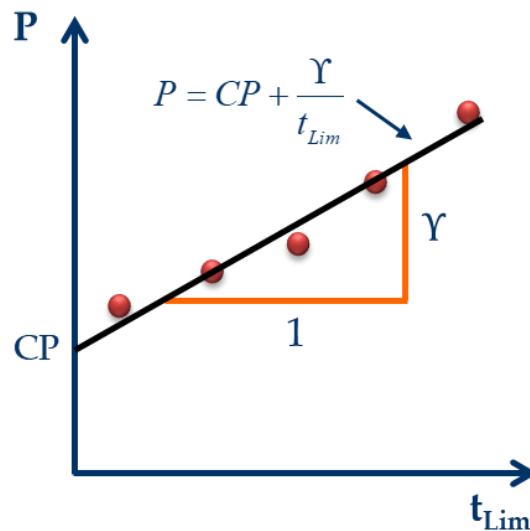
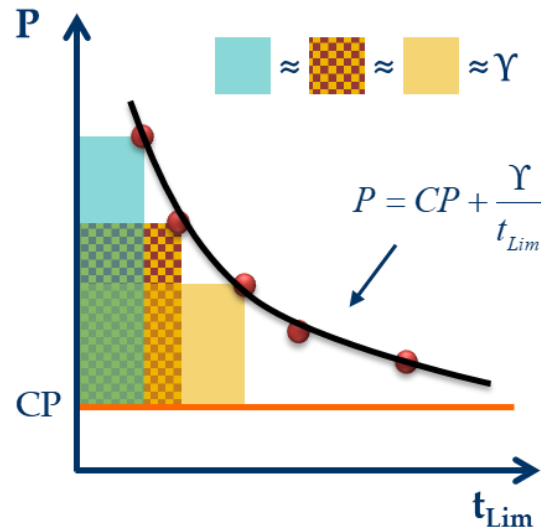


Figure 2-1. The 2-parameter model, (a) the hyperbolic form and (b) the linear transformation with Critical Power (CP) as the y-intercept and curvature constant (Υ) as the slope.

A limitation of the CP concept described by Equation 5 is that as t_{Lim} approaches 0, P tends to infinity (See Figure 2-2). This is not realistic as there is a limit to the instantaneous

maximum power that a human can produce [51], [52]. Moreover, Josephson [53] states that the maximum power output for a muscle occurs at 30% of its maximum shortening velocity (V_{\max}). It takes a short duration of time for the muscle to reach $0.3 V_{\max}$ starting from rest. Therefore, it may be beneficial to define the instantaneous maximum power as the average power-output for one crank rotation [54]. Additionally, some publications have reported that the average duration for which the CP can be maintained is less than an hour [55]–[58], while others have reported that it can be maintained for approximately over an hour [59], [60]. D. W. Hill [49] suggests that the end point of the tests proposed to the subjects in these studies, i.e., 24-30 minutes in [61], [62] and 60-90 minutes in [55], [59] may have influenced the outcome. Several researchers have attempted to address the limitations of the 2-parameter model. These models are shown in Table 2-1.

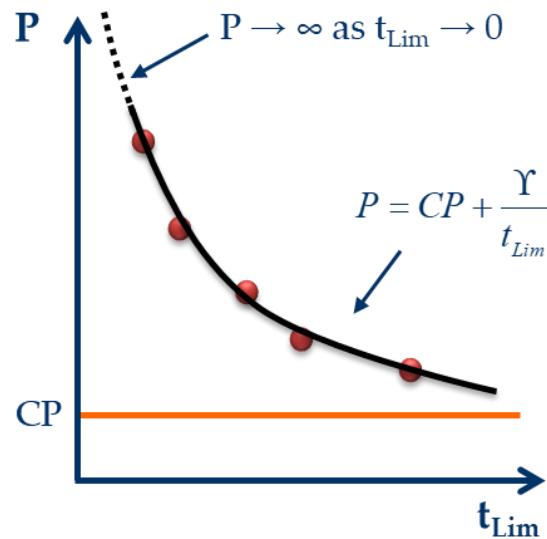


Figure 2-2. The 2-parameter model and its limitations. As t_{Lim} tends to 0, P tends to ∞ , and Critical Power (CP) is the power asymptote at $t_{Lim} = \infty$.

Table 2-1. Models that address the limitations of the 2-parameter model.

Researchers	Model	Model terms
Ward-Smith [3] (1985) Running	$P(t) = (P_{\max} - R) \cdot e^{(-\lambda \cdot t)} + R$	P_{\max} : Maximum available anaerobic power, R: Maximum aerobic power, and λ : A constant.
Hopkins and colleagues [63] (1989) Treadmill running	$I_t = I_{\infty} + (I_0 - I_{\infty}) \cdot e^{(-t/\tau)}$	I_t : Inclination at time t, I_{∞} : Inclination pertaining to infinite t, I_0 : Instantaneous maximum inclination, and τ : A time constant.
Morton [64] (1996), Cycling	$t = \frac{AWC}{P - CP} + k, \quad k = \frac{AWC}{CP - P_{\max}}$	P_{\max} : Instantaneous maximum power.
Weyand and colleagues [65] (2003), Cycling	$P(t) = P_{\text{aer}} + (P_{\text{mech max}} - P_{\text{aer}}) \cdot e^{(-k_{\text{cycle}} \cdot t)}$	P_{aer} : Maximum aerobic power, $P_{\text{mech max}}$: Maximum power for a 3s effort, and k_{cycle} : A constant.
Morton [66] (2009), Running/Cycling	$P(t) = CP + (P_{\max} - CP) \cdot e^{(t/k)}$	P_{\max} : Instantaneous maximum power producible and k: A constant.

#The model shown is a simplified form. The complete model can be found in the original article by Ward-Smith [3].

Models from Ward-Smith [3], Hopkins and colleagues [63], Weyand and colleagues [65], and Morton (2009) [66] are all fundamentally the same with

- (i) R , I_{∞} , and P_{aer} analogous to CP
- (ii) P_{max} , I_0 , $P_{mech\ max}$ representing the instantaneous maximum power that can be produced, and
- (iii) λ , τ , k_{cycle} , and k representing constants whose values and signs are dependent on the regression fit.

Figure 2-3 shows three models (2-parameter, 3-parameter, and exponential) plotted against experimental data presented by Gaesser and colleagues [48]. The values of CP, $\dot{V}O_2$, and P_{max} were taken from [48] and data points were extracted using the open source software Plot Digitizer. Table 2-2 summarizes the estimates from each method.

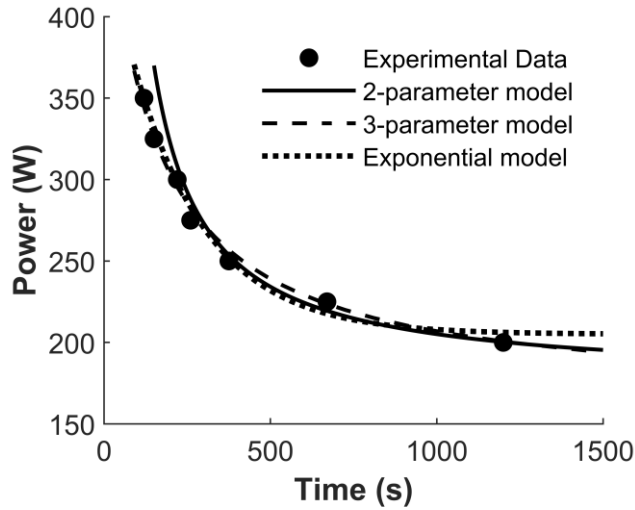


Figure 2-3. The 2-parameter model (solid line), the 3-parameter model (dashed line), and the exponential model (dotted line) fitted to the same experimental data (solid circles) presented by Gaesser and colleagues [48]. Data extracted from Figure 2 in [34] (p. 1434) and redrawn with permission using the values reported in the original article.

Table 2-2. Summary of estimates from all models fit to the data presented by Gaesser and colleagues [48].

Model	CP (W)	Υ (J)	P_{\max} (W)	Additional model parameters
				(λ , τ , k_{cycle} , or k) (s)
2-parameter	176	29100	NA	NA
3-parameter	165	47900	491	- 146.93
Exponential	205	NA	452	0.0044 or - 225.2867*

*Morton's [66] $k = -225.2867$, Hopkins' [63] $\tau = 225.2867$, which are same as Weyand's [65] $-1/k_{\text{cycle}}$ and Ward-Smith's [3] $-1/\lambda$.

There are other models available in literature that predict performance with higher accuracy (For example: Peronnet and Thibault [67] for race performance and Morton [68] for endurance at incremental and constant power exercises). However, these models, like Ward-Smith's complete model [3] are complex and need determination of several parameters, which involves a greater investment of time and resources. Furthermore,

algebraic manipulations of the 2-parameter model shown in Equation 5 have been presented in literature. However, these models yield different estimates of CP and \dot{V} at the individual level for the same data as seen in [48], [69], [70]. These differences in estimates could originate from the rounding off approximations of reciprocals such as $1/t_{Lim}$. CP estimates from different models are reported to be in close agreement with each other in [48], [69], [70]. However, as illustrated in Table 2-2, the estimation of \dot{V} remains elusive as the same data can yield different estimates depending on the model used even though CP estimates are comparable [48], [52], [69]–[75]. The 2-parameter model, though having limitations ($P = \infty$ at $t = 0$ and CP lasting indefinitely), owing to its simplicity, can potentially be used to optimize performance as well as determining strategies by estimating time-to-exhaustion [27], [28], [76].

2.2. Methods and protocols to estimate CP and \dot{V}

The first experimental protocol to estimate CP and \dot{V} was derived from Monod and Scherrer's [2] work. Subjects completed at least three constant work-rate (CWR) to exhaustion tests. From these tests, the experimental results are fit to the 2-parameter model resulting in CP and \dot{V} estimates. Hill [49] suggests the use of the linear model (P versus $1/t_{Lim}$) with at least 4-5 CWR tests to arrive at CP and \dot{V} estimates.

While less prevalent in literature, Morton [72] demonstrated another method to determine estimates of CP and \dot{V} from ramp exercises to exhaustion by deriving an equation between time-to-exhaustion and ramp slope given by,

$$T = \frac{CP}{S} + \sqrt{\frac{2 \cdot Y}{S}} \quad (6)$$

where, T is the time-to-exhaustion in seconds and S is the ramp slope in Watts/second. Morton suggested that subjects complete 4-5 ramp tests to exhaustion at different slopes. The time-to-exhaustion from these tests are then plotted against the slopes and Equation 6 would be fitted to the data to determine CP and Y. Morton claims that the estimates from this protocol appear to be lower than those from the CWR protocol thus, addressing the overestimation of CP reported in a few publications cited earlier. The ramp protocol was compared to the CWR protocol by Morton and colleagues [77] showing an underestimation of Y and no statistical difference for CP. However, a closer inspection shows underestimation of Y by approximately 10kJ, 4kJ, 3kJ, and 9kJ for subjects 1, 2, 3, and 6 respectively and an overestimation of Y by approximately 8kJ, 6kJ, and 3kJ for subjects 4, 9, and 10 respectively (see Table 1 in [77]).

Vanhatalo and colleagues [78] more recently proposed the 3 min all-out test (3MT) to determine CP and Y in fewer laboratory visits. This test involves pedaling at all-out intensity for 3 minutes with CP estimated by the average power from the last 30 seconds and Y given by the area under the curve above CP [71], [78]. Figure 2-4 shows the schematic representation of a notional 3MT. Parallels can be drawn between the 3MT and the Wingate anaerobic test [79], which is essentially a 30s all-out test. Studies that compare Y to the anaerobic capacity from the Wingate test report a correlation coefficient of ~0.7 [80], [81]. Therefore, the anaerobic capacity from the Wingate test and Y cannot be used interchangeably.

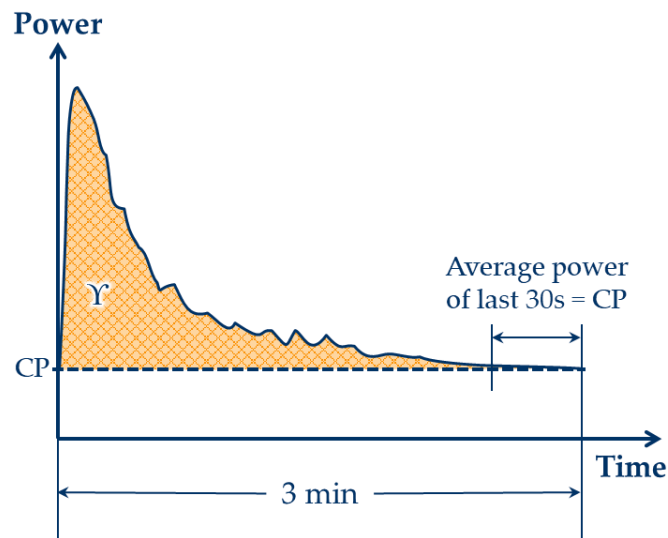


Figure 2-4. Schematic representation of a 3-min all-out test to determine Critical Power (CP) and the curvature constant (γ). The average power of the last 30s yields CP and the area below the curve and above CP yields γ .

The estimates from the 3MT have been compared to those from the CWR tests in [43], [74], [82] and thereby, validating the 3MT. Burnley and colleagues [83] saw (in 7 out of 11 subjects) a steady state blood lactate and oxygen uptake profile in 30 minutes of exercise at 15 W below CP determined from the 3MT. The same subjects pedaled at 15 W above CP which resulted in an average time-to-exhaustion of 13 ± 7 minutes. Black and colleagues [76] used the CP determined from the 3MT to successfully estimate a 16.1 km time trial performance. However, studies have reported that the time-to-exhaustion at CP derived from the 3MT to be 14.79 ± 8.38 minutes and 12.5 ± 6.5 minutes in [84] and [85] respectively. These are similar to 13 ± 7 minutes for exercise at 15 W above CP reported by Burnley and colleagues [83]. Moreover, γ from 3MT has also been reported to be overestimated in comparison to CWR protocol (11.37 ± 3.84 kJ vs 9.55 ± 4 kJ) in [86]. However, as discussed in [87] the errors observed in the estimates could be attributed to not using the same equipment, or not adhering to the test procedure laid out in [78].

Additionally, the inherent day-to-day or trial-to-trial variability within subjects, referred to as the intra-individual variability (IIV), may have contributed to the shorter time-to-exhaustion observed at CP [28], [52]. Hence, exercise outside a subject's 95% confidence interval of CP, i.e. outside the bounds of the IIV associated with CP (similar to 15 W above and below CP in [83]), will yield better insights into reliability of the 3MT.

2.2.1. Limitations of the protocols used to determine CP and $\dot{V}O_{2max}$

The CWR protocol is considered as the “gold-standard” to estimate CP and $\dot{V}O_{2max}$ as it was the first method to be proposed. However, the CWR protocol is not devoid of shortcomings. Using the CWR protocol, Bishop and colleagues [88] and Jenkins and colleagues [89] illustrated that the duration of the predicting trials influences the estimates with both CP and $\dot{V}O_{2max}$ computed from three shortest duration trials being significantly greater than those from the three longest trials. Furthermore, CP estimates from the CWR protocol at 60rpm have been found to be significantly greater than those at 100rpm [90]. Considering these limitations, Muniz-Pumares and colleagues [75] suggest the use of the 2 parameter hyperbolic model with at least three CWR trials of durations > 2 minutes and < 15 minutes and freely chosen cadence to arrive at reliable estimates.

The 3MT avoids the need to do multiple tests to arrive at CP and $\dot{V}O_{2max}$. However, there are reports of overestimation of CP from the 3MT [84], [85], [91], which are comparable to other reports of overestimation of CP from the CWR tests in [55]–[58]. The 3MT appears to reliably predict a 16.1 km time trial performance [76], which is in accordance with other studies that report the validity of CP to be 40 minutes to over 1 hour [49], [59], [60]. These

contradictory results can be attributed to equipment, test method, validation methods, and the day to day variability of the participants [28], [52], [87].

It has been shown that the day-to-day (or trial-to-trial) variability within a person, i.e. IIV, affects performance during physical activities in [92]. The CWR tests, depending on the fit and the model used, yield standard errors of estimation (SEEs) for CP and \dot{V}_O . These SEEs give a measure of goodness of fit and not the IIV. To capture and quantify IIV using the CWR protocol, exercise to exhaustion at each work-rate must be repeated multiple times. CP and \dot{V}_O estimates for each set of tests could be determined, which can then be averaged to arrive at a grand mean for CP and \dot{V}_O (See Figure 2-5). On similar lines, Triska and colleagues [93] conducted maximal effort time trials spanning 3, 7, and 12 minutes with each trial repeated thrice (One familiarization and two repeats), and computed CP and \dot{V}_O for each data set using the 2-parameter hyperbolic model. They found higher reliability between the post familiarization trials with intra-class correlation coefficient of 0.95 and 0.94 and a coefficient of variation of 2.6% and 8.2% for CP and \dot{V}_O respectively. However, an average CP and \dot{V}_O for all three sets of data (or post familiarization trials) could be computed to yield grand means for CP and \dot{V}_O for each subject with their IIVs as shown in Figure 2-5. Although costly in terms of time, this method leads to a more complete understanding of \dot{V}_O , which has been shown to be ambiguous and significantly dependent on the mathematical model used [48], [69]–[71], [73]–[75].

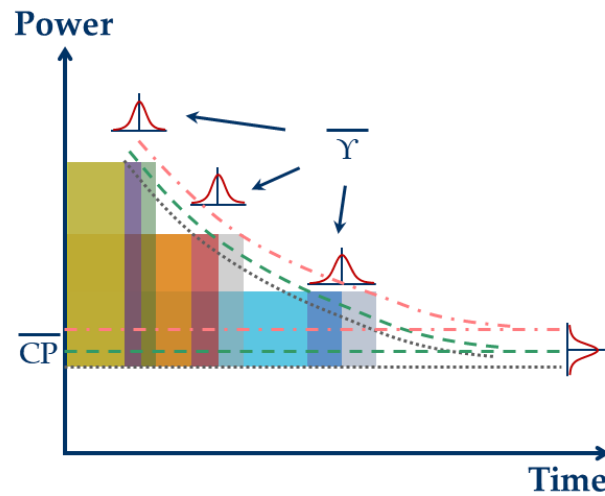


Figure 2-5. Repeated constant work-rate (CWR) tests to capture intra-individual variability (IIV) associated with Critical Power (CP) and curvature constant (\dot{Y}) estimates. The dotted, dashed, and dot-dashed lines show the fits to the different sets of data and their respective asymptotes. The grand means for CP and \dot{Y} are obtained by averaging the respective parameters estimates from each curve fitting.

Though the 3MT has been shown to be repeatable in [83], a closer investigation of the Bland-Altman plots presented in the first paper on 3MT [83] (p.1998, Figure 1, panel D) shows the bias and 95% limits of agreement of -1 ± 15 W resulting from the variability associated with each subject's CP estimate across two trials. A 15 W change in CP between two 3MTs contributes to a difference of 2700 J of \dot{Y} across the 3 minutes of the test. This IIV needs to be accounted for before prescribing training schedules and interventions based on the 3MT. The estimates from the CWR protocol have associated SEEs for CP and \dot{Y} , whereas it is not possible to get a standard error for \dot{Y} from a 3MT. A possible way to arrive at SEEs for CP and \dot{Y} from the 3MT is by fitting a curve to the data. Morton [66] used a bi-exponential extension to his exponential model [66] (last row in Table 2-1) to be applicable to all-out efforts given by,

$$P(t) = CP + (P_{\max} - CP) \cdot e^{t/k} + P_{\text{IN}} \cdot e^{-t/k'} \quad (7)$$

where, P is the power at any time t , CP is the critical power, P_{\max} is the instantaneous maximum power, P_{IN} is the power required to overcome the initial inertial resistance of the ergometer flywheel, and k and k' are constants. The P_{IN} term accounts for 0-5s of the all-out test. The model in Equation 7 is shown to fit the all-out test data with $R^2 = 0.985$ in [66]. However, it has a few limitations that are discussed below.

At $t = 0$, $P(0) = P_{\max} + P_{\text{IN}}$, which is not possible as the instantaneous maximum power that can be generated is P_{\max} . Instead, at $t = 0$, $P(0) = P_{\max} - P_{\text{IN}}$ is a more realistic power output. The $P_{\max} - P_{\text{IN}}$ correction is a mathematical quirk and may appear to lack physiological basis. However, P_{\max} could be assumed to be equal to either the average power output of one crank-rotation [54] or the power output of 3s trial [65] which accounts for the physiological constraints of producing an instantaneous P_{\max} . Furthermore, if the all-out interval starts from rest, then at $t=0$, $P(0) = 0$, is a more valid initial condition as power is defined as energy-expended/time and no energy is expended before starting the exercise.

Morton fit the model to Burnley's data in [83] which resulted in the $CP = 336.3 \pm 1.2$ W, $P_{\max} = 959.3 \pm 7.9$ W, $P_{\text{IN}} = 512.1 \pm 13.8$ W, $k = -29.9 \pm 0.5$ s, $k' = 3.14 \pm 0.16$ s. Using these values in Equation 7 and plotting against time (from 0 to 180s) does not result in the desired shape of the 3MT as shown in Figure 2-4 (See Figure 2-6). If P_{IN} were to be negative, the resulting shape would be similar to that of Figure 2-4. However, a negative resistance for the flywheel is unrealistic.

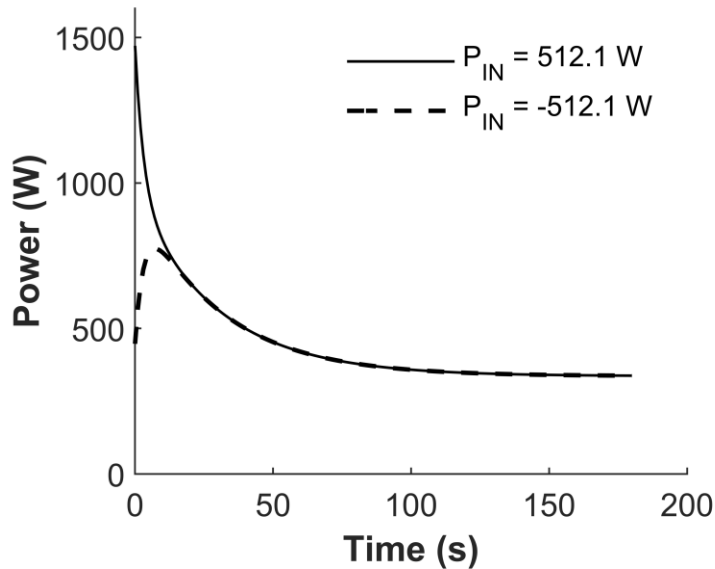


Figure 2-6. model [66] plots showing positive inertial resistance of ergometer flywheel, P_{IN} (solid line) and negative P_{IN} (dashed line). The positive P_{IN} term does not yield the shape shown in Figure 2-4.

The power required to overcome the inertial resistance of the flywheel can be computed using the Newton's second law for rotational motion as shown in [94]. The P_{IN} term is a function of torque and acceleration. Thus, there is no reason to assume an exponential decay as shown in Equation 7. A piecewise model could be developed for a 3MT with the first piece to account for the power needed to overcome the flywheel's inertia and the second to account for the decline from peak power to CP. Furthermore, the time taken by the muscle to reach P_{max} needs to be accounted for in the first piece where the muscles are overcoming the flywheel resistance while reaching their maximal power output.

The SEEs from curve fitting, as mentioned earlier, do not quantify the IIV associated with CP and \dot{Y} for an individual. Conducting multiple tests and computing grand means for CP and \dot{Y} from each set of tests significantly increases the time investment. There is a need for better methods to capture the IIV from a 3MT, minimize the number of testing days, and

statistically compare two 3MTs to arrive at reliable estimates of CP and \dot{V} for an individual. Furthermore, most studies report the average of their participant groups. While this is convenient in terms of comparing them with estimates from other methods and protocols, they give little information pertaining to the repeatability and variability at the individual level. It is, therefore, practical to consider individuals rather than groups and arrive at athlete-specific models. This is important in terms of modeling recovery of \dot{V} which could be appended to the 2-parameter CP model, thereby aiding in performance optimization.

2.3. Adding recovery to the 2-parameter model

The CP concept has been discussed using a hydraulic vessel analogy by Morton [52]. Morton [52] discusses that the aerobic and anaerobic domains are analogous to energy vessels connected by a tube of fixed diameter, with the anaerobic vessel being limited in capacity and the aerobic being unlimited (See Figure 2-7). Morton suggests that when functioning above CP, energy is derived from the anaerobic vessel, whereas when exercising below CP, energy is supplied by the aerobic vessel. Morton's hydraulic analogy considers CP to be the boundary between aerobic and anaerobic domains, and AWC to be equal to \dot{V} as it was published around the same time as the Deckerle and colleagues' study [47] that showed that AWC and \dot{V} cannot be used interchangeably.

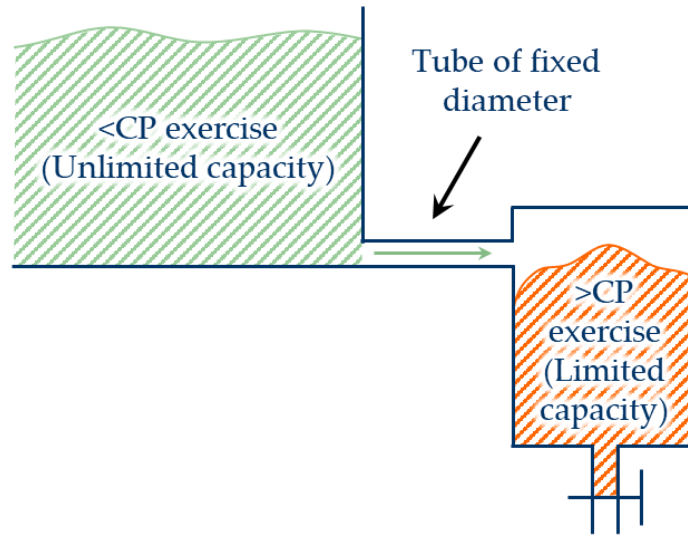


Figure 2-7. Critical power (CP) concept using Morton's hydraulic vessel analogy [52]: Energy domains show sub-CP and supra-CP vessels connected by a tube of fixed diameter. Morton's aerobic and anaerobic vessels are replaced by <CP and >CP respectively as the curvature constant (Υ) and Anaerobic Work Capacity (AWC) cannot be used interchangeably.

Ignoring the assumption of AWC and Υ being equal, Morton's analogy suggests that while below CP, the curvature constant Υ (limited capacity tank in Figure 2-7) is refilled or recovered. This suggestion presents the possibility of modeling the recovery of Υ while exercising below CP and thereby, together with the 2-parameter model, optimizing performance. While there are models to estimate the depletion of Υ , there are only a few models that attempt to estimate its recharge/recovery while below CP.

The first model considering recovery of Υ was proposed by Morton and Billat [95]. Morton and Billat [95], based on the 2-parameter model, derived an equation for time-to-exhaustion for intermittent exercise by assuming that the rates of recharge and expenditure of Υ were equal given by,

$$t = \frac{n \cdot (t_w + t_r) + \Upsilon - n \cdot [(P_w - CP) \cdot t_w - (CP - P_r) \cdot t_r]}{(P_w - CP)} \quad (8)$$

where, t is the total duration of the intermittent exercise, n is the number of intervals, t_w and t_r are respective durations of intervals above and below CP, and P_w and P_r are respective power outputs of intervals above and below CP. Ferguson and colleagues [96] were first to quantify recovery of $\dot{V}O_2$ by proposing that it is “curvilinear” and not proportional to its depletion as assumed by Morton and Billat [95]. Acknowledging this curvilinear nature of recovery of $\dot{V}O_2$, Skiba and colleagues [97]–[100] proposed a model which assumed the behavior to be exponential given by,

$$W'_{bal} = W'_{exp} - \int_0^t W'_{exp} \cdot e^{-\left(\frac{t-u}{\tau_{W'}}\right)} du \quad (9)$$

where, W'_{bal} is the $\dot{V}O_2$ -balance at any time during exercise, W'_{exp} is the amount of $\dot{V}O_2$ expended, $(t - u)$ is the duration of the recovery interval, and $\tau_{W'}$ is the time constant of reconstitution of $\dot{V}O_2$ in seconds given by,

$$\tau_{W'} = 546 \cdot e^{(-0.01D_{CP})} + 316 \quad (10)$$

where, D_{CP} is the difference between CP and average power output during all intervals below CP. Equation 10 is a non-linear regression obtained by plotting $\tau_{W'}$ values (calculated by setting $W'_{bal} = 0$ in Equation 9 at the termination of exercise) against respective D_{CP} s.

Skiba’s model was validated in [98] where an average $\dot{V}O_2$ -balance at exhaustion of 0.5 ± 1.3 kJ was reported. However, the model cannot be used to determine $\dot{V}O_2$ -balance in real time [87] (p.78) as the $\tau_{W'}$ term needs W'_{bal} to be zero which is not known until the termination of each test. Moreover, three forms of the W'_{bal} model have been published by Skiba and colleagues [97]–[100]. The first [97] contains only the integrand and not the differential variable. The second [98], [99] contains the differential “ du ” as shown in

Equation 9, whereas the third [100] has “dt” as its differential variable. Changing the differential variable from “du” to “dt” yields different results upon integration. Additionally, inspecting Equation 9 reveals that the integral term on the right-hand side has units of Joules-second causing an inequality as the units of the left-hand side is Joules. The detailed derivation of the mathematical solutions for both “du” and “dt” as the differential term of the W'_{bal} model illustrating the difference in results as well as the imbalance of units is available in Appendix A. Furthermore, the standard errors associated with the estimation of CP and \dot{Y} may cause a negative balance of \dot{Y} -balance (can be seen in [98], Figure 2, p.903). Skiba and colleagues [99] proposed a biconditional W'_{bal} model which resolves the inequality of units (can be seen in Appendix 1 of [99]) given by,

$$\begin{aligned} \text{If } P \geq CP, \quad W'_{bal} &= W'_0 - [(P - CP) \cdot t] \\ \text{If } P < CP, \quad W'_{bal} &= W'_0 - W'_{exp} \cdot e^{\left(\frac{-t}{\tau}\right)} \end{aligned} \quad (11)$$

where, W'_0 is \dot{Y} at time $t = 0$ and $\tau = W'_0/D_{CP}$. Bartram and colleagues [101] illustrated that Equation 11 (referred to as SK2 in Chapter 4) underestimates the recovery of W' in elite athletes and proposed that τ be modified as,

$$\tau = 2287.2 \cdot D_{CP}^{-0.688} \quad (12)$$

They also suggested deriving group/athlete-specific time constants to be able to accurately estimate \dot{Y} recovery. The model using the τ from Equation 12 will henceforth be referred to as BAR in chapter 4. Bickford and colleagues [102] developed a model of recovery of \dot{Y} which was derived from limited data and thus needs refinement.

Apart from the models presented above, at the time of submission, there are no models available in literature that attempt to model the recovery of \dot{Y} . These models need to be

improved for accurately modeling the recovery of \dot{V} and combining them with the models of exertion that are well established in the literature. There is potential in extending the 2-parameter model to include the recovery of \dot{V} . A combined exertion-recovery/discharge-recharge model of \dot{V} will be worthwhile in estimating the time-to-exhaustion of endurance efforts and optimizing performance. The potential of optimizing performance to accomplish a 2-hour marathon has been illustrated by Nike's Breaking2 project [103] which has inspired modeling studies by Hoogkamer and colleagues [104]–[106] based on the 2-parameter CP model with exponential recovery similar to Equation 11, biomechanical improvements, shoe design improvements, and drafting strategy. Furthermore, the successful completion of a sub 2-hour marathon by Eliud Kipchoge as a part of the INEOS 1:59 challenge in Vienna in October 2019 provides encouraging signs for investigative studies focusing on optimization of performance in other endurance sports.

2.3.1. Applications of a combined expenditure-recovery model of \dot{V}

In the literature reviewed thus far, studies modeling recovery of \dot{V} are not common. A limited number of studies attempt to address the need for a combined expenditure-recovery model. Skiba's first model [97] is similar to the mono-exponential ventilatory gas exchange model for moderate intensity cycling proposed by Whipp and colleagues [107] and Vandewalle and colleagues' aerobic power model [81]. The exponential assumption of recovery seems logical as sub-CP exercise is considered to be supported by aerobic mechanisms [52]. The τ_W relation in Equation 10 is representative of the 7 recreational

athletes from whose data it was derived. Though the model was validated using data from 8 triathletes in [98], it may not be able to predict the recovery of Y for athletes of higher or lower caliber. This is illustrated by Caen and colleagues [108] where faster recovery of Y was observed. Skiba's second model (also mono-exponential) [99], derived from first principles with valid assumptions, addresses some limitations of the earlier version. However, it has not been validated, and like its predecessor, has been shown to have slower recovery kinetics for elite athletes by Bartram and colleagues [101].

De Jong and colleagues [109] used the 2-parameter model to simulate the optimization of a 5km time-trial performance. However, a recovery model in combination with the 2-parameter model will aid in optimizing performance over longer durations and distances. There have been other attempts at combining the 2-parameter model with a recovery model [102], but the limited data results in the need for refinement. The advantage of an exertion-recovery model is the ability to accurately predict the time-to-exhaustion during endurance exercises. Furthermore, modeling fatigue, exhaustion, and recovery has applications not only in the field of athletic training and performance but also in the fields of medicine and health monitoring [15], [27], [28].

With an exertion-recovery model based on the CP concept, an energy management system can be designed that will regulate the expenditure and recovery of Y . The optimization objectives would be minimizing time and maximizing distance by maximizing power output with the help of an exertion-recovery model. For example, in cycling races, 3-4 cyclists form pelotons to reduce drag. It has been shown that the cyclists in the middle of a peloton experience up to 40% less drag [110]. A potentially successful race strategy for

the peloton group can be derived from the exertion-recovery model using CPs and Ys of the individual riders. A similar drafting strategy was employed by Eliud Kipchoge in the INEOS 1:59 challenge where he completed a full marathon in 1 hour 59 minutes and 40.2 seconds. Another application is an energy management system for foot missions of soldiers. Time to exhaustion in long foot missions, where soldiers carry all the load from ammunition, food, and water can be accurately estimated with an exertion-recovery model. Additionally, in team sports like football, rowing, lacrosse, and soccer, CP and Y could be used in team selection, determining team strategies, planning individual training needs, and training interventions [111]. Furthermore, the combined model can be used to link Y-balance to performance quality, and to estimate injury-risk. Together with wearable sensors, the model could potentially be used to determine team strategies in terms of player substitutions and avoiding fatigue-related injuries, and for real-time performance optimization. The rise in popularity of wearable sensors has resulted in their use in health monitoring [112] and physical activity tracking [112], [113] and provides opportunities to mitigate dependence on laboratory equipment. Therefore, models of human performance can be tested and validated outside the laboratory.

2.4. Research opportunities in modeling human performance

The research opportunities identified in this chapter are cross-functional encompassing the areas of human performance, exercise physiology, health, and engineering. Though the themes belong to different backgrounds, they are not independent of each other. Table 2-3 summarizes the theme-wise research opportunities and applications that have been identified in this chapter.

Developing mathematical models of fatigue will not only aid athletes, but also defense personnel in mission planning and healthcare professionals who study the effect of physical exertion on overall health. The ability to quantify the day-to-day variability aids the measurement of training effectiveness and training prescription. Furthermore, the theory of expenditure of Y is explained well by the 2-parameter model. However, a robust model for recovery of Y is yet to be proposed.

Table 2-3. Research opportunities and applications of human performance modeling.

Themes	Research opportunities and applications
Groups versus individuals	Models derived from the data pertaining to a group of individuals may not accurately model performance of athletes outside the group, thus, suggesting a need for individual specific models [101].
Influence of mathematical modeling on Y	Understanding of Y is still ambiguous as it is model dependednt [48], [69]–[71], [73]–[75]. Quantifying the natural day-to-day/trial-to-trial variability within subjects, i.e. IIV, may yield a better understanding of Y .
Natural variability within an individual	Methods need to be developed to quantify the IIV associated with physiological parameters, which will be useful in measuring training effectiveness, developing higher fidelity models, and optimizing performance.

Table 2-3 (continued). Research opportunities and applications of human performance modeling.

Themes	Research opportunities and applications
Recovery of Υ	Current models described in [97]–[102] need improvement. The Υ -balance can potentially be correlated to fatigue related injuries and the risk of injury could be estimated.
Performance optimization	The recovery model in conjunction with the 2-parameter model enables optimization of time-trial performance as illustrated in [105], [106], [109], [114].
Wearable sensor integration	Wearable sensors provide opportunities in real-time performance tracking, optimization, and mitigate the reliance on laboratory equipment. Similar to studies in [115], [116], commercially available sensors could be validated against laboratory equipment and used in-situ for developing higher fidelity models.
Individual and team performance	Athlete-specific models could be used in determining team strategies, training interventions, planning training needs, and team selection as illustrated in [105], [111].
Physical exertion and health	Models of human performance could be used to gain insight into the effect of physical exertion on overall health and well-being as discussed in [27], [28].

2.5. Key conclusions and research objectives

The 2-parameter CP concept reliably estimates fatigue due to severe intensity exercise in the range of 2 minutes to 1 hour and is also suitable to model sprint performances of appropriate durations. Alternate models predict the power and time relationship in the severe intensity domain with better accuracy, but these models require the determination of more parameters, thereby, increasing complexity. CP and \dot{V} can be estimated using multiple models and protocols with the 3MT being the least time-consuming method. The 3MT, despite its advantages, has a limitation of not capturing the IIV associated with CP and \dot{V} estimates. Standard errors associated with the estimates from the power-time regression of CWR tests could help in better quantifying this variability. However, they only give a measure of goodness of fit and do not capture the IIV. None of the models available accommodate the IIV associated with the parameter estimates, regardless of the method of estimation used. Thus, the following are the key areas identified in this chapter:

- Mathematical models of human energy expenditure and recovery present opportunities in quantifying, evaluating, and optimizing performance.
- Established models are focused on energy expenditure and the available models that focus on recovery need refinement to be used in real-time performance optimization.
- Existing models derived from group data neglect the intra-individual variability (IIV) which is critical in evaluating improvements and optimizing performance at the individual level.

Until methods to capture IIV are proposed and validated, subject-specific training prescription and subsequent performance optimization will be limited in precision and

accuracy. Additionally, models derived from group data do not represent the population as several factors and variables have a bearing on human performance. Individualized athlete-specific models need to be derived to potentially improve performance through training prescriptions. The CP concept, owing to its simplicity, is promising and robust in terms of modeling fatigue in the severe intensity domain. However, it is incomplete due to the lack of proper understanding of the recovery behavior of $\dot{V}O_2$ in the moderate and heavy intensity domains. Attempts have been made to address this gap, but with limited success. The models available provide a good starting point to develop higher accuracy models with fewer assumed parameters. A combined exertion-recovery model will lead to optimized performance realized through an energy management control system. The combined model could lead to a straightforward way of assessing fatigue, risk of injury, and have implications with respect to the influence of exercise on overall health. Thus, the following research objectives were formulated to address the key gaps identified from the literature review with the overall goal of developing an energy management system to help in optimizing cycling performance.

Research objective 1: Establish a method to quantify the individual variability of CP and $\dot{V}O_2$ as determined by the 3MT.

Research objective 2: Develop a testing protocol to understand expenditure and recovery of power and $\dot{V}O_2$.

Research objective 3: Establish recovery profiles in terms of recovery power and recovery duration.

Research objective 4: Combine recovery with established expenditure for energy management.

The next chapter describes the method proposed to quantify the individual variability of CP and \dot{V} as determined from the 3MT.

CHAPTER THREE: REPEATABILITY AND VARIABILITY OF THE 3MT AT THE SUBJECT LEVEL²

The purpose of this chapter is:

- *To investigate the repeatability of the 3MT at the subject level.*
- *To propose a new method to compare a pair of 3MTs at the subject level.*
- *To propose a minimum number of 3MTs to arrive at the intra-individual variability (IIV) of CP and Y.*

3.1. Background

Performance in any endurance activity depends on the ability to sustain the highest possible work-intensity for extended time periods [117]. The critical power concept presents opportunities in planning training prescriptions aimed at performance improvement [118] as certain training interventions have shown to increase CP [119] and $\dot{V}O_{2max}$ [117], [120]. However, the natural variability of CP and $\dot{V}O_{2max}$ for an athlete will have a bearing on the effectiveness of such training prescriptions and has received little attention in literature. None of the existing studies pay attention to subject level analysis and are focused on group level analysis.

CP and $\dot{V}O_{2max}$ are shown to be variable between trials at the subject level by Triska and colleagues [93] (can be seen in the supplementary document available with [93]). Hickey

² The work presented in this chapter stems from the following paper that is under review:

Sreedhara, V. S. M., Mocko, G. M., & Hutchison, R. E. "Repeatability and variability of the 3-minute all-out test at the subject level". Under review in SSEJ (submitted in March 2020).

and colleagues [121] and Kuiper and colleagues [92] have illustrated the variability associated with time-to-exhaustion in CWR tests, which in turn results in a variability for CP and \dot{V} . It is not possible to determine the intra-individual variability (IIV), of CP and \dot{V} with one test at each work-rate (See Figure 2-5). If this variability is not accounted for, then training prescriptions designed at eliciting improvements in CP and \dot{V} may result in false positives or negatives.

Instead of repeating the CWR tests multiple times at each power level, the 3-minute all-out test (3MT) [78] can be repeated a few times as it has been shown to reliably estimate CP and \dot{V} in one test. The repeatability of the 3MT has been assessed using Intraclass Correlation Coefficient (ICC), Typical Error (TE), and Coefficient of Variation (CV) using data from two trials [74], [83]. Hickey and colleagues [121] report average subject level CVs for repeated trials of isokinetic cycling. These average subject level CVs give an idea of the IIV, but they are generally not reported for CP and \dot{V} . Furthermore, the 3MT has not been repeated more than two times and similar to the CWR studies, the subject level CVs are not reported either.

While the repeatability metrics (ICC, TE, and CV) indicate whether a test is repeatable at the group level, they do not estimate the repeatability or the trial-to-trial variability at the subject level. Estimating IIV and establishing a 95% confidence interval (CI) is critical in modeling performance, planning training interventions aimed at improving CP and \dot{V} , and subsequent performance optimization. Furthermore, these CIs will aid in measuring the effectiveness of training prescriptions at the subject level.

The standard deviation of CP (SD_{CP}) can be determined using the power data of the last 30 seconds of the 3MT (i.e. the standard deviation of the power output of the last 30 seconds of the test). Subsequently, using SD_{CP} , an SD and a CI can be determined for \dot{V} by applying SD_{CP} across the power output of the entire 3MT. However, this CI may not be a valid estimation of the variation in an individual's \dot{V} . Weir [122] suggests the construction of 95% CIs for measured parameters and minimal detectable differences using ICC and TE. However, this approach is catered to estimate the variability associated with the measurement errors and is not helpful determining the IIV. Thus, there exists an opportunity to develop methods to estimate the repeatability of the 3MT at the subject levels and arrive at an IIV for CP and \dot{V} . Therefore, the goal of this study is to investigate the repeatability of the 3MT (both at group and subject levels) and arrive at an IIV for each subject's CP and \dot{V} . At the group level, it is hypothesized that the CP and \dot{V} as determined from the 3MT are consistent across all trials. To assess the repeatability of the 3MT at the subject level, we propose a new method to compare two tests using the peak power (P_p), the time to P_p (T_{P_p}), and the total work done (TW) during the test. P_p and TW are used as they demonstrate that the subject is performing maximally in the early phases of the test and the subject's willingness to maintain the maximal effort throughout the test. Once the repeatability is determined, the IIV is computed as the 95% CI using the standard error from the repeated trials.

3.2. Estimating the repeatability and IIV

In repeatability studies, ideally, the test must be repeated several times with the same subject, equipment, and operator, but in practice several subjects repeat the test a few times

[123]. The repeatability is assessed by computing ICC, TE, and CV. These metrics, while useful in validating the repeatability of a method, fail in comparing two 3MTs at the subject level or computing the IIV as the data are averaged for all subjects. To address this limitation, we propose to compare two 3MTs by computing the absolute difference, δ (expressed in %) as,

$$\delta = \frac{|Prm_i - Prm_j|}{(Prm_i + Prm_j) / 2} \times 100 \quad (13)$$

where, Prm_i and Prm_j are parameters (CP, Υ , Pp, and TW) from trials i and j respectively with $i, j = 1, 2, 3, 4$. The denominator of Equation 13 is the average of the parameters from trials i and j . The absolute difference as computed from Equation 13 is similar to the bias computed in the Bland-Altman analysis. However, any two trials at the subject level can be compared using δ .

The following procedure can be used to compare two 3MTs and arriving at an IIV for CP and Υ .

Step 1: Check if T_{Pp} in both the tests has occurred within the first 10 seconds [78], [86].

Step 2: Compute δ for Peak Power (Pp) and Total work (TW) to ensure repeatability of the trials.

Step 3: Compute CP and Υ for both, average them and arrive at mean \pm SE and establish 95% CI for CP and Υ as,

$$95\% CI = \overline{Prm} \pm t_{0.025, (n-1)} \cdot \frac{S}{\sqrt{n}} \quad (14)$$

where, \overline{Prm} is the average of the parameter from all the trials, t is the t-distribution value from t-tables, S is the standard deviation of the parameter, and n is the number of trials. Equation 14 gives the uncertainty associated with CP or \dot{V} at the individual level, which is the IIV estimated using the data from repeated trials. Specific cut-off values for T_{PP} , δ_{PP} , and δ_{TW} are presented in Sections 3.4 and 3.5.

The following sections discuss the experimental study conducted to validate the method of estimating repeatability and variability of CP and \dot{V} at the subject level and its results.

3.3. Experimental Procedures and Analyses

3.3.1. Subjects

Seven competitive amateur cyclists (4 males, 3 females, Age: 42 ± 10 years, Weight: 76 ± 14 kg, Height: 1.78 ± 0.08 m) participated in the study. The subjects were recruited using a survey on their activity levels. All subjects trained 3-5 days a week and their training load was in the range of 100-200 km/week. The study was approved by the university's institutional review board and signed consent forms were obtained from each subject.

3.3.2. Procedures

The subjects were given instructions to bring their own bicycle as well as their clip-in shoes on each testing day. The bicycle was mounted onto Racermate CompuTrainer and secured using the rear axle. The trainer was calibrated per the manufacturer's guidelines. The use of CompuTrainer to conduct the 3MT has been validated by Clark and colleagues [124]. During all tests, heart rate and muscle oxygenation data were collected using Garmin chest-

strap heartrate monitor and MOXY monitor respectively. Subjects were not allowed to change gears during the tests. A gear inch range of 52-57 inches was chosen to account for different gear combinations on subjects' bicycles. Perfpro-Studio software was used to program the protocols on the trainer. Only the cadence was shown to the subjects during the tests. The subjects visited the laboratory five times with at least 24 hours between each visit. On the first visit, an incremental ramp test was conducted using COSMED Quark CPET apparatus to determine the subject's $\dot{V}O_{2peak}$ and Gas exchange threshold (GET), and a 3min all-out familiarization test was conducted. On each subsequent visit, the subjects performed a 3MT at the same time of the day (± 2 hours). The room temperature in the laboratory was 19-22°C. Subjects were instructed not to do any strenuous physical activity for at least 24 hours prior to each test. Additionally, the subjects were instructed to avoid alcohol consumption for at least 24 hours prior to the test, avoid consuming caffeinated drink for at least 3 hours before the test, and consume a carbohydrate rich meal at least 90 minutes before the test.

3.3.3. Incremental ramp test

The warmup for the ramp test involved pedaling at 100W and 80rpm for 5 minutes, followed by a 5-minute passive interval, followed by 3 minutes of unloaded pedaling at 80rpm. After the unloaded interval, the ramp interval started at 100W with an increase of $0.5 \text{ W}\cdot\text{s}^{-1}$ ($30 \text{ W}\cdot\text{min}^{-1}$). The subjects were instructed to maintain 80rpm until termination of the test, which was determined by a drop of 5rpm in the subject's cadence for more than 10 seconds [83]. Strong verbal encouragement was given to the subjects by repeatedly

instructing them to hold 80rpm. A schematic representation of the test is shown in Figure 3-1.

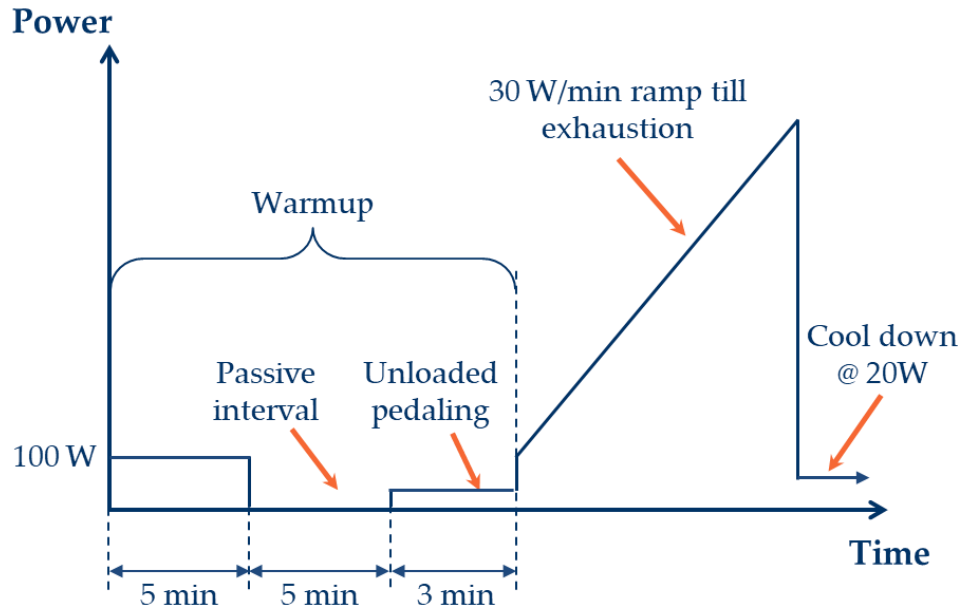


Figure 3-1. Schematic representation of the incremental ramp test protocol.

Data from the ramp test were saved at 10-second intervals to determine $\dot{V}O_{2max}$ and GET [78], [125]. GET is defined as the point at which CO_2 expiration increases relative to O_2 consumption [126]. The GET was determined using the v-slope method [125] and $\dot{V}O_{2peak}$ was calculated as the highest 30-second average $\dot{V}O_2$ during the ramp test [78]. The maximum power during the ramp test (P_{mx}) and the power at GET (P_{GET}) were noted from the power data file. P_{mx} and P_{GET} were used to determine a gradient for the 3MT on the CompuTrainer, thus resulting in end power halfway between P_{mx} and P_{GET} at approximately 80rpm.

3.3.4. 3min all out test

The 3MT was conducted as described by Vanhatalo and colleagues [78] on a CompuTrainer instead of a cycle ergometer. The warmup for the 3MT was identical to that of the ramp test. However, in the last 5 seconds of the unloaded interval, the subjects were instructed to increase their cadence to at least a 110rpm. The 3-minute all-out effort immediately followed the unloaded pedaling interval. The subjects were given strong verbal encouragement throughout the 3-minute all-out interval and were constantly instructed to keep their cadence as high as possible. The verbal encouragement was standardized. For each 3MT, CP was calculated as the average power of last 30 seconds and \dot{V} was calculated by numerical integration of power values above CP, and total work (TW) was calculated by numerical integration of power values over the entire duration of the test. A schematic representation of the test protocol is shown in Figure 3-2.

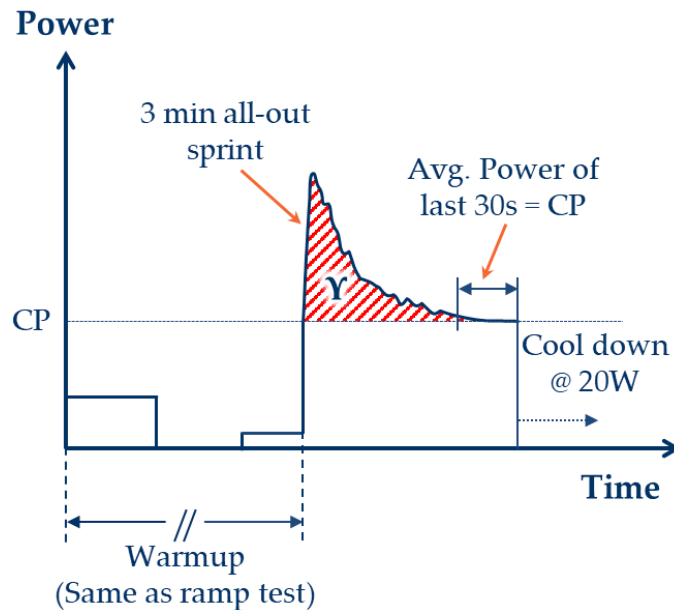


Figure 3-2. Schematic representation of the 3-minute all-out test protocol.

3.3.5. Statistical Analyses

A one-way repeated-measures ANOVA was conducted to determine if CP, γ , TW, and Pp differed across the four trials. The repeatability of the test (all trials together) was evaluated using ICC, TE, and CV [123]. The TEs were calculated as the square-root of the mean square error term from the ANOVA table and their 95% confidence intervals (95% CI) were calculated using the inverse Chi-squared distribution tables [123]. The CVs and their 95% CIs were calculated as TE/mean of all four trials [123]. ICCs, TEs, and CVs were also computed for consecutive pairs of trials (i.e. T2-T1, T3-T2, and T4-T3). Shapiro-Wilk and Mauchly's tests were used to test the assumptions of the repeated-measures ANOVA (normality and sphericity) before analyzing the data. Greenhouse-Geisser correction was used to account for violation of the sphericity assumption. Bonferroni post-hoc test was conducted wherever appropriate. To check for learning/fatiguing effects across the four

trials, a one-way ANOVA was conducted on the biases of consecutive trials determined from Bland-Altman analysis. Standard error of measurement (SEM) and 95% limits of agreement (LOA) were also computed for the Bland-Altman analysis [123]. The data are represented as mean \pm SD and a level of significance of 0.05 was chosen for statistical analysis. The analyses were conducted in SPSS Statistics 25 (IBM Corp., Armonk, NY).

3.4. Results

A summary of $\dot{V}O_{2max}$, $\dot{V}O_{2peak}$, GET, P_{mx} , and P_{GET} for all subjects are reported in Table 3-1. At the group level, the average relative $\dot{V}O_{2max}$ was $51.8 \pm 6.49 \text{ mL}\cdot\text{kg}^{-1}\cdot\text{min}^{-1}$, the average relative GET was $34.83 \pm 4.39 \text{ mL}\cdot\text{kg}^{-1}\cdot\text{min}^{-1}$, and the average relative $\dot{V}O_{2peak}$ was $50.37 \pm 6.49 \text{ mL}\cdot\text{kg}^{-1}\cdot\text{min}^{-1}$.

Table 3-1. Summary of parameters from the ramp test: $\dot{V}O_{2max}$, GET, and $\dot{V}O_{2peak}$ for all subjects.

Subject	$\dot{V}O_{2max}$ ($\text{L}\cdot\text{min}^{-1}$)	GET ($\text{L}\cdot\text{min}^{-1}$)	$\dot{V}O_{2peak}$ ($\text{L}\cdot\text{min}^{-1}$)	P_{mx} (W)	P_{GET} (W)
1	4.76	3.05	4.48	425	255
2	2.87	2.01	2.85	270	190
3	4.51	3.03	4.33	360	235
4	4.01	2.84	3.90	316	224
5	3.96	2.59	3.82	409	236
6	2.88	2.05	2.86	275	156
7	4.60	2.87	4.53	445	215
Mean \pm SD	3.94 ± 0.78	2.64 ± 0.44	3.82 ± 0.71	357 ± 72	216 ± 33

The parameters CP, Υ , Pp, and TW for all subjects across all trials are reported in Table 3-2. The average CP of the four trials was 0.99Δ (Δ = halfway between P_{mx} and P_{GET}) with 131% of P_{GET} and 80% of P_{mx} . The peak power output, Pp, was seen within the first 7 seconds of the test ($3.82 \pm 1.12\text{s}$) for all subjects.

Table 3-2. Summary of the parameters from the four trials of the 3MT for all subjects.

Subject	Parameter	T1	T2	T3	T4	Mean \pm SD
1	CP (W)	335	334	327	343	335 ± 7
	Υ (kJ)	14.15	15.81	16.09	14.32	15.09 ± 1.00
	Pp (W)	978	1068	1059	1068	1043 ± 44
	TW (kJ)	74.14	75.68	74.64	75.91	75.09 ± 0.84
2	CP (W)	211	215	220	224	217 ± 6
	Υ (kJ)	6.04	5.33	5.02	6.19	5.65 ± 0.56
	Pp (W)	449	440	416	448	438 ± 15
	TW (kJ)	43.25	42.99	43.77	45.76	43.94 ± 1.26
3	CP (W)	330	359	359	354	351 ± 14
	Υ (kJ)	12.11	7.77	8.65	9.68	9.55 ± 1.87
	Pp (W)	786	730	803	869	797 ± 57
	TW (kJ)	71.27	71.61	72.88	72.92	72.17 ± 0.85
4	CP (W)	246	237	245	242	242 ± 4
	Υ (kJ)	8.18	8.09	7.56	7.52	7.84 ± 0.34
	Pp (W)	555	508	569	562	549 ± 28
	TW (kJ)	51.92	50.40	51.07	50.62	51.00 ± 0.67
5	CP (W)	319	319	333	337	327 ± 9
	Υ (kJ)	12.19	12.79	10.74	10.57	11.58 ± 1.09
	Pp (W)	718	809	815	802	786 ± 46
	TW (kJ)	69.29	69.99	70.11	70.73	70.03 ± 0.59
6	CP (W)	195	217	212	200	206 ± 10
	Υ (kJ)	10.82	8.27	8.08	9.38	9.14 ± 1.26
	Pp (W)	405	396	457	426	421 ± 27
	TW (kJ)	45.80	47.30	46.06	45.28	46.11 ± 0.86

Table 3-2 (continued). Summary of the parameters from the four trials of the 3MT for all subjects.

Subject	Parameter	T1	T2	T3	T4	Mean \pm SD
7	CP (W)	295	305	319	327	311 \pm 14
	Y (kJ)	12.75	14.41	11.88	11.58	12.65 \pm 1.27
	Pp (W)	785	898	838	829	838 \pm 47
	TW (kJ)	65.44	69.01	68.74	70.08	68.32 \pm 2.00
Group Mean \pm SD	CP (W)	276 \pm 58	284 \pm 60	288 \pm 60	290 \pm 65	
	Y (kJ)	10.89 \pm 2.83	10.35 \pm 3.95	9.72 \pm 3.58	9.89 \pm 2.66	
	Pp (W)	668 \pm 207	693 \pm 253	708 \pm 234	715 \pm 241	
	TW (kJ)	60.16 \pm 12.85	61 \pm 13.52	61.04 \pm 13.47	61.61 \pm 13.7	

The ICCs, TEs, and CVs for consecutive pairs of trials are shown in Table 3-3. The results from Bland-Altman plots for consecutive pairs for CP, Y, Pp, and TW are shown in Figure 3-3. The biases, SEMs, and LOAs across the three combinations of trials (T2-T1, T3-T2, and T4-T3) are reported in Table 3-4.

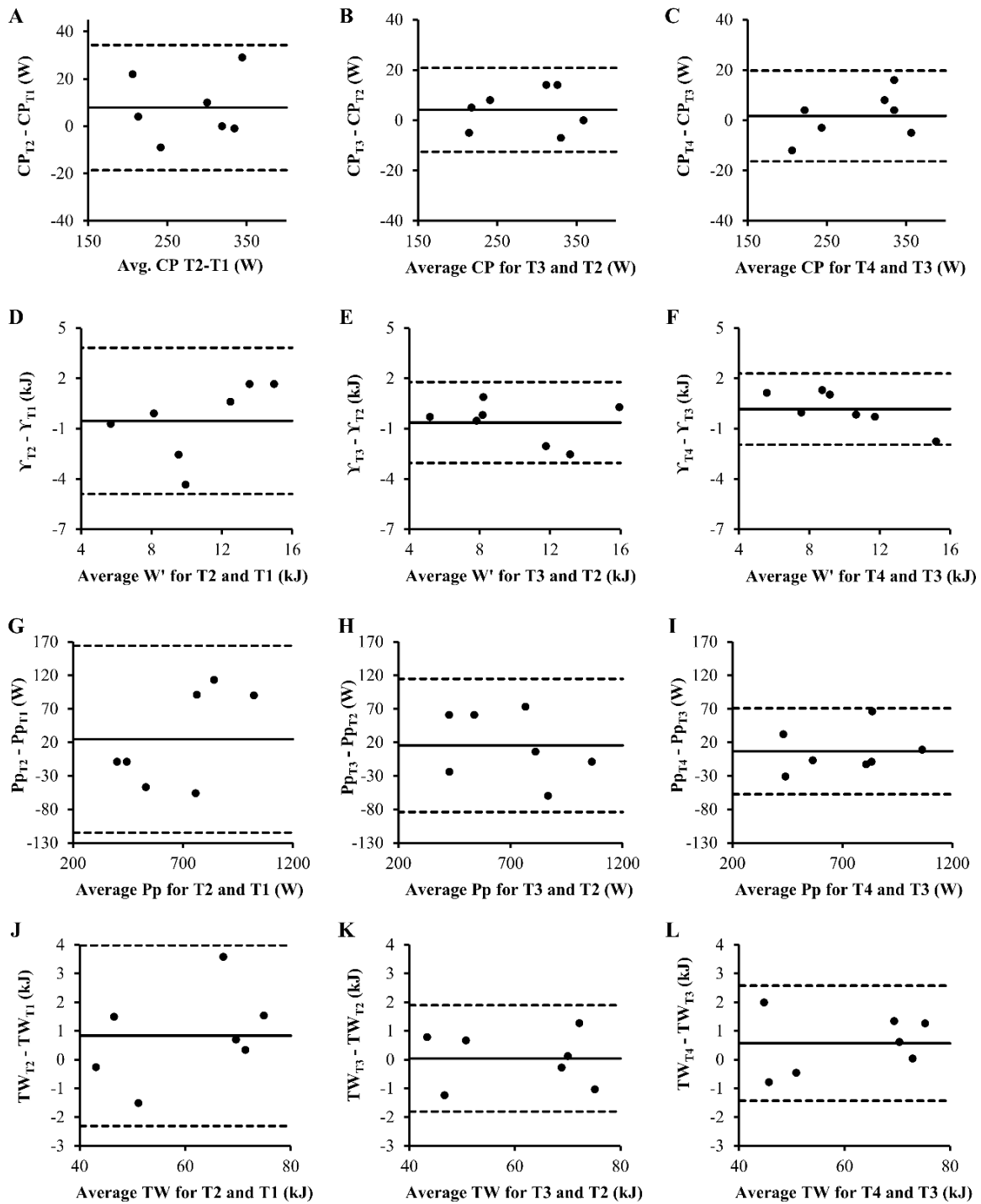


Figure 3-3. Bland-Altman plots for consecutive trials. Panel A, B, C: Plots for CP, panels D, E, F: Plots for γ , panels G, H, I: Plots for Pp, and panels J, K, L: Plots for TW.

Table 3-3. ICCs, TEs, CVs, and their 95% CIs for consecutive pairs of trials in parentheses.

Parameter	T2-T1			T3-T2			T4-T3		
	ICC	TE	CV (%)	ICC	TE	CV (%)	ICC	TE	CV (%)
CP	0.969	10W (7, 14)	3.41	0.989	6W (5, 9)	2.11	0.99	7W (5, 10)	2.26
	(0.834,		(2.57,	(0.943,		(1.59,	(0.948,		(1.71,
	0.995)		5.04)	0.998)		3.12)	0.998)		3.34)
Y	0.804	1.574kJ	14.82	0.941	0.87kJ	8.66	0.948	0.767kJ	7.82
	(0.244,	(1.189,	(11.2,	(0.721,	(0.657,	(6.55,	(0.736,	(0.579,	(5.91,
	0.963)	2.328)	21.91)	0.989)	1.286)	12.81)	0.991)	1.134)	11.57)
Pp	0.954	50W (38, 74)	7.40	0.979	36W (27, 53)	5.11	0.991	23W (17, 34)	3.25
	(0.782,		(5.59,	(0.898,		(3.86,	(0.954,		(2.11,
	0.992)		10.94)	0.996)		7.56)	0.999)		4.80)
TW	0.992	1.134kJ	1.87	0.998 (0.988, 1)	0.668kJ	1.09	0.997	0.722kJ	1.18
	(0.956,	(0.857,	(1.41,		(0.505,	(0.83,	(0.981,	(0.546,	(0.89,
	0.999)	1.677)	2.77)		0.988)	1.62)	0.999)	1.068)	1.74)

Table 3-4. Results from Bland-Altman analysis on all parameters from consecutive pairs of trials.

Parameter	T2-T1			T3-T2			T4-T3		
	SEM	Bias	95% LOA	SEM	Bias	95% LOA	SEM	Bias	95% LOA
CP (W)	10	8	-19, 34	6	4	-13, 21	7	2	-16, 20
Y (kJ)	1.574	-0.539	-4.903, 3.824	0.870	-0.634	-3.045, 1.776	0.767	0.169	-1.956, 2.294
Pp (W)	50	25	-115, 164	36	15	-84, 115	23	7	-57, 71
TW (kJ)	1.134	0.838	-2.306, 3.982	0.668	0.043	-1.808, 1.894	0.722	0.572	-1.429, 2.574

The one-way repeated-measures ANOVA showed that there was not a significant difference between Υ , Pp, and TW across the four trials (see Table 3-5). The trial to trial differences in CP at group level is illustrated by the p-value ($p = 0.03$) of the one-way repeated measures ANOVA even though the ICCs showed strong agreement. However, the average CP across all trials did not show significant differences on the post-hoc Bonferroni test. The possibility of training effects was minimized by having the familiarization trial [121] and all the tests being completed within 10 days of the first visit. The normality assumption was verified using the Shapiro-Wilk test and the resulting p-values were ≥ 0.05 (except for Trial 4 of TW where the p-value was 0.049). The ANOVA is generally robust to minor violations of the normality assumption, but may lead to false positives [127]. The normality violation did not result in a false positive as the p-value for TW was 0.125 (>0.05). The ICCs, the TEs, the CVs, their 95% CI, and the average absolute difference between all trials for all subjects (δ_g) computed for the four trials are presented in Table 3-5. The strongest agreement was seen in TW followed by CP, Pp, and Υ , which was also seen in δ_g . Furthermore, in 5 out of 7 subjects, when the difference in TW between any two trials was less than 2.5%, CP and Υ showed an inverse relationship with an increase in CP resulting in a decrease in Υ and a decrease in CP resulting in an increase in Υ .

Table 3-5. One-way repeated measures, ICCs, TEs, CVs, their 95%CI, and δ_g for CP, Υ , Pp, and TW for the four trials.

Parameter	p-value and partial- $\eta^{2\#}$	ICC(A,1)	TE	CV	δ_g
CP	0.030* (0.384)	0.974 (0.914, 0.995)	8W (6, 12)	2.94% (2.22, 4.35)	4.06%
Υ	0.253 (0.208)	0.879 (0.685, 0.975)	1.11kJ (0.838, 1.641)	10.87% (8.21, 16.07)	12.83%
Pp	0.155 (0.271)	0.971 (0.912, 0.994)	37W (28, 54)	5.29% (4, 7.83)	6.42%
TW	0.125 (0.293)	0.993 (0.978, 0.999)	1.004kJ (0.759, 1.485)	1.65% (1.24, 2.44)	2.09%

[#]Values are from a one-way repeated measures ANOVA. *The post-hoc Bonferroni test did not show any significant differences between the trials with p-values of 0.31 and 0.15 for trial1-trial 3 and trial1-trial4 combinations respectively.

3.5. Discussion

This study determined the subject-level repeatability of the 3MT and computed the IIV of CP and Υ from the four trials. Based on the results, thresholds for TPp (7 seconds), δPp (10%), and δTW (3%) are proposed to determine subject-level repeatability between any two 3MTs (reasons for these thresholds are discussed later). Subsequently, the IIV is

estimated using the 95%CI from repeated trials. Additionally, the similarity of ICC, TE, and CV of the consecutive trials suggest that the parameters become steady between trials T2 and T4.

The Bland-Altman plots (Figure 3-3) show a decreasing trend across the trials. However, the one-way ANOVA on its biases did not show any learning/fatiguing effects as the SEMs were greater than the biases (Table 3-4), indicating subject-level variability. Furthermore, as observed in Table 3-3, the similarity of ICC, TE, and CV for trial pairs T3-T2 and T4-T3 (except Pp) shows the parameters stabilizing from T2 to T4 suggesting that three trials may be sufficient in obtaining consistent estimates from the 3MT. The advantage of repeating the 3MT thrice versus twice [74], [83] is the extra data point to compute the IIV. Establishing a 95%CI using t-tables for three trials outweighs the additional time investment to better estimate the IIV ($t_{0.025,1} = 12.706$ versus $t_{0.025,2} = 4.303$).

The group-level reliability statistics for CP (ICC = 0.974, TE = 8W, and CV = 2.94%) were stronger than those reported by Johnson and colleagues [74] (ICC = 0.93, TE = 15W, and CV = 6.7%) and similar to Burnley and colleagues [83] (ICC = 0.99, TE = 7W, CV = 3%). With respect to Υ , the ICC and TE (0.878, 1.11kJ) were similar to Johnson and colleagues [74] (0.87, 1.456kJ) while the CV was stronger (10.87% versus 20.7%). A stronger reliability was seen in CP as opposed to, which is echoed in other studies [71], [74]. Furthermore, stronger reliability statistics were observed in Pp (ICC = 0.971, TE = 37W, and CV = 5.29%) and TW (ICC = 0.993, TE = 1.004kJ, and CV = 1.65%) compared to Υ . These metrics indicate that the 3MT produces consistent responses at group-level, but they are not useful to assess subject-level repeatability. This is illustrated in Subject 7's data

where TW and from T2, T3, and T4 were 5.47%, 5.05%, and 7.09% more than T1 respectively. Similarly, CP from T2, T3, and T4 were 3.58%, 8.26%, and 10.94% more than T1 respectively. Furthermore, the SD of any parameter across all trials and all subjects (i.e. Global Mean \pm SD) is limited in estimating the individual variability. For example, the global mean and SD for CP across all trials is 284 \pm 58 W, while the mean and SD for Subject 1 is 335 \pm 7 W. The SD of CP for the individual subjects ranges from 7% to 25% of the global SD. This is also illustrated in Figure 3-4, where the PDF for Subject 3's and Subject 6's CP are overlaid on that of the group highlighting the overestimation of IIV by group SD. Additionally, the trial-to-trial differences in CP and \dot{V} at the subject level get distributed when they are averaged at group level resulting in similar means and SDs across the four trials.

Hickey and colleagues [121] report the average subject-level CV for time-to-exhaustion in the range of 0.95% to 2.43% illustrating the IIV. However, they did not determine CP and \dot{V} from their data and consequently those CV are unavailable. The average subject-level CVs from this study is compared to those calculated from Triska and colleagues [93] in Table 3-6 This comparison is made as there are no other studies which report CVs for CP and \dot{V} or share their data.

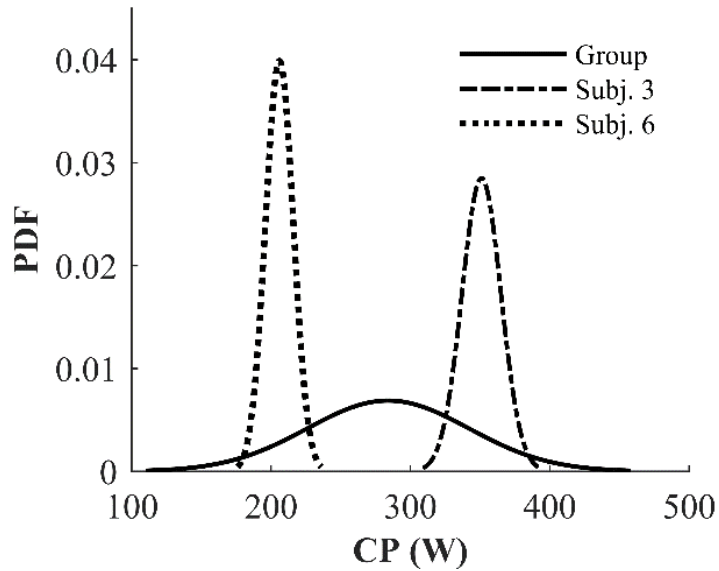


Figure 3-4. Group and subject level probability density functions (PDF) of CP plotted with $\pm 3SD$. Subjects 3 and 6 were shown as they had the highest and the lowest CP among the group respectively. Solid line shows the group PDF. Dash-dot line shows Subject 3's PDF, and dotted line shows Subject 6's PDF. The figure illustrates the overestimation of IIVs by the group level SDs.

Table 3-6. Comparison of average CV at the subject level for CP and Υ computed from Triska and colleagues [93].

Study	No. of subjects	Average CV at the subject level with its range in parentheses (%)	
		CP	Υ
		Triska and colleagues [93]	10
Current study	7	3.26 (1.76 to 4.97)	10.55 (4.40 to 19.63)

The subject level CVs from both studies are comparable for CP, while those for Υ are higher in the current study. This difference could be attributed to the difference in subject populations (well-trained male triathletes versus male and female competitive amateur cyclists), the number of trials (2 versus 4), and the differences between the Υ estimates

from CWR and 3MT protocols observed in previous studies [43], [70]. The subject level CVs have not been previously reported for 3MT. Studies either report the group averages or the average value of the two repeated trials for individual subjects. Moreover, even if the subject level CVs were available, the values cannot be extrapolated to other subjects regardless of the similarities in their level of training and caliber [121].

Therefore, at the subject level, the absolute difference between two tests, δ (from Equation 13), gives more information as it compares the parameter estimates between two trials. Additionally, the average absolute difference for all subjects across all trials, δ_g , for TW and Pp (2.09% and 6.43%) were less than the 12.83% of Υ . This reiterates the larger variability observed in Υ as compared to TW and Pp. Furthermore, in 5 subjects, δ for TW (δ_{TW}) across the four trials was less than 2.5%. Additionally, in all subjects, when δ_{TW} was small (~3%), there was an inverse relationship between CP and Υ . An increase in CP resulted in a decrease in Υ and vice-versa illustrating the IIV associated with these parameters. A similar inverse relationship has been observed previously by Black and colleagues [128] and Vanhatalo and colleagues [129]. Thus, at the subject level to quantify the IIV, the procedure described in the methods section is refined as follows:

Step 1: Check if T_{Pp} has occurred within the first 7 seconds for both tests.

Step 2: Compute δ_{Pp} and δ_{TW} for both tests. If $\delta_{Pp} \leq 10\%$ and $\delta_{TW} \leq 3\%$, then it must be concluded that the two tests being compared agree with each other.

Step 3: Compute the 95% CI for CP and Υ using Equation 14, which gives the IIV.

This procedure provides a comparison of two 3MTs at the subject level and computes the IIV for CP and Υ . The average IIV observed was 15 ± 6 W (range 7 to 23 W) for CP and

1.68±0.8 kJ (range 0.55 to 2.98 kJ) for Υ . The choices for T_{Pp} , δ_{Pp} , and δ_{TW} are based on the results from this study. The conservative choice of 10% for δ_{Pp} is due to the larger variability seen in overcoming the inertia of the flywheel in first 5-10 seconds of the 3MT. Vanhatalo and colleagues [78] also highlight this and suggest that flywheel inertia to be the reason for the discrepancy between Υ estimates from 3MT and CWR protocols. Furthermore, the average CP occurring at $0.8P_{max}$ was higher than $0.7P_{max}$ reported by Vanhatalo and colleagues [78]. The power of the repeated measures ANOVA of 34% (Υ), 47% (Pp), 52% (TW), and 71% (CP) could not be compared to studies by Burnley [83] and Johnson [74] as they do not report their power analysis and effect sizes. It is suggested that similar studies in the future should aim for a statistical power $\geq 80\%$.

In this study, the estimates from the 3MTs were not compared to those from the CWR protocol, which is considered to result in reliable estimates of CP and Υ [49]. The standard errors of estimation of CP and Υ from the CWR tests measure the goodness of fit and do not actually capture the IIV. To capture the IIV associated with CP and Υ , the CWR tests need to be repeated multiple times at each work-rate. This would yield an average Υ for each work-rate and an average CP from all possible model fits (See Figure 2-5). The repeatability of the 3MT can then be verified by comparing the values of CP and Υ averaged from multiple trials to the average of those estimated from the CWR tests repeated multiple times at each power level as shown in Figure 3-5.

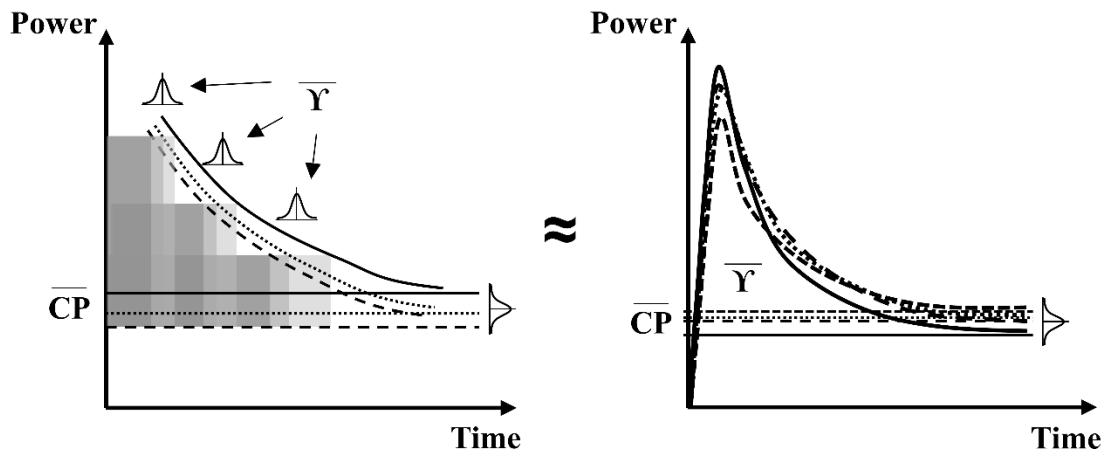


Figure 3-5. Comparison of average CP and \bar{Y} from CWR tests with multiple trials at each work-rate (total number of CWR tests ≥ 6 with at least two per work-rate) with those from multiple 3MT trials (total number of repeats ≥ 3).

The investigative study shown in Figure 3-5 would address the concerns pertaining to the reliability of estimates the 3MT presented in several publications [84]–[86]. Additionally, the behavior of IIV with respect to the power level can also be investigated. Depending on the athlete, the variation of \bar{Y} at different power levels above CP can be investigated. Moreover, developing a field version of the 3MT will be useful to determine a field-grade CP and \bar{Y} similar to the maximal time-trials used to determine CP and \bar{Y} [40]. Though the CP estimates from a 3MT have been shown to predict a 16.1 km time-trial performance [76], a 3-min all-out effort can potentially be carried out on an outdoor velodrome similar to the study by Karsten and colleagues [130], thereby testing its field-readiness and validity. It has been shown that a highly trained athlete’s variability of power within the 3MT is less than that of a recreational athlete [74]. However, further investigation is required to verify if the same can be said about the IIV associated with CP and \bar{Y} . Furthermore, understanding and quantifying IIV associated with CP and \bar{Y} from either the

CWR test protocol or the 3MT may aid in gaining a better understanding of Υ , which has been shown to be elusive in several publications [52], [71]–[73].

3.6. Key findings

The study presented in this chapter has illustrated a method to determine the subject-level repeatability of the 3MT and compute the IIV of CP and Υ . This is the first study to compute the subject-level variability of CP and Υ based on repeated trials. Multiple trials require additional time, but it is suggested that the 3MT be repeated at least three times to capture the IIV by establishing a 95% CI. Training plans should be designed to account for the natural variability of the individual athlete. It is proposed that the cut-offs for T_{Pp} (7 seconds), δ_{Pp} (10%), and δ_{TW} (3%) be used as guidelines to determine subject-level repeatability before computing the IIV for CP and Υ . Additionally, the investigative study involving the repeated CWR tests may help in understanding the underlying causes for the variability seen in Υ .

The next chapter describes the hypothesized behavior of the recovery of Υ , the experimental study to model the same, and discusses the results from the experiments.

CHAPTER FOUR: MODELING THE RECOVERY OF Y^3

The purpose of this chapter is:

- *To introduce the hypothesized model of Y recovery.*
- *To develop an exercise protocol to understand recovery of Y .*
- *To investigate the behavior of Y with respect to recovery powers and recovery durations.*
- *To present a case of performance optimization.*
- *To discuss the results from the experimental testing.*

4.1. Hypothesized behavior of recovery of Y

An intermittent cycling session refers to a series of cycling bouts comprising of exertion and recovery intervals. Figure 4-1 shows one such session comprising of a recovery interval (below CP) sandwiched between two exertion intervals (above CP). The subject would exert above CP at a power for a known amount of time, which will discharge a portion of his/her Y . Then the subject would go below CP and recover at a known power

³ The work presented in this chapter stems from the following four papers:

1. Sreedhara, V. S. M., Mocko, G. M., & Hutchison, R. E. (2018). "An Experimental Protocol to Model Recovery of Anaerobic Work Capacity". In: The Engineering of Sport (ISEA 2018), Brisbane, Australia, 26-29 March 2018. (Vol. 2, No. 6, p. 208).
2. Ashtiani, F., Sreedhara, V. S. M., Vahidi, A., Hutchison, R., & Mocko, G. (2019, July). Experimental Modeling of Cyclists Fatigue and Recovery Dynamics Enabling Optimal Pacing in A Time Trial. In 2019 American Control Conference (ACC) (pp. 5083-5088). IEEE.
3. Sreedhara, V. S. M., Ashtiani, F., Mocko, G. M., Vahidi, A., & Hutchison, R. E. Modeling the recovery of W' in the moderate to heavy exercise intensity domain. Under review in MSSE: Submitted in February 2020.
4. Ashtiani, F., Sreedhara, V. S. M., Mocko, G. M., Vahidi, A., & Hutchison, R. E. Optimal Pacing of a Cyclist in a Time Trial Based on Experimentally Calibrated Models of Fatigue and Recovery. In preparation: To be submitted in April 2020.

level (P_{rec}) for a known time duration (t_{rec}) and then go back above CP to exert at a constant power level till he/she is exhausted.

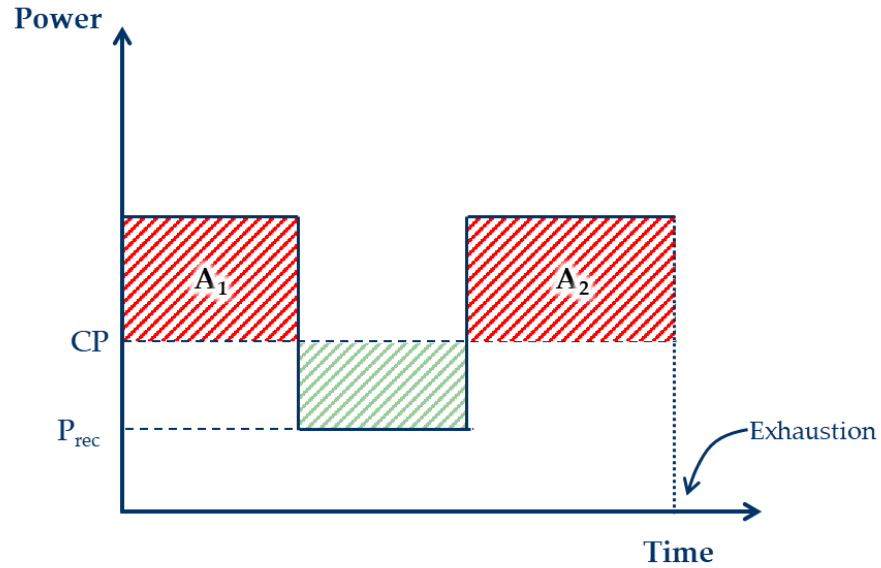


Figure 4-1. Example of an intermittent cycling session; A1 and A2 are areas of the two exertion intervals.

The recovery power is represented by the term β , which is given by

$$\beta = \frac{P_{rec}}{CP} \quad (15)$$

where, P_{rec} is the recovery power in Watts and CP is critical power in Watts. The areas A_1 and A_2 represent the amount of Υ expended in the two exertion intervals. Hence, the amount of Υ recovered (E_{rec}) during recovery is given by,

$$E_{rec} = A_1 + A_2 - \Upsilon \quad (16)$$

Normalizing E_{rec} with respect to Υ yields % Υ_{rec} given by,

$$\% \Upsilon_{rec} = \frac{E_{rec}}{\Upsilon} \quad (17)$$

The amount of Υ recovered is a function of both P_{rec} and t_{rec} . Figure 4-2 shows the hypothesized behavior of Υ recovered with respect to recovery powers and recovery durations. Figure 4-2 illustrates that as β tends to 0 all of Υ is recovered, while none is recovered when β is equal to CP. Figure 4-2(a) is similar to Skiba's τ_w versus D_{CP} curve in [97], however, instead of τ_w , % Υ recovered is plotted against recovery power. Figure 4-2(b) shows a trend similar to that seen by Ferguson and colleagues in [96].

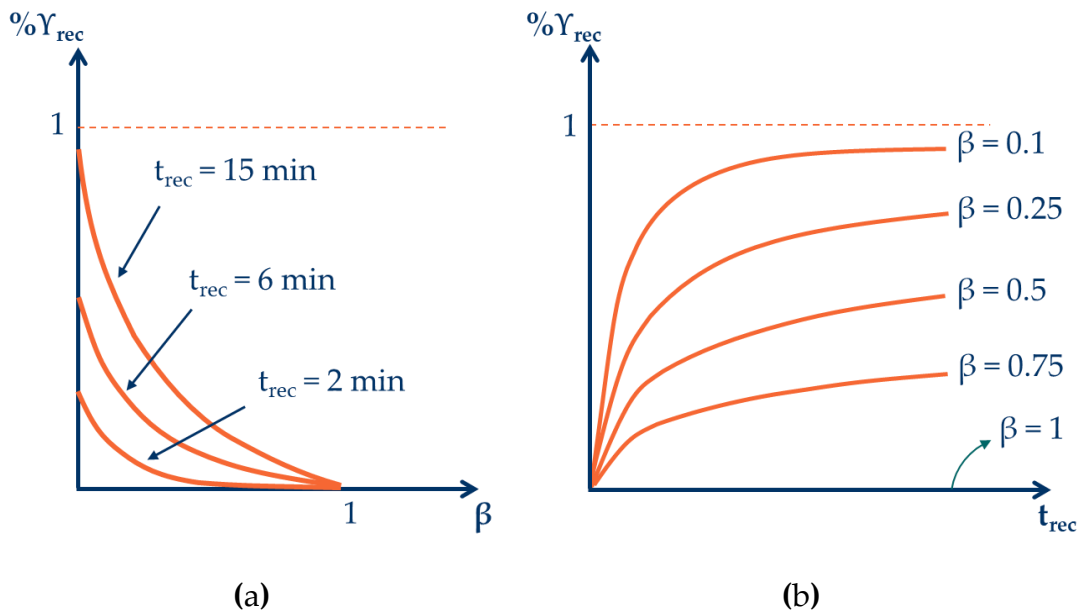


Figure 4-2. Hypothesized behavior of % Υ recovered, (a) as a function of recovery power (β) and (b) as a function of recovery duration t_{rec} .

The curves shown in Figure 4-2 need to be determined and it is hypothesized that the trends will be different for different individuals. Additionally, it is hypothesized that the recovery power β will have a greater influence on the amount of Υ recovered. To determine the behavior of recovery Υ in terms of recovery powers and durations, an experimental study was conducted which is discussed in the following sections.

4.2. Experimental Procedures and Analyses

4.2.1. Subjects

Seven recreational cyclists (4 males, 3 females, Age: 36 ± 11 years, Weight: 73 ± 14 kg, Height: 1.76 ± 0.08 m) volunteered to participate in the study and completed all the tests. The subjects were recruited using a survey on their activity levels. All subjects trained 3-5 days a week and their training load was in the range of 100-200 km/week. Each subject signed an informed consent approved by university's institutional review board. Each testing day was approximately 2 hours long.

4.2.2. Procedures

The instructions given to subjects were the same as those described in Section 3.3.2. The total duration to complete all tests was 4-7 weeks per subject. Each subject visited the laboratory fourteen to sixteen times. The first day consisted of a ramp test, and a 3min all-out familiarization test. In the next two or four visits (Subjects A and B were able to perform only two 3MTs, the rest performed four), subjects performed unfatigued 3MTs to determine their CP and $\dot{V}_{O_{2max}}$. The next visit involved the familiarization trial of the intermittent cycling test. In the next two visits, subjects repeated their first intermittent test. In the next eight visits, the remaining intermittent tests were conducted. The order of the intermittent cycling tests was randomized.

4.2.3. Incremental ramp test and the 3MTs

The incremental ramp test and the 3MTs procedures were the same as those described in Sections 3.3.3 and 3.3.4 respectively.

4.2.4. Intermittent cycling tests

The intermittent cycling test protocol shown in Figure 4-3 was developed based on the following assumptions:

- The 3 min all-out test accurately estimates CP and Υ [74], [78], [82].
- Exercise above CP results only in the expenditure of Υ , not its recovery [99].
- Exercise below CP results in recovery of Υ , thus increasing the Υ -balance [95]–[97], [99].
- The recovery of Υ is a function of the level of power below CP and the recovery duration [95]–[97].
- The power held during recovery interval is constant. The behavior of power versus time below CP is unknown, and hence the power below needs to be constant to mathematically model the recovery of Υ .

The warmup for the intermittent test protocol was same as that of the ramp test. The intermittent test protocol comprised of (i) a 2-minute exertion interval at CP₄, the power at which a subject would exhaust all of their Υ in 4 minutes (calculated using Equation 5, Chapter 2), (ii) a recovery interval at three recovery powers, P_{rec} [Low (L): 20 W, Medium (M): $0.9 \cdot P_{\text{GET}}$, and High (H): $P_{\text{GET}} + 0.5 \cdot (\text{CP} - P_{\text{GET}})$] and three recovery durations, t_{rec} (2, 6, and 15 minutes) to result in a full factorial design of 9 tests, and (iii) a 3-min all-out interval.

The exertion interval was designed to expend ~50% of the subjects $\dot{V}O_2$. For the recovery interval, the powers were chosen for comparison purposes to previously published studies by Skiba and colleagues [97] and Chidnok and colleagues [131], while the recovery durations were chosen from Ferguson and colleagues [96].

The subjects were instructed to maintain 80 rpm in the warmup, exertion, and recovery intervals. In the last 5 seconds of the recovery interval, the subjects were instructed to ramp up to at least 110 rpm. To ensure an all-out effort, the subjects were instructed to pedal as hard as possible in the 3-min all-out interval. Strong verbal encouragement was given throughout the test. A cool down at 20 W immediately followed the all-out interval.

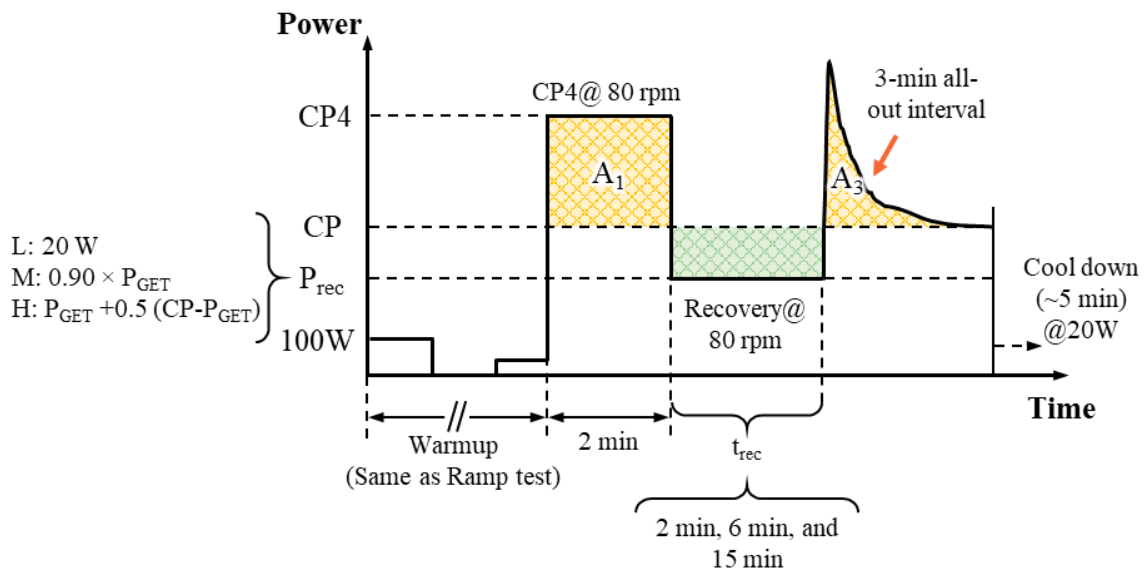


Figure 4-3. Schematic representation of the intermittent cycling test protocol.

The amount of $\dot{V}O_2$ expended in the CP4 and the 3-min all-out intervals, A_1 and A_3 , were calculated by numerical integration of power values above CP. The area of the recovery interval is larger than the amount of $\dot{V}O_2$ recovered. Hence, the amount of $\dot{V}O_2$ recovered in the recovery interval was expressed as a percentage of $\dot{V}O_2$ and was computed using the formula,

$$\% \Upsilon_{rec} = \frac{A_1 + A_3 - \Upsilon}{\Upsilon} \quad [18]$$

4.2.5. Optimization tests

One subject participated in the optimization tests. Optimization tests involved two tests: (i) a self-strategy test, and (ii) an optimal strategy test. The subject chose a course 18 km long, which was then simulated on the CompuTrainer. The warmup for both tests that lasted ~15 minutes (left to the discretion of the subject). On the first test, the subject was advised to employ their own strategy to complete the course as quickly as possible. The subject was shown the distance covered during the test. For the optimal strategy test, the entire distance of the course was discretized into 100-meter segments. Optimal power for each segment was determined using the subject's individual fatigue and recovery model as illustrated in our previous work in [114]. The subject was shown both the target power and their real time power during the test and was instructed to try and match the target power. The distance covered was not shown to the subject during optimal strategy test. The subject could change gears during the tests and strong verbal encouragement was provided for both the tests.

4.2.6. Statistical analysis

The repeatability was evaluated using Intraclass correlation coefficient (ICC), typical error (TE), and coefficient of variation (CV) [123], and their average values were used in analysis. CP, Υ , Pp, and TW from the 3MTs, and TW and Pp during the 3-min all out interval of the two repeated trials of the intermittent test were compared for repeatability.

A two-way repeated measures ANOVA was conducted to investigate the effects of P_{rec} and t_{rec} on $\% \dot{Y}_{\text{rec}}$. Subject 7 was not included in the repeated measures ANOVA as they recovered all the \dot{Y} expended in each of the 9 intermittent tests (refer to the Results section for detailed explanation). Post-hoc tests were conducted using the Bonferroni correction. To investigate the influence of the intermittent test on CP, fresh CPs from the four 3MTs (CP_{fr}) and fatigued CPs from the intermittent tests (CP_{fi}) were compared at both group and subject levels using independent sample t-tests as the sample sizes were not equal. Mann-Whitney U tests were conducted in case of a violation of the normality assumption. Similarly, the actual \dot{Y} -balance at the end of recovery interval (given by A_3) was compared to \dot{Y} -balance predicted from SK2 and BAR models. Effect sizes are reported as η^2 and Cohen's d wherever appropriate. The violations to assumptions of normality, sphericity, and homogeneity of variance were checked using Shapiro Wilk's, Mauchly's, Levene's tests respectively. The data are represented as mean \pm SD. All statistical analyses were conducted in SPSS Statistics 25 (IBM Corp., Armonk, NY) and the level of significance was 0.05.

4.3. Results

A summary of $\dot{V}O_{2\text{max}}$, $\dot{V}O_{2\text{peak}}$, GET, P_{mx} , and P_{GET} is reported in Table 4-1. The average relative $\dot{V}O_{2\text{max}}$ was $53.38 \pm 6.44 \text{ mL}\cdot\text{kg}^{-1}\cdot\text{min}^{-1}$, the average relative GET was $36.25 \pm 4.51 \text{ mL}\cdot\text{kg}^{-1}\cdot\text{min}^{-1}$, and the relative $\dot{V}O_{2\text{peak}}$ was $51.91 \pm 6.27 \text{ mL}\cdot\text{kg}^{-1}\cdot\text{min}^{-1}$.

Table 4-1. Summary of parameters from the ramp test: $\text{VO}_{2\text{max}}$, GET, and $\text{VO}_{2\text{peak}}$ for all subjects.

Subject	$\text{VO}_{2\text{max}}$ (L/min)	$\text{VO}_{2\text{peak}}$ (L/min)	GET (L/min)	P_{mx} (W)	P_{GET} (W)
A	4.15	4.04	2.79	374	244
B	3.72	3.56	2.62	320	180
1	4.76	4.48	3.05	425	255
2	2.87	2.85	2.01	270	190
4	4.01	3.90	2.84	316	224
6	2.88	2.86	2.05	275	156
7	4.60	4.53	2.87	445	215
Mean \pm SD	3.86 ± 0.75	3.75 ± 0.69	2.60 ± 0.41	346 ± 70	209 ± 36

The CP, \dot{V} , TW, and Pp from all the 3MTs were averaged and are reported in Table 4-2.

The T_{Pp} during the 3MT occurred between 3.82 ± 1.23 seconds (range 3-7 seconds). The

P_{GET} and P_{mx} from the ramp test were 0.81CP and 1.33CP respectively.

Table 4-2. Summary of the parameters form the four trials of the 3MT for all subjects. Data presented as Mean \pm SD.

Subj.	No. of 3MTs	CP (W)	Y (kJ)	TW (kJ)	Pp (W)
A	2	269 \pm 3	12.03 \pm 0.58	60.08 \pm 0.22	766 \pm 6
B	2	233 \pm 2	10.10 \pm 0.33	51.69 \pm 0.63	714 \pm 8
1	4	335 \pm 7	15.09 \pm 1.00	75.09 \pm 0.84	1043 \pm 44
2	4	217 \pm 6	5.64 \pm 0.56	43.94 \pm 1.26	438 \pm 15
4	4	242 \pm 4	7.84 \pm 0.34	51.00 \pm 0.67	549 \pm 28
6	4	206 \pm 10	9.14 \pm 1.26	46.11 \pm 0.86	421 \pm 27
7	4	311 \pm 14	12.65 \pm 1.27	68.32 \pm 2.00	838 \pm 47

4.3.1. Repeatability of 3MTs and the intermittent test

The reliability statistics for the repeated 3MTs and the repeated intermittent tests are reported in Table 4-3. The reliability metrics for the 3MTs and the intermittent cycling tests indicate excellent agreement between the trials. Subject 4 performed only one trial of their first intermittent test as the second trial was unsuccessful due to their shoes coming unclipped from the pedal, and the test was not repeated so as not to delay the schedule.

Table 4-3. Summary of the reliability metrics with their 95% CI for the repeated trials of the 3MT and the intermittent test.

Parameter	Reliability	3MT	Intermittent test
	metric		
CP	ICC	0.994 (0.977, 0.999)	0.990 (0.937, 0.999)
	TE	9 W (6, 14)	9 W (5, 21)
	CV	3.26% (2.34, 5.38)	3.18% (1.99, 7.81)
Y	ICC	0.984 (0.938, 0.998)	
	TE	0.998 kJ (0.716, 1.648)	NA
	CV	9.91% (7.11, 16.36)	
Pp	ICC	0.996 (0.985, 1)	0.990 (0.941, 0.999)
	TE	34 W (24, 56)	30 W (19, 73)
	CV	5.14% (3.68, 8.48)	4.39% (2.74, 10.76)
TW	ICC	0.998 (0.993, 1)	0.999 (0.994, 1)
	TE	1.197 kJ (0.858, 1.976)	0.547 kJ (0.341, 1.341)
	CV	2.10% (1.51, 3.47)	0.97% (0.61, 2.38)

4.3.2. Effect of recovery power (P_{rec}) and recovery duration (t_{rec}) on Y recovery

Each subject's recovery profile is shown in Figure 4-4. Subject 7 was excluded from the analysis as their CP kept increasing from 3MT1 to 3MT4. Subject 7's CPs across the four 3MT trials were 295, 305, 319, and 327 Watts. This caused an inaccurate estimation of

CP4, which resulted in less Υ being expended in the CP4 interval. This in-turn resulted in similar Υ_{rec} for all intermittent tests as seen in Figure 4-4 (xiii) and (xiv).

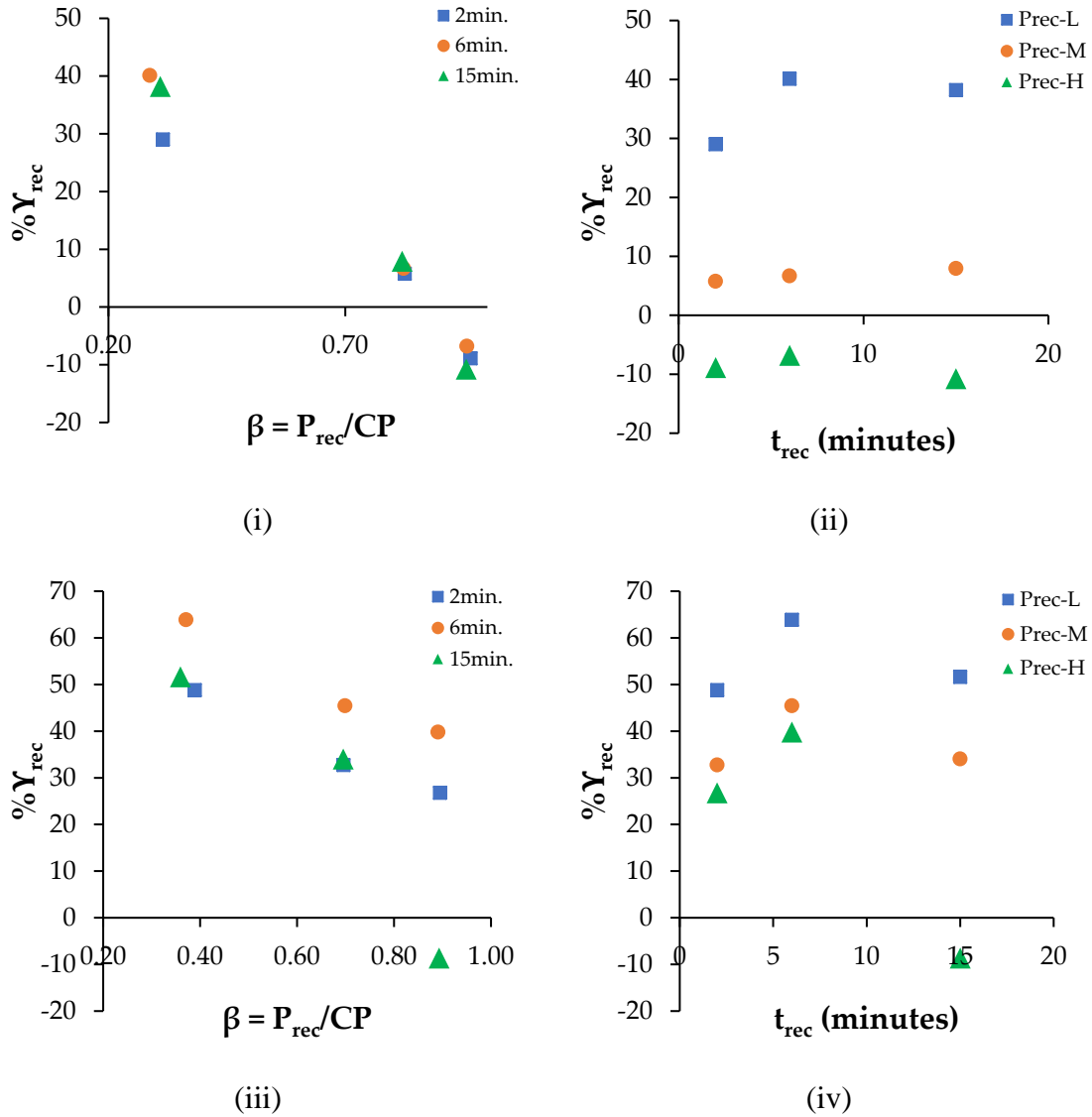
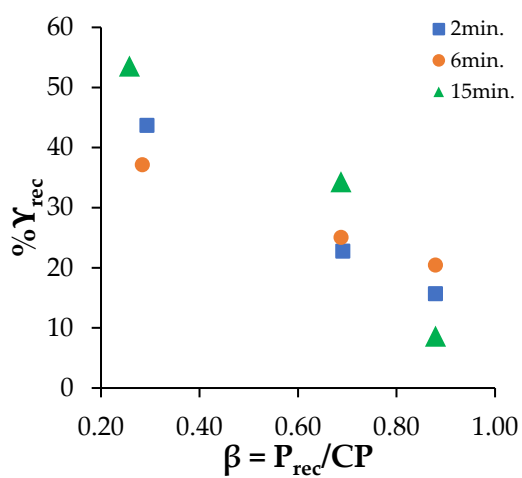
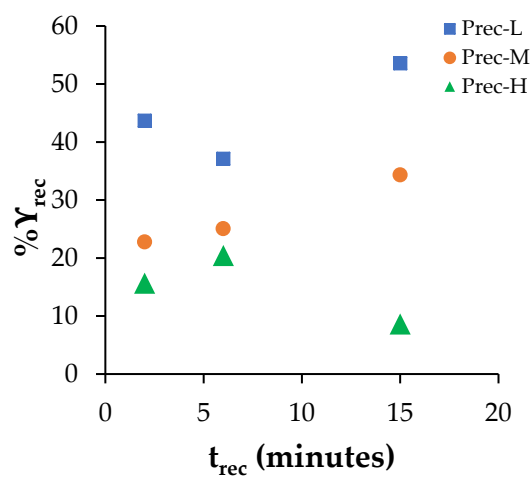


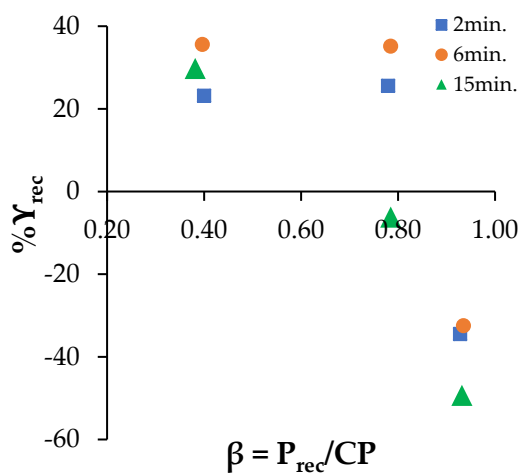
Figure 4-4. Recovery profiles of all subjects. Subject A: (i) and (ii), Subject B: (iii) and (iv), Subject 1: (v) and (vi), Subject 2: (vii) and (viii), Subject 4: (ix) and (x), Subject 6: (xi) and (xii), and Subject 7: (xiii) and (xiv).



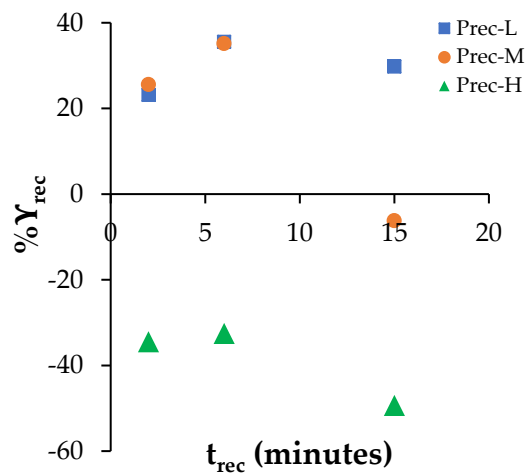
(v)



(vi)

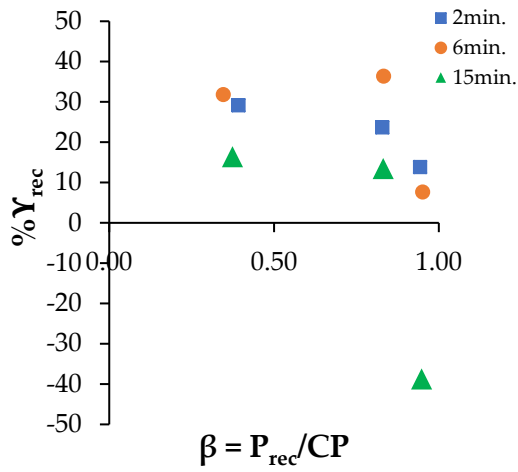


(vii)

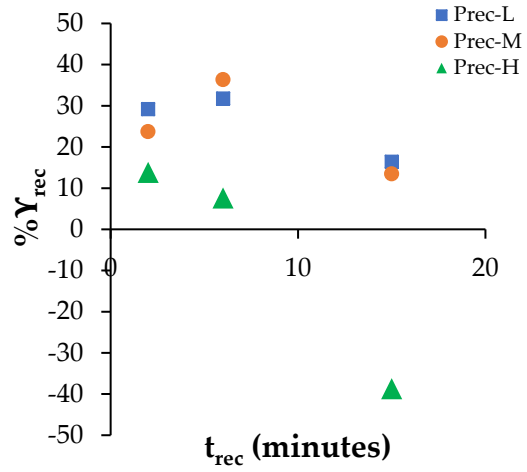


(viii)

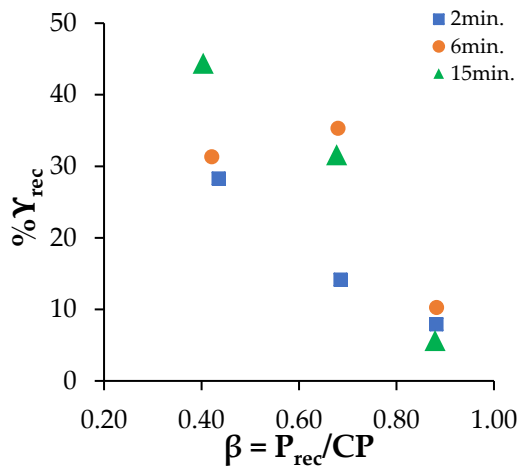
Figure 4-4 (continued). Recovery profiles of all subjects. Subject A: (i) and (ii), Subject B: (iii) and (iv), Subject 1: (v) and (vi), Subject 2: (vii) and (viii), Subject 4: (ix) and (x), Subject 6: (xi) and (xii), and Subject 7: (xiii) and (xiv).



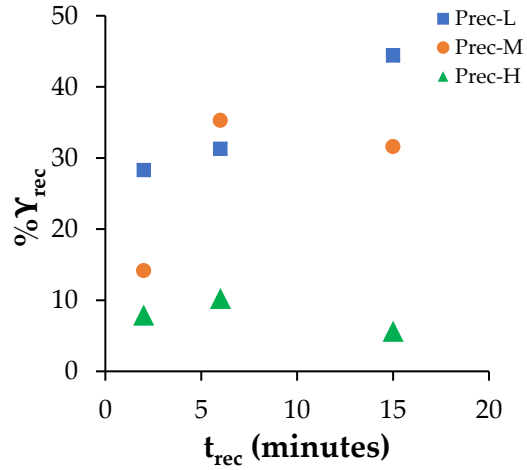
(ix)



(x)

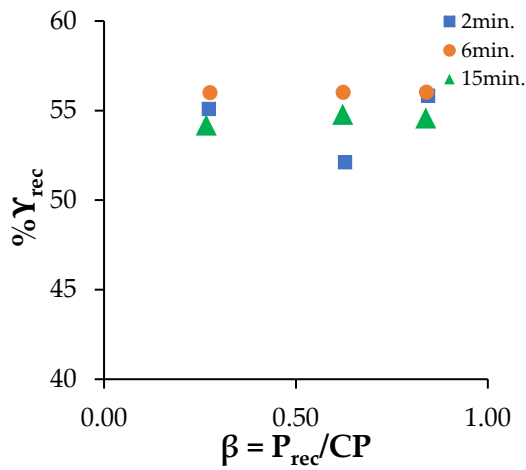


(xi)

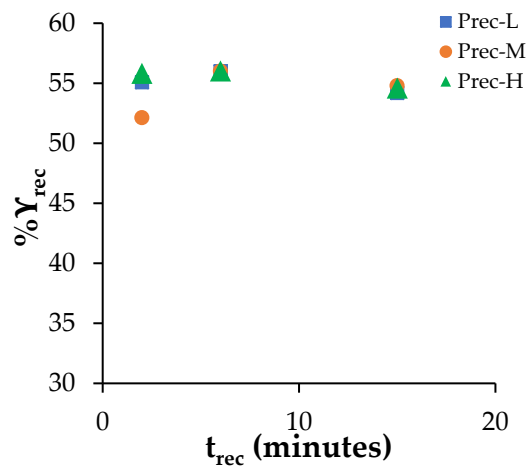


(xii)

Figure 4-4 (continued). Recovery profiles of all subjects. Subject A: (i) and (ii), Subject B: (iii) and (iv), Subject 1: (v) and (vi), Subject 2: (vii) and (viii), Subject 4: (ix) and (x), Subject 6: (xi) and (xii), and Subject 7: (xiii) and (xiv).



(xiii)



(xiv)

Figure 4-4 (continued). Recovery profiles of all subjects. Subject A: (i) and (ii), Subject B: (iii) and (iv), Subject 1: (v) and (vi), Subject 2: (vii) and (viii), Subject 4: (ix) and (x), Subject 6: (xi) and (xii), and Subject 7: (xiii) and (xiv).

The hypothesized behavior of $\%Y_{rec}$ versus β and t_{rec} was not observed in most subjects. However, a statistically significant two way interaction effect was observed between P_{rec} and t_{rec} on Y_{rec} across all subjects ($p = 0.004$, $\eta^2 = 0.52$), which is also illustrated in Figure 4-5A. Assumption of sphericity was not violated as indicated by Mauchly's met for the two-way interaction, $\chi^2(9) = 5.547$, $p = 0.812$.

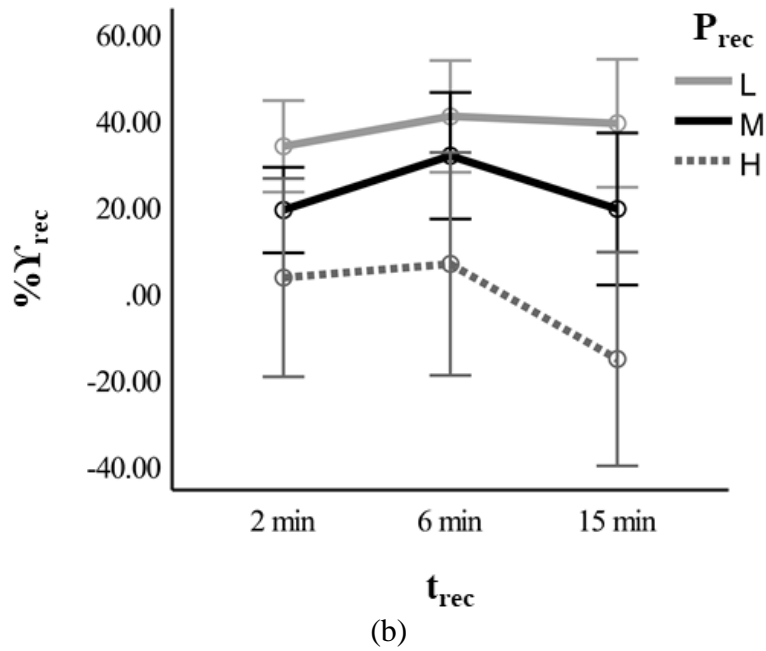
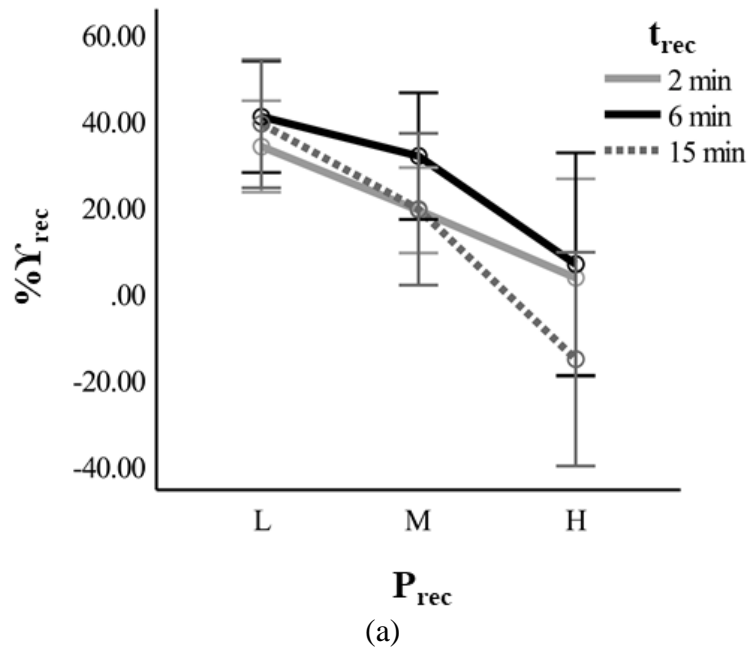


Figure 4-5. Interaction plots. A: Y_{rec} vs P_{rec} , and B: Y_{rec} vs t_{rec} . Simple main effects are present at all t_{rec} between mean Y_{rec} at the three P_{rec} , there are no simple main effects at all P_{rec} between mean Y_{rec} at the three t_{rec} .

Simple main effects analyses were conducted due to the presence of interaction effects between P_{rec} and t_{rec} . There was a statistically significant difference in mean Y_{rec} at $t_{rec} =$

2min ($p = .001$, $\eta^2 = 0.747$), at $t_{\text{rec}} = 6\text{min}$ ($p = 0.006$, $\eta^2 = 0.640$), and at $t_{\text{rec}} = 15\text{ min}$ ($p < 0.001$, $\eta^2 = 0.914$). Table 4-4 shows the summary of the simple main effects analysis.

Table 4-4. Mean Y_{rec} at different t_{rec} and P_{rec} with summary of simple main effects of P_{rec} at each t_{rec}

t_{rec} (min)	Mean Y_{rec} (%)		
	$P_{\text{rec-L}}$	$P_{\text{rec-M}}$	$P_{\text{rec-H}}$
2	33.7% \pm 10.1% ^{#, †}	18.95% \pm 9.42%	3.31% \pm 21.84%
6	40.6% \pm 12.3% ^{††}	31.51% \pm 13.97%	6.47% \pm 24.56%
15	39% \pm 14.12% ^{##, ‡}	19.20% \pm 16.77% ^{‡‡}	-15.53% \pm 23.58%

[#]Statistically significantly different from $P_{\text{rec-M}}$ (mean difference = 14.75%, 95%CI [4.84, 24.66], $p = 0.01$).

[†]Statistically significantly different from $P_{\text{rec-H}}$ (mean difference = 30.39%, 95%CI [8.06, 52.72], $p = 0.015$).

^{††}Statistically significantly different from $P_{\text{rec-H}}$ (mean difference = 34.15%, 95%CI [4.53, 63.77], $p = 0.029$).

^{##}Statistically significantly different from $P_{\text{rec-M}}$ (mean difference = 19.81%, 95%CI [2.63, 36.99], $p = 0.029$).

[‡]Statistically significantly different from $P_{\text{rec-H}}$ (mean difference = 54.54%, 95%CI [34.05, 75.02], $p = 0.0007$).

^{‡‡}Statistically significantly different from $P_{\text{rec-H}}$ (mean difference = 34.72%, 95%CI [15.87, 53.57], $p = 0.004$).

The negative mean Y_{rec} seen at $P_{\text{rec-H}}$ indicates that the subjects did not recover any W' but depleted it in the recovery interval suggesting that they were functioning above CP. This indicates a fluidity associated with CP either within or between exercise bouts.

With regards to simple main effects of t_{rec} at the three P_{rec} , there was no statistically significant difference in mean Y_{rec} at the different t_{rec} for $P_{\text{rec-L}}$, $p = 0.303$ ($\eta^2 = 0.213$).

Similar results were observed at $P_{\text{rec-M}}$, $p = 0.094$ ($\eta^2 = 0.376$), and at $P_{\text{rec-H}}$, $p = 0.052$ ($\eta^2 = 0.536$) (Greenhouse-Geisser correction was applied for $P_{\text{rec-H}}$ as epsilons for Greenhouse-

Geisser and Huynh-Feldt corrections were 0.570 and 0.628 respectively). Please see Appendix B for data and the statistical analyses presented in this section.

4.3.3. Comparison of actual Y -balance (A_3) and W'_{bal} predicted by SK2 and BAR models

Mann-Whitney U tests were conducted to determine if there were differences between actual balance (A_3) and W'_{bal} predicted by SK2 (Y_{SK2}) and BAR (Y_{BAR}) due to a violation of the normality assumption. Distributions of the A_3 and Y_{SK2} , and A_3 and Y_{BAR} were not similar, as assessed by visual inspection. Comparing A_3 and Y_{SK2} , A_3 was statistically significantly lower than Y_{SK2} , $p = 0.035$. Similarly, A_3 was statistically significantly lower than Y_{BAR} , $p = 0.015$. Please see Appendix C for data and details pertaining to statistical analyses presented in this section.

4.3.4. Influence of intermittent test on CP

The influence of the intermittent test on CP was analyzed by comparing CP_{fr} and CP_{ft} at both group and subject levels (excluding Subject 7). Data from Subjects A and B were not analyzed at the subject level as there were only two data points for CP_{fr} . At the group level, a Mann Whitney U test was conducted due to a violation of the normality assumption. The mean CP_{fr} was not statistically different from that of CP_{ft} , $p = 0.327$.

At the subject level, there were no violations of assumptions as assessed by Shapiro Wilk's and Levene's tests for each subject. Independent samples t-test indicated no statistically significant difference between the mean CP_{fr} and mean CP_{ft} for Subject 2 ($p = 0.166$, $d = 0.89$) and Subject 6 ($p = 0.517$, $d = 0.40$). Whereas, mean CP_{ft} was statistically significantly higher than mean CP_{fr} for Subject 1 ($p = 0.025$, $d = 1.56$), Subject 4 ($p = 0.032$, $d = 1.46$).

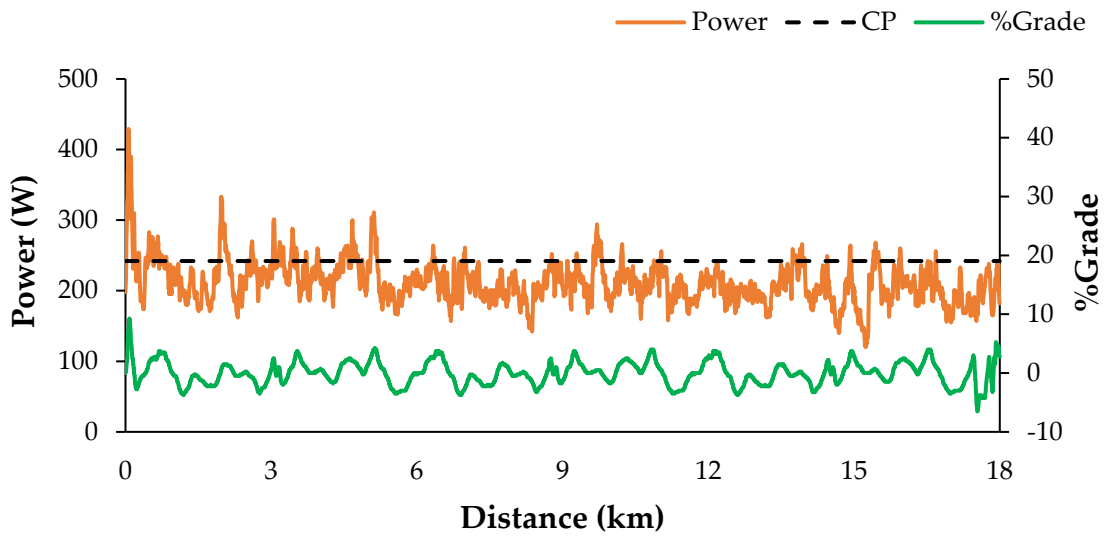
The p-values along with the effect sizes for Subjects 1 and 4 indicate the within subject variability of CP. Please see Appendix D for data and details pertaining to statistical analyses presented in this section.

4.3.5. Optimization tests

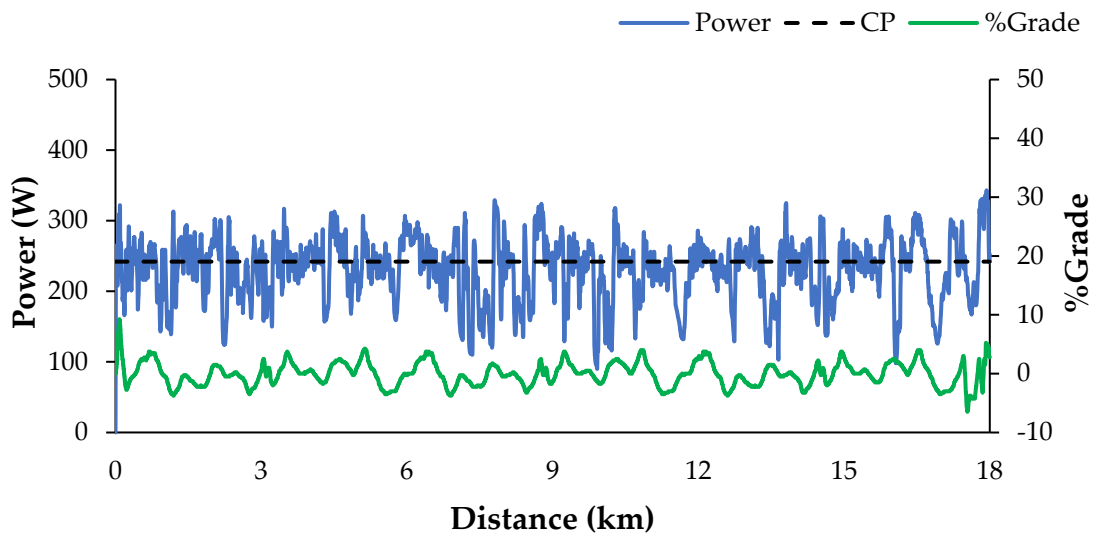
The goal of the optimization was to minimize time by managing the Y-balance. Subject 4 volunteered to participate in the optimization tests and chose the 18 km course that was simulated on the CompuTrainer. The subject's individual data was used to arrive at a recovery model and to determine the optimal power profile for the test (refer to our previous work in [114] for methodology). Table 4-5 summarizes the results from both tests and Figure 4-6 shows the power versus distance profiles for both self and optimal strategies, while Figure 4-6 (c) shows the Y-balance during the optimal test plotted against the distance.

Table 4-5. Comparison of results between self-strategy and optimal strategy tests.

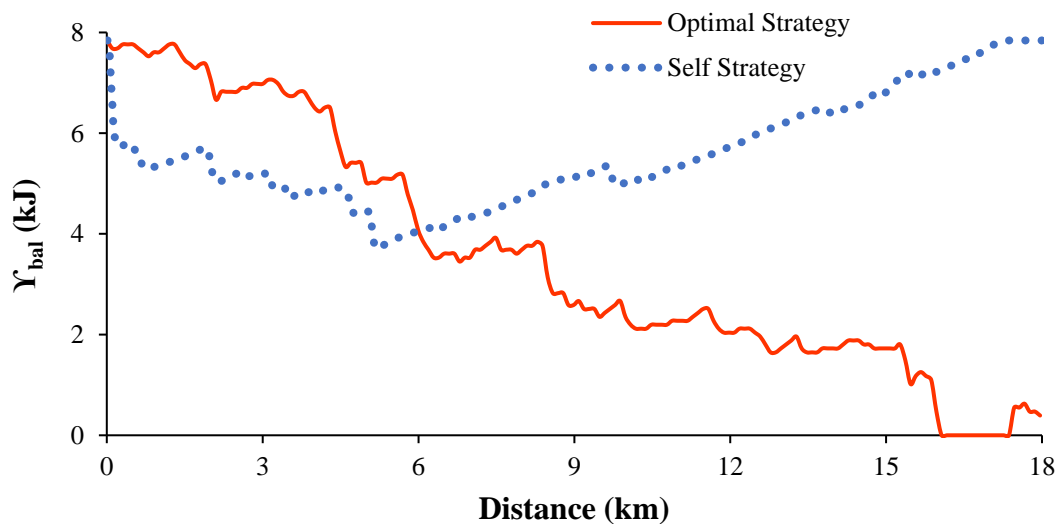
Parameter	Self-strategy test	Optimal strategy test
Time (min:sec)	34:08	33:13
Average Power (W)	212	219
Max Power (W)	429	343
Total Work (kJ)	435	456
Average velocity (mph)	31.64	32.51
Average heart rate (bpm)	148	146



(a)



(b)



(c)

Figure 4-6. Results from the optimization tests: (a) Power vs distance profile for self-strategy, (b) Power vs distance profile for optimal strategy, and (c) Υ -balance vs distance for the optimal strategy test. The course grade is shown below the power profiles and is plotted on the secondary axis.

The optimal strategy tests show an improvement of 55 seconds from the self-strategy. In the self-strategy test, as seen Figure 4-6 (a), the subject began the test at higher powers and then settled below their CP for the last 2/3rds of the course. Whereas, in the optimal strategy test (Figure 4-6 (b)), the subject pedaled above and below CP giving them ample recovery to finish the test faster. The Υ -balance plot in Figure 4-6 (c) has a 0 balance toward the end of the test (not exactly at the finish line). This can be attributed to (i) the variability of Subject 4's Υ and (ii) the constraint that the maximum power which can be generated at Υ -balance = 0 is CP. Overcoming the uphill section at the end of the course at CP results in an increased race completion time. Hence, it is optimal to recover before the uphill section to go up the hill faster.

4.4. Discussion

The objectives of this study were to investigate (i) the effect of P_{rec} and t_{rec} on Y_{rec} after a semi-exhaustive interval above CP, (ii) if Y recovery as calculated from SK2 and BAR models accurately predict the actual Y recovered, (iii) real-time performance optimization using the individual specific recovery data with one subject.. A significant result of this study was the two-way interaction effect between recovery parameters, P_{rec} and t_{rec} , followed by the simple main effects of P_{rec} on Y_{rec} . This illustrates that recovery power has a greater influence on the recovery of Y in comparison to recovery duration. Furthermore, the overestimation of Y -balance at the end of the recovery interval by both SK2 and BAR models illustrates the need to establish athlete-specific models echoing the conclusions from Bartram and colleagues [101]. Moreover, the results from the optimization tests performed with one subject show the potential of athlete-specific models in performance optimization.

The assumptions of this study were that the 3MT estimates CP and Y reliably and Equation 5 accurately describes the expenditure of Y in the severe intensity domain. From the 3MTs, the P_{GET} occurred at 0.81CP, which is higher than that reported by Vanhatalo and colleagues [78] of ~0.625CP. A limitation of the study was that the actual power output in 20W recovery interval was 75-90 W for all subjects. It was not possible to generate a power output of 20W at 80 rpm due to the rolling resistance calibration recommendations.

The repeatability statistics reported in Table 4-3 for CP (ICC = 0.994, TE = 9W, and CV = 3.26%) were stronger than those reported by Johnson and colleagues [74] (ICC = 0.93, TE = 15W, and CV = 6.7%), and similar to those by Burnley and colleagues [83] (ICC =

0.99, TE = 7W, CV = 3%). Similarly, reliability statistics for \dot{Y} (ICC = 0.984, TE = 0.998kJ, and CV = 9.91%) were stronger than those by Johnson and colleagues [74] (ICC = 0.87, TE = 1.456kJ, and CV = 20.7%). Burnley and colleagues [83] did not compute repeatability statistics for \dot{Y} and therefore a comparison with this study is not possible. The stronger repeatability along with the subject-level coefficient of variance for CP (range: 0.86% to 4.85%) and \dot{Y} (range: 3.27% to 13.79%), gives us reason to believe that the higher variability of \dot{Y} (compared to CP) did not substantially influence the outcomes of the study. Similar results of lower variability of CP compared to \dot{Y} have been reported in other studies [71], [74].

The statistical powers observed for the two-way interaction and the simple main effects of P_{rec} were >0.9 illustrate that these analyses were appropriately powered. However, the low statistical power observed on simple main effects of t_{rec} could be due to the low sample size used in the study. The two-way interaction effect between P_{rec} and t_{rec} on \dot{Y}_{rec} was not observed by Caen and colleagues [108]. The simple main effects of lower P_{rec} resulting in greater \dot{Y} recovery has also been illustrated by Bickford and colleagues [102] with P_{rec} having a greater influence on \dot{Y} recovered than t_{rec} . Furthermore, the lack of simple main effects with respect to t_{rec} contrasts the results from Caen and colleagues [108]. They reported main effects with respect to recovery duration with more energy recovered at 6 min ($59.4\% \pm 4.1\%$) when compared to 2 min ($46\% \pm 2.1\%$). Similar results to Caen and colleagues [108] were observed by Ferguson and colleagues [96] with greater \dot{Y} recovery as recovery duration increased. This difference in results could be attributed to the CP4 exertion interval where $\sim 50\%$ of \dot{Y} (linear depletion as per Skiba and colleagues [99]) was

expended while all of $\dot{V}O_2$ was expended prior to the recovery interval in the aforementioned studies. The rate of $\dot{V}O_2$ recovery could be different for recovery intervals that follow exhaustive intervals versus semi-exhaustive intervals, like this study.

Another significant result from this study was that SK2 and BAR models overestimated the actual $\dot{V}O_2$ -balance at the end of the recovery interval. This finding is in contrast to the results found by Bartram and colleagues [101] where SK2 underestimated $\dot{V}O_2$ -balance. The reason for this could be that the athletes who participated in this study were competitive amateur cyclists as compared to elite cyclists in Bartram and colleagues' study [101]. Additionally, SK1, SK2, and BAR assume the recovery of $\dot{V}O_2$ to be exponential with respect to time. The results from this study did not find any such trends (see Figure 4-5). There was an increase in $\dot{V}O_2$ recovered between 2 minutes and 6 minutes while a negative trend was seen in one case for two subjects, which could be attributed to the intra-individual variability of the subjects. This was the reason for comparing TW and Pp to establish repeatability of the intermittent testing protocol which showed less variability as indicated by the ICC, TE, and CV (Table 4-3).

None of the existing literature accounts for the variability of CP and $\dot{V}O_2$ at the subject level as it opposes the assumptions of these parameters being discrete and constant throughout the experiments. In the present study, in some cases, depletion of $\dot{V}O_2$ was observed at the highest recovery power P_{rec-H} , indicated by the negative $\dot{V}O_{2rec}$. This can be attributed to the variability of $\dot{V}O_2$ data around GET [125], which resulted in P_{GET} being in the range of $\sim 0.9CP$. This could be the reason for not observing the hypothesized behavior as depicted in Figure 4-2. Regardless, the subjects were pedaling above CP (i.e. their actual CP on that

day or during that exercise bout) even though it was meant to be a recovery interval. This suggests that there is a variability associated with CP at the individual level, which is illustrated by the increase in CP seen in 2 out of 4 subjects (excluding Subject 7) who repeated the fresh 3MT four times. Similar results were reported by Miura and colleagues [132], where prior exercise in the heavy intensity domain resulting in increased CP estimates. Furthermore, prior heavy intensity exercise has also shown to increase Υ [133], [134]. However, these studies used the constant work-rate protocol to determine CP and Υ as opposed to the 3MT used in this study. The heavy intensity exercise at $P_{\text{rec-M}}$ and $P_{\text{rec-H}}$ may have acted as an additional warmup [133], [134]. These results indicate that CP and Υ have an associated variability which could be a trial-to-trial phenomenon or an intra-trial phenomenon, thus pointing towards individualized time constants or models as suggested in several studies [100], [101], [108].

Another contribution of this study is the real-time performance optimization performed with one subject. However, there are a few limitations to the optimal power profile calculation. First, the recovery of Υ was assumed to depend only on recovery power for the purpose of dynamic programming. Second, the subject would hover above and below the suggested optimal power and was unable to match it exactly at each instant within the 100 m interval. Third, the effects of drag were ignored while determining the optimal strategy as both tests were conducted in the laboratory. Fourth, the trainer was unable to simulate the effect of coasting in the downhill sections of the course. Fifth, there was more than a 4 weeks gap between the completion of the intermittent tests and the optimization tests that could have resulted in changes in the subject's CP, Υ , and recovery mechanisms.

Sixth, the same study with elite cyclists instead of one competitive amateur, may yield a better comparison between the self and optimal strategy tests. Finally, the improved performance may be due to other factors such as the subject's psychological aspects and the novelty of the test. Hence, similar studies in the future should conduct the optimization test at least two times and determine its repeatability.

Considering all these limitations, the improvement of 55 seconds provides encouraging signs for future studies investigating Υ recovery to be used in real-time in-situ performance optimization. The recovery of Υ may not be exponential as suggested by the results of this study in the range of 2 to 15 minutes when a semi-exhaustive exertion interval precedes the recovery interval. The semi-exhaustive exertion interval is a more realistic representation of a race/interval training scenario. The optimal power profile suggested by our method, changes the target power every 100 m, which at a speed of 15 mph is covered in ~15 seconds. This approach is similar to the micro-interval training, which as suggested by Skiba and colleagues [100], is a common coaching practice.

4.5. Key findings

The experimental study presented in this chapter illustrated the interaction effect between recovery characteristics (i.e. recovery power and duration) on recovery of Υ . The study showed that recovery power has a greater influence on the recovery of Υ in comparison to recovery duration as indicated by the simple main effects. Moreover, in some cases, depletion of Υ was observed when the recovery power was in the vicinity of 0.9CP indicating the variability of CP. Additionally, the present study showed that the SK2 and BAR models overestimated Υ -balance at the end of the recovery intervals suggesting that

recovery of Υ may not be exponential in nature for all cyclists, thus, highlighting the need for athlete-specific recovery models. Furthermore, the results of the optimal strategy test show promising signs for in-situ real-time performance optimization using the CP concept. The next chapter summarizes key findings from each chapter, lists research contributions, and discusses potential future research opportunities.

CHAPTER FIVE: CONCLUSIONS AND FUTURE WORK



5.1. Conclusions

By surveying the literature for power-based models of exertion and recovery, it was found that the critical power concept, owing to its simplicity, offers the prospect of a combined exertion-recovery model to optimize performance. Additionally, the lack of methods to quantify the within subject variability (i.e. the IIV) of CP and $\dot{V}O_2$ pose problems in modeling and optimizing performance. The literature review also revealed a scarcity of high-fidelity models for recovery of $\dot{V}O_2$ leading to the following research objectives:

Research objective 1: Establish a method to quantify the individual variability of CP and $\dot{V}O_2$ as determined by the 3MT.

Research objective 2: Develop a testing protocol to understand expenditure and recovery of power and $\dot{V}O_2$.

Research objective 3: Establish recovery profiles in terms of recovery power and recovery duration.

Research objective 4: Combine recovery with established expenditure for energy management.

Research objective 1 was addressed by repeating the 3MT four times with seven subjects and developing a method to compare any two trials of 3MT at the subject level. The developed method ensures repeatability at the subject level using TW and Pp and then the IIV is computed by calculating the 95% confidence interval using the standard deviation from the repeated trials.

Research objective 2 was addressed by developing an intermittent testing protocol to understand the effect of the recovery powers and durations on \dot{Y} recovery. The experimental comprised of a semi-exhaustive interval above CP followed by recovery interval where the recovery power and the recovery duration was manipulated. There was a total of nine different recovery interval manipulations. Seven recreationally active cyclists completed the experimental protocol, thus establishing their individual recovery profiles and addressing Research objective 3. A finding common across all subjects was that the recovery power P_{rec} having a greater influence on \dot{Y}_{rec} than t_{rec} in the recovery duration range of 2 – 15 minutes.

Research Objective 4 was accomplished with one subject whose race time was reduced by 55 seconds compared to their self-strategy by using the subject-specific models and dynamic programming to optimize performance⁴. Though having limitations, the results provide encouraging signs to use subject-specific modeling in performance optimization.

The next steps of the research and are discussed in the following section.

⁴ This was accomplished in collaboration with Faraz Ashtiani and the methodology can be found in the following paper:

Ashtiani, F., Sreedhara, V. S. M., Vahidi, A., Hutchison, R., & Mocko, G. (2019, July). Experimental Modeling of Cyclists Fatigue and Recovery Dynamics Enabling Optimal Pacing in A Time Trial. In 2019 American Control Conference (ACC) (pp. 5083-5088). IEEE.

5.2. Future Work

5.2.1. Reducing the number of testing days

The current experimental testing comprises of 14-16 testing days spread over 5 weeks (including rest days), which is a significant time commitment for cyclists. The results from Chapter 3 indicated that the 3MT could be repeated three times to estimate CP and $\dot{V}O_2$ along with their IIVs. Moreover, the possibility of conducting two 3MTs separated by 12 hours can be investigated. Two testing days can be saved if 12 hours rest results in similar estimates of CP and $\dot{V}O_2$ compared to 24 hours rest.

The results from Chapter 4 has shown that there was an interaction effect between P_{rec} and t_{rec} on recovery of $\dot{V}O_2$. Furthermore, there were no trends seen at the subject level as hypothesized in Figure 4-2. However, trends were observed at P_{rec-L} and P_{rec-H} at t_{rec} of 2 minutes and 6 minutes. Additionally, P_{rec-H} resulted in negative $\dot{V}O_{2rec}$ in 4 out of 7 subjects at P_{rec-H} . Therefore, an exercise protocol with P_{rec} in the range of 0.3CP – 0.8CP and t_{rec} in the range of 2 – 6minutes may result in trends as hypothesized in Figure 4-2. It is proposed that four P_{rec} levels (0.35CP, 0.5CP, 0.65CP, and 0.8CP) and two t_{rec} levels (2min and 4min) be used for the intermittent tests resulting in 8 manipulations instead of 9. Table 5-1 shows an updated testing protocol where the number of testing days is reduced to 12 days.

Table 5-1. Proposed testing schedule to reduce the number of testing days.

Testing Day	Test/s
Day-1	Ramp test, 3MT familiarization, and 3MT1 (12 hours between familiarization and 3MT1 [#])
Day-2	3MT2, 3MT3 (12 hours rest), and Intermittent test familiarization
Day-3	Intermittent test 1
Day-4	Intermittent test 2
Day-5	Intermittent test 3
Day-6	Intermittent test 4
Day-7	Intermittent test 5
Day-8	Intermittent test 6
Day-9	Intermittent test 7
Day-10	Intermittent test 8
Day-11	Self-strategy test
Day-12	Optimal strategy test

[#]This assumes that there is no difference in CP and Y determined from two 3MTs separated by 12 hours and 24 hours rest.

All tests, including the optimization tests, can be completed between 2 to 4 weeks depending on whether tests are conducted every day or every other day. The next section discusses the in-situ testing and validation.

5.2.2. Surrogate models using muscle-oxygenation (MO_2) and heart rate

Surrogate models to recovery of \dot{V} could potentially be derived by investigating the relationship between \dot{V} behavior, muscle oxygenation, and heart rate. Bickford [135] showed that the MO_2 and heart rate either decreased or remained constant in the recovery interval. Similar analyses can be conducted on the data from the study presented in Chapter 4 and the existence of any relationships or correlations between \dot{V} recovery, MO_2 , and heart rate can be investigated. If such correlations exist, then MO_2 and heart rate can be used as surrogates to the recovery models that are based on power and energy.

5.2.3. In-situ testing and validation using a multiple sensor network

The studies presented in this dissertation were all conducted in the laboratory. The models and methods need to be validated and modified to be used in the field. The validation can be accomplished by using the latest trainers on the market that can simulate the effects of drag and downhill coasting. Alternatively, the tests could be conducted in a velodrome using commercially available bicycle power meters. The 3MT and the intermittent tests can be conducted in the velodrome to estimate and establish CP, \dot{V} , the IIVs, and \dot{V} recovery profiles. The self and optimal strategy tests can then be conducted on a known course using a multiple sensor network as shown in Figure 5-1. The network will comprise the following sensors:

1. Power meter (pedal/crank/hub)
2. GPS sensor (usually integrated with the bike computer/cellphone)
3. Heart-rate monitor

4. Muscle oxygenation sensor
5. Raspberry pi
6. Bike computer/cellphone

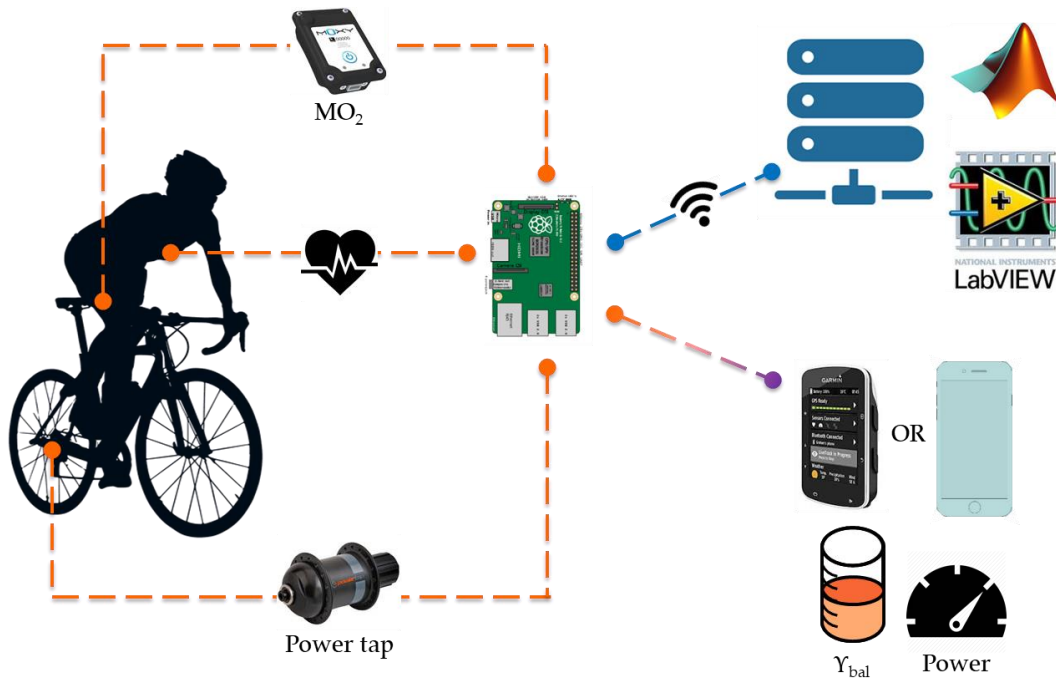


Figure 5-1. Multiple sensor network for real-time in-situ performance optimization.

The known course would be discretized into 100-meter segments and the optimization algorithm would calculate the optimal power profile for all the segments and store it on the remote server/computer. The muscle oxygenation sensor, the heart-rate monitor, and the power meter send data to the raspberry pi mounted on the bike. The raspberry pi will send the acquired data to the computer/server via internet, which will process the data using MATLAB and LabVIEW. The computer/sever compares the average power held in the previous 100-meter segment to its optimal power and calculates an updated optimal power. The computer then sends the updated optimal power to be held in the next 100m segment

to the bike computer via the raspberry pi so that the cyclist can adapt and change their power output. This multiple sensor system can be realized by following the cyclist in a car which can host a Wi-Fi hotspot for the bike mounted raspberry pi to communicate with the either a remote server or a computer in the car.

5.2.4. Modeling performance of endurance sports

There is existing work that applies the CP concept to running [5] and swimming [6] with analogous parameters. The possibility of modeling running and swimming performance in the same vein as presented in the previous chapters can be investigated. Furthermore, with the models for swimming and running, the effect of prior exercise on performance can be investigated. This will lead to modeling and potentially optimizing duathlon and triathlon performances.

5.2.5. Training and in-game strategies for team sports

The CP concept can potentially be used to investigate fatigue related injuries in sports comprising of sprint work such as football, soccer, and lacrosse. Sprinters tend to have a large Υ and recover faster in between their sprints. This faster Υ recovery can be investigated and the learnings can be extended to develop specific training interventions based on different outfield positions. Furthermore, the possibility of linking risk of injury-occurrence to Υ -balance can be investigated and the learnings could potentially be helpful in devising team strategies based on ever changing game situations.

5.2.6. Exercise and health

The critical power concept has been applied to different forms of exercise in many studies [2], [6], [7] and provides a framework that can be useful in understanding the physiological

underpinnings of fatigue in relation to heart disease and muscle atrophy [28]. Mezzani and colleagues [136] conducted CWR tests on patients suffering from chronic heart failure to understand their limits of prolonged aerobic performance. Neder and colleagues [137] investigated the power-duration relationship in patients with chronic obstructive pulmonary disease to arrive at “sustainable” and “non-sustainable” exercise domains. Similarly, future studies can explore training prescriptions for patients suffering from other diseases like diabetes, and diseases that cause muscle atrophy to improve their overall health. Furthermore, the critical power concept has the potential to assess muscle health of astronauts who are prone to develop muscular atrophy during space missions [138].

5.3. Research Contributions

1. None of the work reviewed in this research attempts to model/address/quantify IIV associated with CP and $\dot{V}O_2$. All studies attempt to develop global models without accounting for this IIV. The work presented here has laid the foundation for quantifying IIV to mitigate under/overestimation of performance.
2. The available studies pertaining to $\dot{V}O_2$ recovery investigate the effect of either recovery duration [96] or recovery powers [97] on recovery of $\dot{V}O_2$. There are only a few studies that investigate the effect of both recovery powers and durations on $\dot{V}O_2$. This work investigated the effect of both on recovery of $\dot{V}O_2$ and the results suggest that $\dot{V}O_2$ recovery may not be exponential for all cyclists and highlights the need for athlete specific models.
3. This research presented a case of performance optimization using an energy management system with subject-specific models derived from the experimental

data to successfully reduce the race time by approximately 2 minutes. This was one of the first attempts at real-time performance optimization.

5.3.1. Publications

Journal articles

1. Sreedhara, V. S. M., Mocko, G. M., & Hutchison, R. E. “A survey of mathematical models of human performance using power and energy”. *Sports Medicine-Open*, vol. 5, no. 1, pp. 1-13, 2019.
2. Sreedhara, V. S. M., Mocko, G. M., & Hutchison, R. E. “Repeatability and variability of the 3-minute all-out test at the subject level”. (submitted to *SSEJ* in March 2020).
3. Sreedhara, V. S. M., Ashtiani, F., Mocko, G. M., Vahidi, A., & Hutchison, R. E. “Modeling the recovery of W’ in the moderate to heavy exercise intensity domain” (submitted to *MSSE* in February 2020).
4. Malley, J. C., Sreedhara V. S. M., Mocko, G. M., Vahidi, A., & Hutchison, R. E. “Cycling fatigue modeling for intermittent exercise: A case study” (to be submitted in May 2020).
5. Ashtiani, F., Sreedhara, V. S. M., Mocko, G. M., Vahidi, A., & Hutchison, R. E. “Optimal Pacing of a Cyclist in a Time Trial Based on Experimentally Calibrated Models of Fatigue and Recovery” (to be submitted in May 2020).

Conference proceedings

1. Ashtiani, F., Sreedhara, V. S. M., Vahidi, A., Hutchison, R., & Mocko, G. (2019, July). “Experimental Modeling of Cyclists Fatigue and Recovery Dynamics Enabling Optimal Pacing in A Time Trial”. In 2019 American Control Conference (ACC) (pp. 5083-5088). IEEE.
2. Sreedhara, V. S. M., Mocko, G. M., & Hutchison, R. E. “An Experimental Protocol to Model Recovery of Anaerobic Work Capacity”. In: The Engineering of Sport (ISEA 2018), Brisbane, Australia, 26-29 March 2018. (Vol. 2, No. 6, p. 208).
3. Bickford, P., Sreedhara, V. S. M., Mocko, G. M., Vahidi, A., & Hutchison, R. E. (2018, February). “Modeling the Expenditure and Recovery of Anaerobic Work Capacity in Cycling”. In International Sports Engineering Association Conference Proceedings, 2018, Brisbane, Australia (Vol. 2, No. 6, p. 219).

REFERENCES

- [1] A. V. Hill, "The Physiological Basis of Athletic Records," *Lancet*, vol. 206, no. 5323, pp. 481–486, 1925.
- [2] H. Monod and J. Scherrer, "The work capacity of a synergic muscular group," *Ergonomics*, vol. 8, no. 3, pp. 329–338, 1965.
- [3] A. J. Ward-Smith, "A mathematical theory of running, based on the first law of thermodynamics, and its application to the performance of world-class athletes," *J. Biomech.*, vol. 18, no. 5, pp. 337–349, 1985.
- [4] T. Moritani, A. Nagata, H. A. Devries, and M. Muro, "Critical Power as a measure of physical work capacity and anaerobic threshold," *Ergonomics*, vol. 24, no. 5, pp. 339–350, 1981.
- [5] R. L. Hughson, C. J. Orok, and L. E. Staudt, "A high velocity treadmill running test to assess endurance running potential," *Int. J. Sports Med.*, vol. 5.01, no. 01, pp. 23–25, 1984.
- [6] K. Wakayoshi *et al.*, "Determination and validity of critical velocity as an index of swimming performance in the competitive swimmer," *Eur. J. Appl. Physiol. Occup. Physiol.*, vol. 64, no. 2, pp. 153–157, 1992.
- [7] M. D. Kennedy and G. J. Bell, "A comparison of critical velocity estimates to actual velocities in predicting simulated rowing performance," *Can. J. Appl. Physiol.*, vol. 25, no. 4, pp. 223–235, 2000.

- [8] S. F. Lewis and R. G. Haller, "Physiologic Measurement of Exercise and Fatigue with Special Reference to Chronic Fatigue Syndrome," *Rev. Infect. Dis.*, vol. 13, no. Supplement_1, pp. S98–S108, 1991.
- [9] M. D. Kennedy, K. A. Tamminen, and N. L. Holt, "Factors that influence fatigue status in Canadian university swimmers," *J. Sports Sci.*, vol. 31, no. 5, pp. 554–564, 2013.
- [10] J. L. Taylor, G. Todd, and S. C. Gandevia, "Evidence for a supraspinal contribution to human muscle fatigue.," *Clin. Exp. Pharmacol. Physiol.*, vol. 33, no. 4, pp. 400–405, 2006.
- [11] M. Amann, "Central and peripheral fatigue: Interaction during cycling exercise in humans," *Med. Sci. Sports Exerc.*, vol. 43, no. 11, pp. 2039–2045, 2011.
- [12] B. Bigland-Ritchie and J. J. Woods, "Changes in muscle contractile properties and neural control during human muscular fatigue," *Muscle Nerve*, vol. 7, no. 9, pp. 691–699, 1984.
- [13] S. Triscott, J. Gordon, A. Kuppaswamy, N. King, N. Davey, and P. Ellaway, "Differential effects of endurance and resistance training on central fatigue," *J. Sports Sci.*, vol. 26, no. 9, pp. 941–951, 2008.
- [14] S. C. Gandevia, "Spinal and Supraspinal Factors in Human Muscle Fatigue," *Physiol. Rev.*, vol. 81, no. 4, pp. 1725–1789, 2001.
- [15] M. P. Davis and D. Walsh, "Mechanisms of Fatigue," *J. Support. Oncol. J Support Oncol*, vol. 8, no. 4, pp. 164–174, 2010.

- [16] C. R. Abbiss and P. B. Laursen, “Models to explain fatigue during prolonged endurance cycling,” *Sport. Med.*, vol. 35, no. 10, pp. 865–898, 2005.
- [17] L. Nybo and N. H. Secher, “Cerebral perturbations provoked by prolonged exercise,” *Prog. Neurobiol.*, vol. 72, no. 4, pp. 223–261, 2004.
- [18] J. A. Kent-Braun, “Central and peripheral contributions to muscle fatigue in humans during sustained maximal effort,” *Eur. J. Appl. Physiol. Occup. Physiol.*, vol. 80, no. 1, pp. 57–63, 1999.
- [19] B. K. Barry and R. M. Enoka, “The neurobiology of muscle fatigue: 15 years later,” *Integr. Comp. Biol.*, vol. 47, no. 4, pp. 465–473, 2007.
- [20] C. M. Laurent and J. M. Green, “Multiple Models Can Concurrently Explain Fatigue During Human Performance,” *Int. J. Exerc. Sci.*, vol. 2, no. 4, pp. 280–293, 2009.
- [21] C. Williams and S. Ratel, Eds., *Human muscle fatigue*. Routledge, 2009.
- [22] M. N. Bourne, K. E. Webster, and T. E. Hewett, “Is Fatigue a Risk Factor for Anterior Cruciate Ligament Rupture?,” *Sport. Med.*, 2019.
- [23] R. M. Enoka and D. G. Stuart, “Neurobiology of muscle fatigue,” *J. Appl. Physiol.*, vol. 72, no. 5, pp. 1631–1648, 1992.
- [24] N. K. Vøllestad, “Measurement of human muscle fatigue,” *J. Neurosci. Methods*, vol. 74, no. 2, pp. 219–227, 1997.
- [25] D. Kay and F. E. Marino, “Fluid ingestion and exercise hyperthermia: Implications for performance, thermoregulation, metabolism and the development of fatigue,” *J. Sports Sci.*, vol. 18, no. 2, pp. 71–82, 2000.

- [26] D. Kay, E. Marino, J. Cannon, A. St, C. Gibson, and T. D. Noakes, “Evidence for neuromuscular fatigue during high-intensity cycling in warm , humid conditions,” *Eur. J. Appl. Physiol.*, vol. 84, no. 1–2, pp. 115–121, 2001.
- [27] D. C. Poole, M. Burnley, A. Vanhatalo, H. B. Rossiter, and A. M. Jones, “Critical Power: An Important Fatigue Threshold in Exercise Physiology,” *Med. Sci. Sport. Exerc.*, vol. 48, no. 11, pp. 2320–2334, 2016.
- [28] J. C. Craig, A. Vanhatalo, M. Burnley, A. M. Jones, and D. C. Poole, “Critical Power: Possibly the Most Important Fatigue Threshold in Exercise Physiology,” in *Muscle and Exercise Physiology*, J. A. Zoladz, Ed. Academic Press, 2019, pp. 159–181.
- [29] F. Ozyener, H. B. Rossiter, S. a Ward, and B. J. Whipp, “Influence of exercise intensity on the on- and off-transient kinetics of pulmonary oxygen uptake in humans,” *J. Physiol.*, vol. 533, no. Pt 3, pp. 891–902, 2001.
- [30] H. Carter, J. S. M. Pringle, A. M. Jones, and J. H. Doust, “Oxygen uptake kinetics during treadmill running across exercise intensity domains,” *Eur. J. Appl. Physiol.*, vol. 86, no. 4, pp. 347–354, 2002.
- [31] E. A. Rose and G. Parfitt, “A quantitative analysis and qualitative explanation of the individual differences in affective responses to prescribed and self-selected exercise intensities,” *J. Sport Exerc. Psychol.*, vol. 29, no. 3, pp. 281–309, 2007.
- [32] E. E. Hall, P. Ekkekakis, and S. J. Petruzzello, “The affective beneficence of vigorous exercise revisited,” *Br. J. Health Psychol.*, vol. 7, pp. 47–66, 2002.

- [33] A. S. Welch, A. Hulley, C. Ferguson, and M. R. Beauchamp, “Affective responses of inactive women to a maximal incremental exercise test: A test of the dual-mode model,” *Psychol. Sport Exerc.*, vol. 8, no. 4, pp. 401–423, 2007.
- [34] R. Beneke, “Methodological aspects of maximal lactate steady state-implications for performance testing,” *Eur. J. Appl. Physiol.*, vol. 89, no. 1, pp. 95–99, 2003.
- [35] V. L. Billat, P. Sirvent, G. Py, J. P. Koralsztein, and J. Mercier, “The Concept of Maximal Lactate Steady State,” *Sport. Med.*, vol. 33, no. 6, pp. 407–426, 2003.
- [36] R. Beneke, R. M. Leithauser, and O. Ochentel, “Blood lactate diagnostics in exercise testing and training,” *Int. J. Sports Physiol. Perform.*, vol. 6, no. 1, pp. 8–24, 2011.
- [37] D. A. Keir *et al.*, “Exercise Intensity Thresholds: Identifying the Boundaries of Sustainable Performance,” *Med. Sci. Sports Exerc.*, vol. 47, no. 9, pp. 1932–1940, 2015.
- [38] A. Vanhatalo *et al.*, “The mechanistic bases of the power–time relationship: muscle metabolic responses and relationships to muscle fibre type,” *J. Physiol.*, vol. 594, no. 15, pp. 4407–4423, 2016.
- [39] M. I. Black *et al.*, “Muscle metabolic and neuromuscular determinants of fatigue during cycling in different exercise intensity domains,” *J. Appl. Physiol.*, vol. 122, no. 3, pp. 446–459, 2017.
- [40] P. T. Morgan *et al.*, “Road cycle TT performance : Relationship to the power-duration model and association with FTP Road cycle TT performance : Relationship to the power-duration model and association with FTP,” *J. Sports Sci.*, vol. 00, no. 00, pp. 1–9, 2018.

- [41] J. S. M. Pringle and A. M. Jones, "Maximal lactate steady state, critical power and EMG during cycling," *Eur. J. Appl. Physiol.*, vol. 88, no. 3, pp. 214–226, 2002.
- [42] J. Dekerle, B. Baron, L. Dupont, J. Vanvelcenaher, and P. Pelayo, "Maximal lactate steady state, respiratory compensation threshold and critical power," *Eur. J. Appl. Physiol.*, vol. 89, no. 3–4, pp. 281–288, 2003.
- [43] F. Mattioni Maturana, D. A. Keir, K. M. McLay, and J. M. Murias, "Can measures of critical power precisely estimate the maximal metabolic steady-state?," *Appl. Physiol. Nutr. Metab.*, vol. 41, no. 11, pp. 1197–1203, 2016.
- [44] A. Vanhatalo, A. M. Jones, and M. Burnley, "Application of Critical Power in Sport," *Int. J. Sports Physiol. Perform.*, vol. 6, pp. 128–136, 2011.
- [45] D. C. Poole, S. A. Ward, and B. J. Whipp, "The effects of training on the metabolic and respiratory profile of high-intensity cycle ergometer exercise," *Eur. J. Appl. Physiol. Occup. Physiol.*, vol. 59, no. 6, pp. 421–429, 1990.
- [46] B. J. Whipp, D. J. Huntsman, T. W. Storer, N. Lamarra, and K. Wasserman, "A constant which determines the duration of tolerance to high-intensity work [abstract]," *Fed. Proc.*, vol. 41, no. 5, p. 1591, 1982.
- [47] J. Dekerle, G. Brickley, A. J. P. Hammond, J. S. M. Pringle, and H. Carter, "Validity of the two-parameter model in estimating the anaerobic work capacity," *Eur. J. Appl. Physiol.*, vol. 96, no. 3, pp. 257–264, 2006.
- [48] G. A. Gaesser, T. J. Carnevale, G. Alan, D. O. Walter, and C. J. Womack, "Estimation of critical power with nonlinear and linear models," *Med. Sci. Sports Exerc.*, vol. 27, no. 10, pp. 1430–1438, 1995.

- [49] D. W. Hill, "The critical power concept," *Sports Med.*, vol. 16, no. 4, pp. 237–254, 1993.
- [50] D. J. Housh, T. J. Housh, and S. M. Bauge, "A methodological consideration for the determination of critical power and anaerobic work capacity.," *Res. Q. Exerc. Sport*, vol. 61, no. 4, pp. 406–409, 1990.
- [51] T. Driss and H. Vandewalle, "The Measurement of Maximal (Anaerobic) Power Output on a Cycle Ergometer : A Critical Review," *Biomed Res. Int.*, 2013.
- [52] R. H. Morton, "The critical power and related whole-body bioenergetic models," *Eur. J. Appl. Physiol.*, vol. 96, no. 4, pp. 339–354, Mar. 2006.
- [53] R. K. Josephson, "Contraction dynamics and power output of skeletal muscle," *Annu. Rev. Physiol.*, vol. 55, no. 1, pp. 527–546, 1993.
- [54] Y. Yoshihuku and W. Herzog, "Optimal design parameters of the bicycle-rider system for maximal muscle power output," vol. 23, no. 10, pp. 1069–1079, 1990.
- [55] S. M. Housh, D. J., Housh, T. J., & Bauge, "The accuracy of the critical power test for predicting time to exhaustion during cycle ergometry.," *Ergonomics*, vol. 32, no. 8, pp. 997–1004, 1989.
- [56] G. Brickley, J. Doust, and C. A. Williams, "Physiological responses during exercise to exhaustion at critical power," *Eur. J. Appl. Physiol.*, vol. 88, no. 1–2, pp. 146–151, 2002.
- [57] T. M. McLellan and K. S. Cheung, "A comparative evaluation of the individual anaerobic threshold and the critical power," *Med. Sci. Sports Exerc.*, vol. 24, no. 5, pp. 543–550, 1992.

- [58] D. G. Jenkins and B. M. Quigley, "Blood lactate in trained cyclists during cycle ergometry at critical power," *Eur. J. Appl. Physiol. Occup. Physiol.*, vol. 61, no. 3–4, pp. 278–273, 1990.
- [59] P. A. Scarborough, J. C. Smith, S. M. Talbert, and D. W. Hill, "Time to exhaustion at the power asymptote in men and women [abstract]," *Med. Sci. Sport. Exerc.*, vol. 23, p. S12, 1991.
- [60] D. W. Hill and J. C. Smith, "Determination of critical power by pulmonary gas exchange," *Can. J. Appl. Physiol.*, vol. 24, no. 1, pp. 74–86, 1999.
- [61] T. J. Overend, D. A. Cunningham, D. H. Paterson, and W. D. F. Smith, "Physiological responses of young and elderly men to prolonged exercise at critical power.," *European J. Appl. Physiol. Occup. Physiol.*, vol. 64, no. 2, pp. 187–193, 1992.
- [62] D. C. Poole, S. A. Ward, G. W. Gardner, and B. J. Whipp, "Metabolic and respiratory profile of the upper limit for prolonged exercise in man," *Ergonomics*, vol. 31, no. 19, pp. 1265–1279, 1988.
- [63] W. G. Hopkins, I. M. Edmond, B. H. Hamilton, D. J. Macfarlane, and B. H. Ross, "Relation between power and endurance for treadmill running of short duration," *Ergonomics*, vol. 32, no. 12, pp. 1565–1571, 1989.
- [64] R. H. Morton, "A 3-parameter critical power model," *Ergonomics*, vol. 39, no. 4, pp. 611–619, 1996.

- [65] P. G. Weyand, J. E. Lin, and M. W. Bundle, “Sprint performance-duration relationships are set by the fractional duration of external force application,” *AJP Regul. Integr. Comp. Physiol.*, vol. 290, no. 3, pp. R758–R765, 2005.
- [66] R. H. Morton, “A new modelling approach demonstrating the inability to make up for lost time in endurance running events,” *IMA J. Manag. Math.*, vol. 20, no. 2, pp. 109–120, 2009.
- [67] F. Péronnet and G. Thibault, “Mathematical analysis of running performance and world running records,” *J. Appl. Physiol.*, vol. 67, no. 1, pp. 453–465, 1989.
- [68] R. H. Morton, “Modelling human power and endurance,” *J. Math. Biol.*, vol. 28, no. 1, pp. 49–64, 1990.
- [69] A. J. Bull, T. J. Housh, G. O. Johnson, and S. R. Perry, “Effect of mathematical modeling on the estimation of critical power,” *Med. Sci. Sports Exerc.*, vol. 32, no. 2, pp. 526–530, 2000.
- [70] H. C. Bergstrom *et al.*, “Differences Among Estimates of Critical Power and Anaerobic Work Capacity Derived From Five Mathematical Models and the Three-Minute All-Out Test,” *J. Strength Cond. Res.*, vol. 28, no. 3, pp. 592–600, 2014.
- [71] I. E. Clark, S. R. Murray, and R. W. Pettitt, “Alternative procedures for the three-minute all-out exercise test,” *J. Strength Cond. Res.*, vol. 27, no. 8, pp. 2104–2112, Aug. 2013.
- [72] R. H. Morton, “Critical power test for ramp exercise,” *Eur. J. Appl. Physiol. Occup. Physiol.*, vol. 69, no. 5, pp. 435–438, 1994.

- [73] G. A. Gaesser and L. A. Wilson, "Effects of continuous and interval training on the parameters of the power-endurance time relationship for high-intensity exercise," *Int. J. Sports Med.*, vol. 9, no. 06, pp. 417–421, 1988.
- [74] T. M. Johnson, P. J. Sexton, A. M. Placek, S. R. Murray, and R. W. Pettitt, "Reliability analysis of the 3-min all-out exercise test for cycle ergometry," *Med. Sci. Sports Exerc.*, vol. 43, no. 12, pp. 2375–2380, 2011.
- [75] D. Muniz-Pumares, B. Karsten, C. Triska, and M. Glaister, "Methodological Approaches and Related Challenges Associated With the Determination of Critical Power and Curvature Constant," *J. Strength Cond. Res.*, vol. 33, no. 2, pp. 584–596, 2019.
- [76] M. I. Black, J. Durant, A. M. Jones, and A. Vanhatalo, "Critical power derived from a 3-min all-out test predicts 16.1-km road time-trial performance," *Eur. J. Sport Sci.*, vol. 14, no. 3, pp. 217–223, 2014.
- [77] R. H. Morton, S. Green, D. Bishop, and D. G. Jenkins, "Ramp and constant power trials produce equivalent critical power estimates.," *Med. Sci. Sports Exerc.*, vol. 29, no. 6, pp. 833–836, 1997.
- [78] A. Vanhatalo, J. H. Doust, and M. Burnley, "Determination of critical power using a 3-min all-out cycling test," *Med. Sci. Sports Exerc.*, vol. 39, no. 3, pp. 548–555, 2007.
- [79] O. Bar-Or, "The Wingate anaerobic test an update on methodology, reliability and validity," *Sport. Med.*, vol. 4, no. 6, pp. 381–394, 1987.

- [80] L. J. Nebelsick-Gullett, T. J. Housh, G. O. Johnson, and S. M. Bauge, “A comparison of methods of measuring anaerobic work capacity,” *Ergonomics*, vol. 31, no. 10, pp. 1413–1419, 1988.
- [81] H. Vandewalle, B. Kapitaniak, S. Grün, S. Raveneau, and H. Monod, “Comparison between a 30-s all-out test and a time-work test on a cycle ergometer,” *Eur. J. Appl. Physiol. Occup. Physiol.*, vol. 58, no. 4, pp. 375–381, 1989.
- [82] A. Vanhatalo, J. H. Doust, and M. Burnley, “Robustness of a 3 min all-out cycling test to manipulations of power profile and cadence in humans.,” *Exp. Physiol.*, vol. 93, no. 3, pp. 383–390, 2008.
- [83] M. Burnley, J. H. Doust, and A. Vanhatalo, “A 3-min all-out test to determine peak oxygen uptake and the maximal steady state,” *Med. Sci. Sports Exerc.*, vol. 38, no. 11, pp. 1995–2003, 2006.
- [84] S. A. McClave, M. LeBlanc, and S. A. Hawkins, “Sustainability of critical power determined by a 3-minute all-out test in elite cyclists,” *J. Strength Cond. Res.*, vol. 25, no. 11, pp. 3093–3098, 2011.
- [85] H. C. Bergstrom *et al.*, “Responses during exhaustive exercise at critical power determined from the 3-min all-out test,” *J. Sports Sci.*, vol. 31, no. 5, pp. 537–545, 2013.
- [86] D. Muniz-Pumares, C. Pedlar, R. Godfrey, and M. Glaister, “A comparison of methods to estimate anaerobic capacity: Accumulated oxygen deficit and W’ during constant and all-out work-rate profiles,” *J. Sports Sci.*, vol. 35, no. 23, pp. 2357–2364, 2017.

- [87] P. F. Skiba, “The Kinetics of the Work Capacity Above Critical Power,” Dissertation, University of Exeter, 2014.
- [88] D. Bishop, D. G. Jenkins, and A. Howard, “The critical power function is dependent on the duration of the predictive exercise tests chosen,” *Int. J. Sports Med.*, vol. 19, no. 2, pp. 125–129, 1998.
- [89] D. Jenkins, K. Krettek, and D. Bishop, “The duration of predicting trials influences time to fatigue at critical power,” *J. Sci. Med. Sport*, 1998.
- [90] T. Barker, D. C. Poole, M. L. Noble, and T. J. Barstow, “Human critical power-oxygen uptake relationship at different pedalling frequencies,” *Exp. Physiol.*, vol. 91, no. 3, pp. 621–632, 2006.
- [91] J. C. Bartram, D. Thewlis, D. T. Martin, and K. I. Norton, “Predicting Critical Power in Elite Cyclists: Questioning the Validity of the 3-Minute All-Out Test,” *Int. J. Sports Physiol. Perform.*, vol. 12, no. 6, pp. 783–787, 2017.
- [92] H. Kuipers, F. T. J. Verstappen, H. A. Keizer, P. Geurten, and G. Van Kranenburg, “Variability of aerobic performance in the laboratory and its physiologic correlates,” *Int. J. Sports Med.*, vol. 6, no. 04, pp. 197–201, 1985.
- [93] C. Triska *et al.*, “Reliability of the parameters of the power-duration relationship using maximal effort time-trials under laboratory conditions,” *PLoS One*, vol. 12, no. 12, pp. 1–12, 2017.
- [94] J. C. Martin, D. L. Milliken, J. E. Cobb, K. L. McFadden, and A. R. Coggan, “Validation of a mathematical model for road cycling power,” *J. Appl. Biomech.*, vol. 14, no. 3, pp. 276–291, 1998.

- [95] R. H. Morton and L. V. Billat, “The critical power model for intermittent exercise,” *Eur. J. Appl. Physiol.*, vol. 91, no. 2–3, pp. 303–307, 2004.
- [96] C. Ferguson, H. B. Rossiter, B. J. Whipp, A. J. Cathcart, S. R. Murgatroyd, and S. A. Ward, “Effect of recovery duration from prior exhaustive exercise on the parameters of the power-duration relationship,” *J. Appl. Physiol.*, vol. 108, no. 4, pp. 866–74, 2010.
- [97] P. F. Skiba, W. Chidnok, A. Vanhatalo, and A. M. Jones, “Modeling the Expenditure and Reconstitution of Work Capacity above Critical Power,” *Med. Sci. Sports Exerc.*, vol. 44, no. 8, pp. 1526–1532, 2012.
- [98] P. F. Skiba, D. Clarke, A. Vanhatalo, and A. M. Jones, “Validation of a novel intermittent W’ model for cycling using field data.,” *Int. J. Sports Physiol. Perform.*, vol. 9, no. 6, pp. 900–904, 2014.
- [99] P. F. Skiba, J. Fulford, D. C. Clarke, A. Vanhatalo, and A. M. Jones, “Intramuscular determinants of the ability to recover work capacity above critical power,” *Eur. J. Appl. Physiol.*, vol. 115, no. 4, pp. 703–713, 2015.
- [100] P. F. Skiba, S. Jackman, D. Clarke, A. Vanhatalo, and A. M. Jones, “Effect of work and recovery durations on W’ reconstitution during intermittent exercise,” *Med. Sci. Sports Exerc.*, vol. 46, no. 7, pp. 1433–1440, 2014.
- [101] J. C. Bartram, D. Thewlis, D. T. Martin, and K. I. Norton, “Accuracy of W’ Recovery Kinetics in High Performance Cyclists – Modelling Intermittent Work Capacity,” *Int. J. Sports Physiol. Perform.*, vol. 13, no. 6, pp. 724–728, 2018.

- [102] P. Bickford, V. S. M. Sreedhara, G. M. Mocko, A. Vahidi, and R. E. Hutchison, “Modeling the Expenditure and Recovery of Anaerobic Work Capacity in Cycling,” in *Proceedings of the 12th Conference of the International Sports Engineering Association; 2018 Mar 26-29: Brisbane (Australia)*, 2018, vol. 2, no. 6.
- [103] “Nike introduces breaking2: the quest to break the two-hour marathon barrier.,” *Nike News*. [Online]. Available: <https://news.nike.com/news/2-hour-marathon>.
- [104] W. Hoogkamer, “How Biomechanical Improvements in Running Economy Could Break the 2-hour Marathon Barrier,” *Sport. Med.*, vol. 47, no. 9, pp. 1739–1750, 2017.
- [105] W. Hoogkamer, K. L. Snyder, and C. J. Arellano, “Modeling the Benefits of Cooperative Drafting : Is There an Optimal Strategy to Facilitate a Sub-2-Hour Marathon Performance?,” *Sport. Med.*, vol. 48, no. 12, pp. 2859–2867, 2018.
- [106] W. Hoogkamer, K. L. Snyder, and C. J. Arellano, “Reflecting on Eliud Kipchoge ’ s Marathon World Record : An Update to Our Model of Cooperative Drafting and Its Potential for a Sub - 2 - Hour Performance,” *Sport. Med.*, vol. 49, no. 2, pp. 167–170, 2019.
- [107] B. J. Whipp, S. A. Ward, N. Lamarra, J. A. Davis, and K. Wasserman, “Parameters of ventilatory and gas exchange dynamics during exercise,” *J. Appl. Physiol.*, vol. 52, no. 6, pp. 1506–1513, 1982.
- [108] K. Caen, J. G. Bourgois, G. Bourgois, T. Van der Stede, K. Vermeire, and J. Boone, “The Reconstitution of \dot{V}' Depends on Both Work and Recovery Characteristics,” *Med. Sci. Sports Exerc.*, vol. 51, no. 8, pp. 1745–1751, 2019.

- [109] J. de Jong, R. Fokkink, G. J. Olsder, and A. Schwab, “The individual time trial as an optimal control problem,” *Proc. Inst. Mech. Eng. Part P J. Sport. Eng. Technol.*, vol. 231, no. 3, pp. 200–206, 2017.
- [110] E. R. Burke and A. L. Pruitt, “Body positioning for cycling,” in *High-Tech Cycling*, 2nd ed., E. R. Burke, Ed. Human Kinetics, 2003, pp. 69–92.
- [111] R. H. Morton, “Isoperformance curves: An application in team selection,” *J. Sports Sci.*, vol. 27, no. 14, pp. 1601–1605, 2009.
- [112] S. Halson, J. Peake, and J. Sullivan, “Wearable Technology for Athletes: Information Overload and Pseudoscience?,” *Int. J. Sports Physiol. Perform.*, vol. 11, pp. 705–706, 2016.
- [113] K. R. Evenson, M. M. Goto, and R. D. Furberg, “Systematic review of the validity and reliability of consumer-wearable activity trackers,” *Int. J. Behav. Nutr. Phys. Act.*, vol. 12, no. 1, p. 159, 2015.
- [114] F. Ashtiani, V. S. M. Sreedhara, A. Vahidi, G. Mocko, and R. Hutchison, “Experimental Modeling of Cyclists Fatigue and Recovery Dynamics Enabling Optimal Pacing in A Time Trial,” in *2019 American Control Conference (ACC)*, 2019, pp. 5083–5088.
- [115] A. R. Novak and B. J. Dascombe, “Agreement of Power Measures between Garmin Vector and SRM Cycle Power Meters,” *Meas. Phys. Educ. Exerc. Sci.*, vol. 7841, no. June, pp. 1–6, 2016.

- [116] A. Bouillod, J. Pinot, G. Soto-Romero, W. Bertucci, and F. Grappe, “Validity, Sensitivity, Reproducibility, and Robustness of the PowerTap, Stages, and Garmin Vector Power Meters in Comparison With the SRM Device.,” *Int. J. Sports Physiol. Perform.*, vol. 12, no. 8, pp. 1023–1030, 2017.
- [117] B. J. Sawyer, D. G. Stokes, C. J. Womack, H. R. Morton, A. Weltman, and G. A. Gaesser, “Strength training increases endurance time to exhaustion during high-intensity exercise despite no change in critical power,” *J. Strength Cond. Res.*, vol. 28, no. 3, pp. 601–609, 2014.
- [118] N. M. Okuno *et al.*, “Physiological and perceived exertion responses at intermittent critical power and intermittent maximal lactate steady state,” *J. Strength Cond. Res.*, vol. 25, no. 7, pp. 2053–2058, 2011.
- [119] D. G. Jenkins and B. M. Quigley, “Endurance training enhances critical power,” *Med. Sci. Sport. Exerc.*, vol. 24, no. 11, pp. 1283–1289, 1992.
- [120] D. G. Jenkins and B. M. Quigley, “The influence of high intensity exercise training on the Wlim-Tlim relationship,” *Med. Sci. Sport. Exerc.*, vol. 25, no. 2, pp. 275–282, 1993.
- [121] M. S. Hickey, D. L. Costill, G. K. McConell, J. J. Widrick, and H. Tanaka, “Day to Day Variation in Time Trial Cycling Performance,” *Int. J. Sports Med.*, vol. 13, no. 06, pp. 467–470, 1992.
- [122] J. P. Weir, “Quantifying the Test-Retest Reliability using the Intraclass Correlation Coefficient and the SEM,” *J. Strength Cond. Res.*, vol. 19, no. 1, pp. 231–240, 2005.

- [123] W. G. Hopkins, "Measures of Reliability in Sports Medicine and Science," *Sport. Med.*, vol. 30, no. 1, pp. 1–15, 2000.
- [124] I. E. Clark, H. E. Gartner, J. L. Williams, and R. W. Pettitt, "Validity of the 3-Minute All-Out Exercise Test on the CompuTrainer," *J. Strength Cond. Res.*, vol. 30, no. 3, pp. 825–829, 2016.
- [125] W. L. Beaver, K. Wasserman, and B. J. Whipp, "A new method for detecting anaerobic threshold by gas exchange," *J. Appl. Physiol.*, vol. 60, no. 6, pp. 2020–2027, 1986.
- [126] J. Hoogeveen, A. R., Schep, G., & Hoogsteen, "The Ventilatory Threshold, Heart Rate, and Endurance Performance: Relationships in Elite Cyclists," *Int. J. Sports Med.*, vol. 20, no. 02, pp. 114–117, 1999.
- [127] M. W. Vasey and J. F. Thayer, "The Continuing Problem of False Positives in Repeated Measures ANOVA in Psychophysiology: A Multivariate Solution," *Psychophysiology*, vol. 24, no. 4, pp. 479–487, 1987.
- [128] M. I. Black, A. M. Jones, S. J. Bailey, and A. Vanhatalo, "Self-pacing increases critical power and improves performance during severe-intensity exercise," *Appl. Physiol. Nutr. Metab.*, vol. 40, no. 7, pp. 662–670, 2015.
- [129] A. Vanhatalo, J. H. Doust, and M. Burnley, "A 3-min all-out cycling test is sensitive to a change in critical power," *Med. Sci. Sports Exerc.*, vol. 40, no. 9, pp. 1693–1699, 2008.

- [130] B. Karsten, S. Jobson, J. Hopker, A. Jimenez, and C. Beedie, “High agreement between laboratory and field estimates of critical power in cycling,” *Int. J. Sports Med.*, vol. 35, no. 4, pp. 298–303, 2013.
- [131] W. Chidnok *et al.*, “Exercise tolerance in intermittent cycling: Application of the critical power concept,” *Med. Sci. Sports Exerc.*, vol. 44, no. 5, pp. 966–976, 2012.
- [132] A. Miura *et al.*, “The effect of prior heavy exercise on the parameters of the power-duration curve for cycle ergometry,” *Appl. Physiol. Nutr. Metab.*, vol. 34, no. 6, pp. 1001–1007, 2009.
- [133] A. M. Jones, D. P. Wilkerson, M. Burnley, and K. Koppo, “Prior Heavy Exercise Enhances Performance during Subsequent Perimaximal Exercise,” *Med. Sci. Sports Exerc.*, vol. 35, no. 12, pp. 2085–2092, 2003.
- [134] M. Burnley, G. Davison, and J. R. Baker, “Effects of priming exercise on $\dot{V}O_2$ kinetics and the power-duration relationship,” *Med. Sci. Sports Exerc.*, vol. 43, no. 11, pp. 2171–2179, 2011.
- [135] P. Bickford, “Understanding the Expenditure and Recovery of Anaerobic Work Capacity Using Noninvasive Sensors,” 2016.
- [136] P. Mezzani, A., Corra, U., Giordano, A., Colombo, S., Psaroudaki, M., & Giannuzzi, “Upper Intensity Limit for Prolonged Aerobic Exercise in Chronic Heart Failure,” *Med. Sci. Sport. Exerc.*, vol. 42, no. 4, pp. 633–639, 2010.

- [137] J. A. Neder, P. W. Jones, L. E. Nery, and B. J. Whipp, "Determinants of the exercise endurance capacity in patients with chronic obstructive pulmonary disease: The power-duration relationship," *Am. J. Respir. Crit. Care Med.*, vol. 162, no. 2 I, pp. 497–504, 2000.
- [138] H. Vandeburgh, J. Chromiak, J. Shansky, Michael Del Tatto, and J. Lemaire, "Space travel directly induces skeletal muscle atrophy," *FASEB J.*, vol. 13, no. 9, pp. 1031–1038, 1999.

APPENDICES

Appendix A

Derivation of the W'_{bal} models demonstrating the imbalance of units

This appendix shows the derivation of mathematical solutions for the different W'_{bal} models presented by Skiba and colleagues [97]–[100]

W'_{bal} model with only the integrand [97]:

$$W'_{bal} = W'_{exp} \cdot e^{-\left(\frac{t-u}{\tau_{W'}}\right)} \quad (\text{A1})$$

W'_{bal} model with “ du ” as the differential variable [98], [99]:

$$W'_{bal} = W'_{exp} \cdot \int_0^t e^{-\left(\frac{t-u}{\tau_{W'}}\right)} du \quad (\text{A2})$$

W'_{bal} model with “ dt ” as the differential variable [100]:

$$W'_{bal} = W'_{exp} \cdot \int_0^t e^{-\left(\frac{t-u}{\tau_{W'}}\right)} dt \quad (\text{A3})$$

In all the forms, W'_{bal} is the Υ balance at any time during exercise, W'_{exp} is the amount of Υ expended, $(t - u)$ is the duration of the recovery interval, and $\tau_{W'}$ is the time constant of reconstitution of Υ in seconds given by,

$$\tau_{W'} = 546 \cdot e^{(-0.01D_{CP})} + 316 \quad (\text{A4})$$

where, D_{CP} is the difference between CP and average power output during all intervals below CP (recovery power). Equation A4 is a non-linear regression obtained by plotting $\tau_{W'}$ values (calculated by setting the $W'_{bal} = 0$ in Equation A2 at the termination of exercise) against respective D_{CP} s.

Biconditional W'_{bal} model proposed by Skiba and colleagues [99]:

$$\begin{aligned}
\text{If } P \geq CP, \quad W'_{bal} &= W'_0 - [(P - CP) \cdot t] \\
\text{If } P < CP, \quad W'_{bal} &= W'_0 - W'_{exp} \cdot e^{\left(\frac{-D_{CP} \cdot t}{W'_0}\right)}
\end{aligned} \tag{A5}$$

where, W'_0 is Y at time $t=0$. The $P > CP$ condition is same as the 2-parameter model for expenditure of Y . The $P < CP$ condition models the recovery of Y .

Equation A1 cannot be integrated due to the absence of the differential term. Hence, in the following section, Equations A2 and A3 will be integrated to show the difference in the obtained solution, and dimensional analyses will be conducted for both solutions to show the imbalance of units. Additionally, a detailed derivation of the $P < CP$ condition of Equation A5 will be presented.

Note: The constant of integration does not appear in the solutions as the limits of integration are known for all the integrals (i.e. they are definite integrals).

Integration of Equations A2 and A3

Integration of Equation A2

Rewriting Equation A2,

$$W'_{bal} = W'_0 - \int_0^t W'_{exp} \cdot e^{-\left(\frac{t-u}{\tau_{W'}}\right)} du$$

Treating W'_{exp} as a constant,

$$W'_{bal} = W'_0 - W'_{exp} \cdot \int_0^t e^{-\left(\frac{t-u}{\tau_{W'}}\right)} du$$

Integrating the exponential term with respect to “ u ” between limits $u = 0$ and $u = t$,

$$\begin{aligned}
W'_{bal} &= W' - \left[W'_{exp} \cdot \left\{ \tau_{W'} \left(e^{\frac{u-t}{\tau_{W'}}} \right) \right\}_{u=0}^{u=t} \right] \\
&= W' - W'_{exp} \cdot \tau_{W'} \left(e^{\frac{t-t}{\tau_{W'}}} - e^{\frac{0-t}{\tau_{W'}}} \right)
\end{aligned}$$

Therefore,

$$W'_{bal} = W' - W'_{exp} \cdot \tau_{W'} \left(1 - e^{\frac{-t}{\tau_{W'}}} \right)$$

Dimensional analysis of the integration of Equation A2

The result of the integration of Equation A2 is

$$W'_{bal} = W' - W'_{exp} \cdot \tau_{W'} \left(1 - e^{\frac{-t}{\tau_{W'}}} \right) \quad (A6)$$

Units of the terms on the left-hand-side (LHS): W'_{bal} is in Joules (J)

Units of the terms on the right-hand-side (RHS): W' is in J, W'_{exp} is in J, $\tau_{W'}$ is in seconds (s). The exponential term is dimensionless as the unit of measurement for both t and $\tau_{W'}$ is seconds.

Therefore, the units will look like:

$$\begin{aligned}
J &= J - J \cdot s \cdot \left(1 - e^{\frac{s}{s}} \right) \\
J &= J - J \cdot s \quad (A7)
\end{aligned}$$

The RHS cannot be computed due to the imbalance of the units.

Integration of Equation A3

Rewriting Equation A3,

$$W'_{bal} = W' - \int_0^t W'_{exp} \cdot e^{-\left(\frac{t-u}{\tau_{W'}}\right)} dt$$

Treating $\tau_{W'} W'_{exp}$ as a constant,

$$W'_{bal} = W' - W'_{exp} \cdot \int_0^t e^{-\left(\frac{t-u}{\tau_{W'}}\right)} dt$$

Integrating the exponential term with respect to “ t ” between limits $t = 0$ and $t = t$,

$$\begin{aligned} W'_{bal} &= W' - \left[W'_{exp} \cdot \left\{ \tau_{W'} \left(-e^{-\frac{u-t}{\tau_{W'}}} \right) \right\}_{t=0}^{t=t} \right] \\ &= W' - W'_{exp} \cdot \tau_{W'} \cdot \left(-e^{-\frac{u-t}{\tau_{W'}}} + e^{-\frac{u-0}{\tau_{W'}}} \right) \\ &= W' - W'_{exp} \cdot \tau_{W'} \cdot \left(-e^{-\frac{u-t}{\tau_{W'}}} + e^{-\frac{u}{\tau_{W'}}} \right) \end{aligned}$$

Therefore,

$$W'_{bal} = W' - W'_{exp} \cdot \tau_{W'} \cdot e^{-\frac{u}{\tau_{W'}}} \left(1 - e^{-\frac{-t}{\tau_{W'}}} \right)$$

Dimensional analysis of the solution to Equation A3

The result of the integration of Equation A3 is

$$W'_{bal} = W' - W'_{exp} \cdot \tau_{W'} \cdot e^{-\frac{u}{\tau_{W'}}} \left(1 - e^{-\frac{-t}{\tau_{W'}}} \right) \quad (\text{A8})$$

Units of the terms on LHS: W'_{bal} is in J

Units of the terms RHS: W' is in J, W'_{exp} is in J, $\tau_{W'}$ is in s. The exponential terms are dimensionless as the unit of measurement for u , t , and $\tau_{W'}$ is seconds.

Therefore, the units will look like:

$$J = J - J \cdot s \cdot e^{\frac{s}{s}} \cdot \left(1 - e^{\frac{s}{s}}\right)$$

$$J = J - J \cdot s \tag{A9}$$

The RHS cannot be computed due to the imbalance of the units, which is the same as the results of the dimensional analysis of Equation A2 in Equation A7.

Derivation of the recovery portion of Equation A5

The derivation below follows that presented by Skiba and colleagues [99] (Refer to Appendix 1 of [99]). It is to be noted that Υ will be referred to as W' in this section.

Case: $P < CP$

Assumption: Rate of change of W' depends on the amount of W' remaining and the power output relative to CP. Additionally, the power below CP is assumed to be constant.

Therefore, the rate of change of W' is given by,

$$\frac{dW'}{dt} = \left(1 - \frac{W'(t)}{W'_0}\right) \cdot (CP - P)$$

Separating dW' and dt and substituting $D_{CP} = CP - P$,

$$\frac{dW'}{\left(1 - \frac{W'(t)}{W'_0}\right)} = D_{CP} \cdot dt$$

The limits of integration on both sides will be for a recovery interval starting at time “ u ” and ending at time “ t ”. Therefore, the limits for $dW' = W'(u)$ to $W'(t)$.

Applying the integral,

$$\int_{W'(u)}^{W'(t)} \frac{dW'}{\left(1 - \frac{W'(t)}{W'_0}\right)} = \int_u^t D_{CP} \cdot dt$$

Integrating by treating (I/W'_0) as a constant,

$$\left[-W'_0 \cdot \ln(W'_0 - W'(t)) \right]_{W'(t)=W'(u)}^{W'(t)=W'(t)} = D_{CP} \cdot (t)_{t=u}^{t=t}$$

Multiplying both sides by (I/W'_0) and applying the limits on the RHS,

$$\ln(W'_0 - W'(t))_{W'(t)=W'(u)}^{W'(t)=W'(t)} = \frac{-D_{CP} \cdot (t-u)}{W'_0}$$

Applying the limits on the LHS,

$$\ln(W'_0 - W'(t)) - \ln(W'_0 - W'(u)) = \frac{-D_{CP} \cdot (t-u)}{W'_0}$$

Using the laws of logarithms,

$$\ln\left(\frac{W'_0 - W'(t)}{W'_0 - W'(u)}\right) = \frac{-D_{CP} \cdot (t-u)}{W'_0}$$

Taking exponential on both sides,

$$\frac{W'_0 - W'(t)}{W'_0 - W'(u)} = e^{\frac{-D_{CP} \cdot (t-u)}{W'_0}}$$

Multiplying by $W'_0 - W'(u)$ on both sides and rearranging,

$$W'(t) = W'_0 - (W'_0 - W'(u)) \cdot e^{\frac{-D_{CP} \cdot (t-u)}{W'_0}}$$

Replacing $W'(t)$ with W'_{bal} , $(W'_0 - W'(u))$ with W'_{exp} , and $(t-u)$ with t gives,

$$W'_{bal} = W'_0 - W'_{exp} \cdot e^{\frac{-D_{CP} \cdot t}{W'_0}} \tag{A10}$$

Equation A10 is identical to the expression representing the recovery portion in Equation A5.

Appendix B

Data and analyses details for the intermittent cycling tests

Table A-1. E_{rec} (%) during each intermittent cycling test for all subjects.

Subject	T1	T2	T3	T4	T5	T6	T7	T8	T9
A	29.02	44.06	38.20	5.76	6.67	7.93	-8.87	-6.80	-10.76
B	48.82	63.90	51.64	32.76	46.05	34.05	26.80	39.81	-8.64
1	43.68	37.11	53.57	22.75	25.05	34.31	14.61	20.44	8.61
2	23.21	35.57	29.80	14.57	35.17	-6.18	-34.44	-32.50	-49.30
4	29.18	31.77	16.41	23.70	36.34	13.45	13.84	7.62	-38.72
6	28.31	31.32	44.42	14.16	39.79	31.61	7.92	10.26	5.65
Mean	33.70	40.62	39.01	18.95	31.51	19.20	3.31	6.47	-15.53
SD	10.10	12.30	14.12	9.42	13.97	16.77	21.84	24.56	23.58

*Subject 7 excluded due to reasons discussed in Chapter 4.

Results of the repeated measures ANOVA:

Table A-2. Results of the repeated measures ANOVA.

Effect	F	Degrees of freedom, Effect, Error	p-value	Partial η^2	Observed power
P_{rec}	25.603	2, 10	<0.001	0.837	1
$t_{rec}^{\#}$	3.29	1.212, 6.062	0.117	0.397	0.355
$P_{rec} \times t_{rec}$	5.395	4, 20	0.004	0.519	0.929

[#]Greenhouse-Geisser correction used as both epsilons from Mauchly's test were <0.7.

Table A-3. Results of the simple main-effects analysis at each t_{rec}^* .

t_{rec} (minutes)	F	Degrees of freedom, Effect, Error	p-value	Partial η^2	Observed power
2	14.745	2, 10	0.001	0.747	0.989
6	8.905	2, 10	0.006	0.640	0.906
15	53.353	2, 10	<0.001	0.914	1

*Pairwise comparisons are reported in Table 2 of the manuscript.

Table A-4. Results of the simple main-effects analysis at each P_{rec} .

P_{rec}	F	Degrees of freedom, Effect, Error	p-value	Partial η^2	Observed power
L	1.25	2, 10	0.303	0.213	0.227
M	3.017	2, 10	0.094	0.376	0.456
H [#]	5.786	1.141, 5.705	0.053	0.536	0.537

[#]Greenhouse-Geisser correction used as both epsilons from Mauchly's test were <0.7.

Appendix C

Data and analysis details of A_3 versus Y_{SK2} and Y_{BAR}

Table A-5. Y_{bal} actual (A_3) vs. Y_{SK2} and Y_{BAR} for all subjects*

Subject	P_{rec}	t_{rec} , minutes	Y_{bal} actual (A_3), kJ	Y_{SK2} , kJ	Y_{BAR} , kJ
A	L	2	10.063	11.135	11.186
	L	6	11.999	12.010	12.012
	L	15	11.375	12.028	12.028
	M	2	7.327	8.619	9.419
	M	6	7.540	10.742	11.459
	M	15	7.724	11.886	12.009
	H	2	5.453	7.007	7.699
	H	6	5.886	8.251	9.731
	H	15	5.248	9.783	11.398
B	L	2	10.169	9.175	9.079
	L	6	11.842	10.076	10.065
	L	15	10.407	10.102	10.102
	M	2	8.631	7.938	8.232
	M	6	9.563	9.671	9.820
	M	15	8.550	10.093	10.099
	H	2	8.040	6.512	7.099
	H	6	8.884	7.969	8.868
	H	15	4.363	9.569	9.967
1	L	2	14.676	13.985	14.325
	L	6	13.674	15.068	15.084
	L	15	17.772	15.092	15.092
	M	2	11.455	11.937	13.071
	M	6	11.844	14.503	14.940
	M	15	13.161	15.078	15.092
	H	2	10.208	9.899	11.385
	H	6	11.081	12.356	14.115
	H	15	9.380	14.462	15.045

Table A-5 (continued). Υ_{bal} actual (A_3) vs. Υ_{SK2} and Υ_{BAR} for all subjects*.

Subject	P_{rec}	t_{rec} , minutes	Υ_{bal} actual (A_3), kJ	Υ_{SK2} , kJ	Υ_{BAR} , kJ
2	L	2	4.481	5.485	5.080
	L	6	5.161	5.645	5.618
	L	15	4.633	5.646	5.646
	M	2	3.802	4.654	4.363
	M	6	4.956	5.507	5.350
	M	15	2.629	5.644	5.635
	H	2	1.164	3.808	3.835
	H	6	1.145	4.550	4.626
	H	15	0.072	5.481	5.509
4	L	2	6.618	7.459	7.134
	L	6	6.644	7.838	7.819
	L	15	5.674	7.841	7.841
	M	2	6.184	5.944	6.027
	M	6	7.072	7.270	7.349
	M	15	5.697	7.811	7.820
	H	2	5.463	5.016	5.296
	H	6	5.204	5.945	6.456
	H	15	1.574	7.078	7.498
6	L	2	7.475	8.172	8.027
	L	6	7.539	9.095	9.070
	L	15	8.704	9.137	9.137
	M	2	5.971	7.189	7.324
	M	6	8.416	8.804	8.867
	M	15	7.575	9.130	9.133
	H	2	5.429	5.883	6.328
	H	6	5.553	7.381	8.019
	H	15	5.086	8.741	9.010
		Mean	7.523	8.835	9.115
		SD	3.549	2.971	3.104

*Subject 7 excluded due to reasons discussed in Chapter 4.

Table A-6. Mann-Whitney U test results for A_3 vs. Y_{SK2} .

Y_{bal}	Mean \pm SD	n	Shapiro-Wilk p-value	Mann-Whitney U test results			
				Mean rank	U	Standardized test-stat, z	p-value
A_3	7.523 \pm 3.549	54	0.540	48.13	1802	2.114	0.035
Y_{SK2}	8.835 \pm 2.971	54	0.022	60.87			

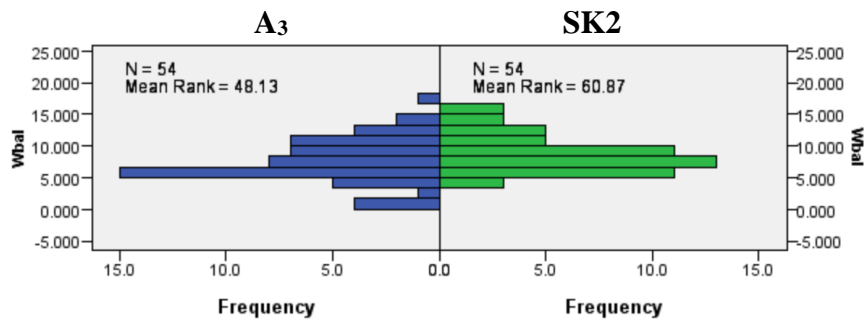


Figure A-1. Dissimilar frequency distributions of A_3 and Y_{SK2} .

Table A-7. Mann-Whitney U test results for A_3 vs. Y_{BAR} .

Y_{bal}	Mean \pm SD	n	Shapiro-Wilk p-value	Mann-Whitney U test results			
				Mean rank	U	Standardized test-stat, z	p-value
A_3	7.523 \pm 3.549	54	0.540	47.18	1853.5	2.430	0.015
Y_{BAR}	9.115 \pm 3.104	54	0.027	61.82			

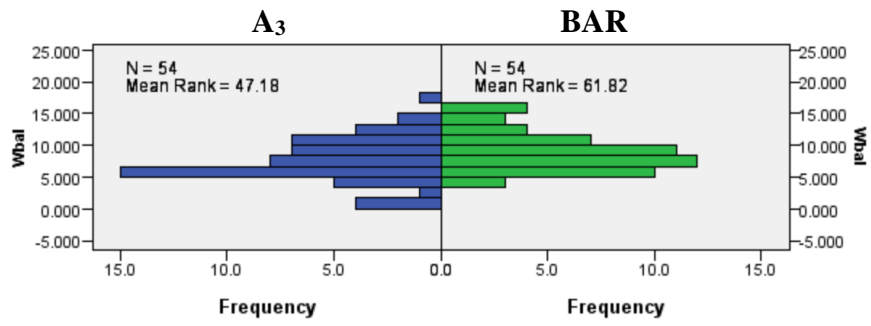


Figure A-2. Dissimilar frequency distributions of A_3 and Y_{BAR} .

Appendix D

Data and analysis details of CP_{fr} versus CP_{ft} for all subjects

Table A-8. CP_{fr} and CP_{ft} for all subjects.

Subject	CP_{fr} (W)	CP_{ft} (W)
1	271	274
	267	278
		284
		277
		274
		278
		285
		273
		285
2	231	282
	234	259
		260
		246
		247
		263
		261
		257
		238

Table A-8 (continued). CP_{fr} and CP_{ft} for all subjects.

Subject	CP_{fr} (W)	CP_{ft} (W)
	335	361
	334	349
	327	360
	343	332
3		348
		352
		348
		352
		340
	211	200
	215	218
	220	227
	224	211
4		218
		201
		207
		203
		191
	246	251
	237	259
	245	244
	242	253
5		258
		254
		254
		263
		237

Table A-8 (continued). CP_{fr} and CP_{ft} for all subjects.

Subject	CP _{fr} (W)	CP _{ft} (W)
	195	203
	217	207
	212	215
	200	194
6		215
		216
		210
		213
		210

Details of statistical analyses:

Group level: Mann-Whitney U test conducted due to a violation of normality assumption.

Table A-9. Mann-Whitney U test results excluding Subject 7*

CP	Mean ± SD	n	Shapiro-Wilk p-value	Mann-Whitney U test results			
				Mean rank	U	Standardized test-stat, z	p-value
CP _{fr}	250 ± 47	20	0.0035	33.48	620.50	0.980	0.327
CP _{ft}	259 ± 49	54	0.0005	38.99			

*Subject 7 excluded due to reasons discussed in Chapter 4.

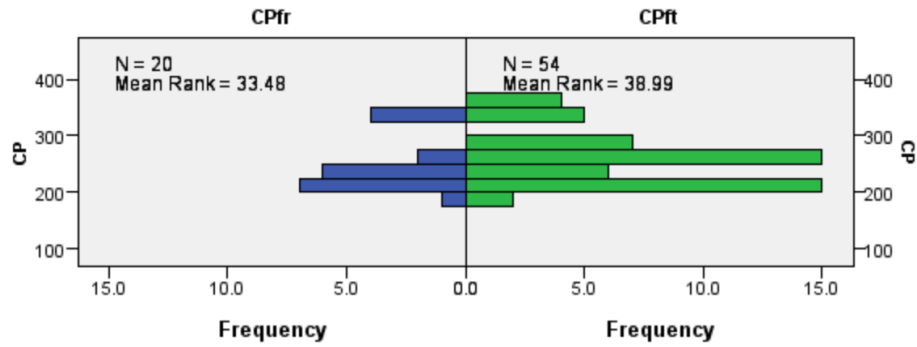


Figure A-3. Dissimilar frequency distributions of CP_{fr} and CP_{ft} .

Subject level: Independent sample t-tests were conducted due to unequal sample sizes. CP data from subjects 1 and 2 were not analyzed at subject level as they did only two fresh 3MTs. Data from Subject 7 were excluded due to reasons discussed in Chapter 4.

Table A-10. Independent t-test results for Subject 1

CP	Mean \pm SD	n	Shapiro-Wilk p-value	Levene's test p-value	Mean diff., 95%CI	t	p-value	Cohen's d
CP_{fr}	335 ± 7	4	0.836	0.476	-13 (-25, -2)	-2.602	0.025	1.56
CP_{ft}	348 ± 9	9	0.765					

Table A-11. Independent t-test results for Subject 2

CP	Mean \pm SD	n	Shapiro-Wilk p-value	Levene's test p-value	Mean diff., 95%CI	t	p-value	Cohen's d
CP_{fr}	217 ± 6	4	0.914	0.201	9 (-4, 22)	1.485	0.166	0.89
CP_{ft}	208 ± 11	9	0.937					

Table A-12. Independent t-test results for Subject 4

CP	Mean ± SD	n	Shapiro-Wilk p-value	Levene's test p-value	Mean diff., 95%CI	t	p- value	Cohen's d
CP _{fr}	242 ± 4	4	0.632	0.396	-10	-2.460	0.032	1.48
CP _{ft}	253 ± 8	9	0.529		(-20, -1)			

Table A-13. Independent t-test results for Subject 6

CP	Mean ± SD	n	Shapiro-Wilk p-value	Levene's test p-value	Mean diff., 95%CI	t	p- value	Cohen's d
CP _{fr}	206 ± 10	4	0.707	0.210	-3	-0.670	0.512	0.40
CP _{ft}	209 ± 7	9	0.078		(-14, 7)			